CYRIL MAYAUD

GROUNDWATER MODELLING IN KARST TERRAINS USING SINGLE-CONTINUUM MODELS

BRIDGING THE GAP BETWEEN STATE-OF-THE-ART TOOLS AND PRACTICAL APPLICATION

A dissertation submitted to the

Faculty of Natural Science
University of Graz
Austria

for the Degree of Doctor of Science

February 2014

In memory of Christoph Rehrl,
To my parents,

“manj strašna noč je v črne zemlje krili,
ko so pod svetlim soncam sužni dnovi!"
France Prešeren, Slovenian poet - 1836
Krst pri Savici (the Baptism on the Savica)

PREAMBLE

Groundwater modelling is of primary importance to assess aquifer hydrological behaviour, flow direction, transport travel times as well as estimation of water resources in karst areas. As groundwater modelling standard approaches do not account for the peculiarities of karst aquifers, there is a need to improve the existing tools used for karst aquifer modelling. Hybrid models, which are frequently employed in basic research, represent karst conduits by a pipe network (allowing laminar and turbulent flow) embedded in a matrix where the flow is laminar. Even if these models present the advantage to reproduce correctly the duality of flow in karst aquifers, they have the significant disadvantage to be hard to implement in practical applications, as many of the required input parameters are rarely available. An alternative to this kind of modelling is the so called single-continuum approach, which is derived from porous aquifer groundwater modelling and presents the advantages to require less input parameters and to be easier to implement. Nevertheless this approach does not explicitly consider the duality of flow reproduced by hybrid models. This lack was filled recently by the development of two compatible MODFLOW packages, allowing the implementation of non-linear and turbulent flow within single-continuum models. The present work has the purpose to investigate to which extent the single-continuum approach (with and without non-linear flow) can be applied to field examples, in order to reproduce hydrological processes occurring in karst aquifers. The present research is based on both generic and field sites (using real data and related problems).

OUTLINE OF THE THESIS

This thesis is divided into five chapters and three appendices.

In **Chapter 1** a general introduction of karst sciences and groundwater modelling in karst terrains is presented. This chapter is important to understand the actual problematic related with groundwater modelling in karst aquifers and the reason why single-continuum models were chosen for this thesis.

Chapter 2 presents a study of a change of hydrological behaviour in an Austrian binary karst system. This study shows that the change of drainage behaviour occurring at one karst spring is caused by a change within the karst aquifer itself and is not driven by a change of weather or land use conditions. This chapter has already been published as:

- **Mayaud, C., Wagner, T., Benischke, R., and Birk, S., 2013.** Understanding changes in the hydrological behaviour within a karst aquifer (Lurbach system, Austria). Carbonate Evaporite. doi: 10.1007/s13146-013-0172-3.

Chapter 3 investigates an overflow behaviour reported in an Austrian binary karst catchment using statistical methods and groundwater modelling. The combination of both approaches helps to determine the overflow location within the karst aquifer. This chapter is currently accepted for publication as:

- **Mayaud, C., Wagner, T., Benischke, R., and Birk, S., 2014.** Single event time series analysis in a binary karst catchment evaluated using a groundwater model (Lurbach system, Austria). doi: 10.1016/j.jhydrol.2014.02.024. Accepted for publication by Journal of Hydrology.

In **Chapter 4** a new numerical package simulating non-linear flow with the Forchheimer equation is introduced. This package was programmed for MODFLOW-2005 and showed a good agreement with three different analytical solutions of the Forchheimer equation for confined and unconfined aquifers. This chapter is currently under review in a peer-reviewed journal:

- **Mayaud, C., Walker, P., Hergarten, S., and Birk, S.,** Non-Linear Flow Process (NLFP): a new package to compute non-linear flow in MODFLOW. Submitted as Methods Note to Groundwater.

Chapter 5 presents the overall conclusions and outlooks of this work.

Appendix A is a contribution where a change of hydrological behaviour within the Lurbach system is investigated with a lumped-parameter model. This appendix has to be read in parallel with Chapter 2 and has already been published as:

- **Wagner, T., Mayaud, C., Benischke, R., and Birk, S., 2013.** Ein besseres Verständnis des Lurbach-Karstsystems durch ein konzeptionelles Niederschlags-Abfluss-Modell. Grundwasser. doi: 10.1007/s00767-013-0234-4.

Appendix B contains five different abstracts presented during the course of this PhD at several national and international conferences where I contributed as a first-author.

Appendix C contains a list of five different abstracts presented during the course of this PhD at several national and international conferences where I contributed as a co-author.

SUMMARY

Karst aquifers represent about 25 % of the total world groundwater reserves and are in many areas the first resource of drinking water. As they are very vulnerable to contamination there is a need to improve the global understanding of their flow behaviour and to better quantify their reserves. In general, groundwater models are widely used to characterize porous aquifers and to make predictions related to groundwater flow and transport phenomena. However, these tools are much less employed in karst areas. One approach used for karst aquifer modelling is the single-continuum model, which represents the conduit system by high contrasts in the hydraulic conductivity of a porous medium. The aim of this PhD thesis is to assess how far this approach is adequate for karst aquifer modelling. To do this, two examples applying a single-continuum model to a real karst system are presented. Both case studies combine the single-continuum approach with other characterization methods (such as time series analysis, master recession curves or tracer test data) and improve significantly the characterization of the aquifer system. Nevertheless, both field examples show the limitations of the currently available packages reproducing turbulent conduit flow through single-continuum models. A new package considering non-linear flow using the Forchheimer equation was developed and proved to compute non-linear flow accurately for three benchmark models and a more realistic field example derived from one of the aforementioned case studies. In summary, the use of single-continuum models for karst aquifer modelling is relevant and should be further considered as a valuable alternative to other modelling approaches.

ZUSAMMENFASSUNG

Karstgrundwasserleiter stellen etwa 25 % der globalen Grundwasservorräte und sind in vielen Gebieten die vorrangige Trinkwasserversorgung. Da sie sehr anfällig gegenüber Schadstoffeinträgen sind, ist es erforderlich, das Verständnis des Fließverhaltens in diesen Grundwasserleitern zu verbessern und die jeweiligen Grundwasservorräte besser zu quantifizieren. Generell werden Grundwassermodelle oft verwendet, um Porengrundwasserleiter zu charakterisieren und Vorhersagen in Bezug auf Strömungs- und Transportvorgänge zu machen. Diese Modellwerkzeuge werden jedoch weit weniger in Karstgebieten eingesetzt. Ein Ansatz für die Modellierung von Karstgrundwasserleitern sind Ein-Kontinuum-Modelle, in denen das Karsthohlraumsystem durch starke Kontraste in der hydraulischen Leitfähigkeit eines porösen Mediums repräsentiert wird. Das Ziel dieser Dissertation ist es, zu beurteilen, inwieweit dieser Ansatz für die Modellierung geeignet ist. Zu diesem Zweck werden zwei Beispiele vorgestellt, in denen ein Ein-Kontinuum-Modell auf ein reales Karstsystem angewendet wird. Beide Fallstudien kombinieren den Ein-Kontinuum-Ansatz mit anderen Methoden (wie etwa Zeitreihenanalyse, Trockenwetterfalllinie oder Markierungsversuche) und verbessern erheblich die Charakterisierung des Aquifersystems. Beide Feldbeispiele zeigen jedoch auch die Limitierungen der derzeit verfügbaren Programmpakete zur Berücksichtigung turbulenter Strömung in Ein-Kontinuum-Modellen auf. Ein neues Programmepaket zur Berücksichtigung nicht-linearer Strömung mit Hilfe der Forchheimergleichung wurde entwickelt und die korrekte Berechnung der nicht-linearen Strömung anhand dreier Benchmark-Modelle sowie einem realistischen Feldbeispiel aus einer der oben erwähnten Fallstudien gezeigt. Zusammenfassend kann festgestellt werden, dass die Verwendung von Ein-Kontinuum-Modellen für Karstgrundwasserleiter relevant ist und als angemessene Alternative zu anderen Modellansätzen gesehen werden sollte.

Contents

CHAPTER I

INTRODUCTION TO KARST SCIENCES AND GROUNDWATER MODELLING IN KARST AQUIFERS

1. Introduction to karst sciences

1.1 Historical and geographical context

Karst is the German translation of kras, a Slovenian word referring originally to a geographical area covering a large part of current southern Slovenia and surrounding the city of Trieste (Italy). This area was already known and investigated during the Austro-Hungarian Empire due to its uncommon landscape including a very sparse surface hydrological network, many large caves, a high density of sinkholes and several intermittent lakes. One of the first detailed scientific descriptions of this region was carried out by the famous Serbian geographer Jovan Cvijić (Das Karstphänomenen, 1893) who also defined almost all the terminology currently used in karst sciences. This area is named the ***"Classical Karst"*** (a part of it can be seen on Fig. 1) and extends from the springs of the Ljubljanica River in the North to the flanks of the Mount Snežnik in the East, the Mediterranean shore and the limestone plateau above Trieste for the southern boundary, and the Slovenian-Italian border with the city of Gorizia in the West. Many famous show caves such as the Postojna cave, the caves of Škocjan or the Križna cave are located within this area.

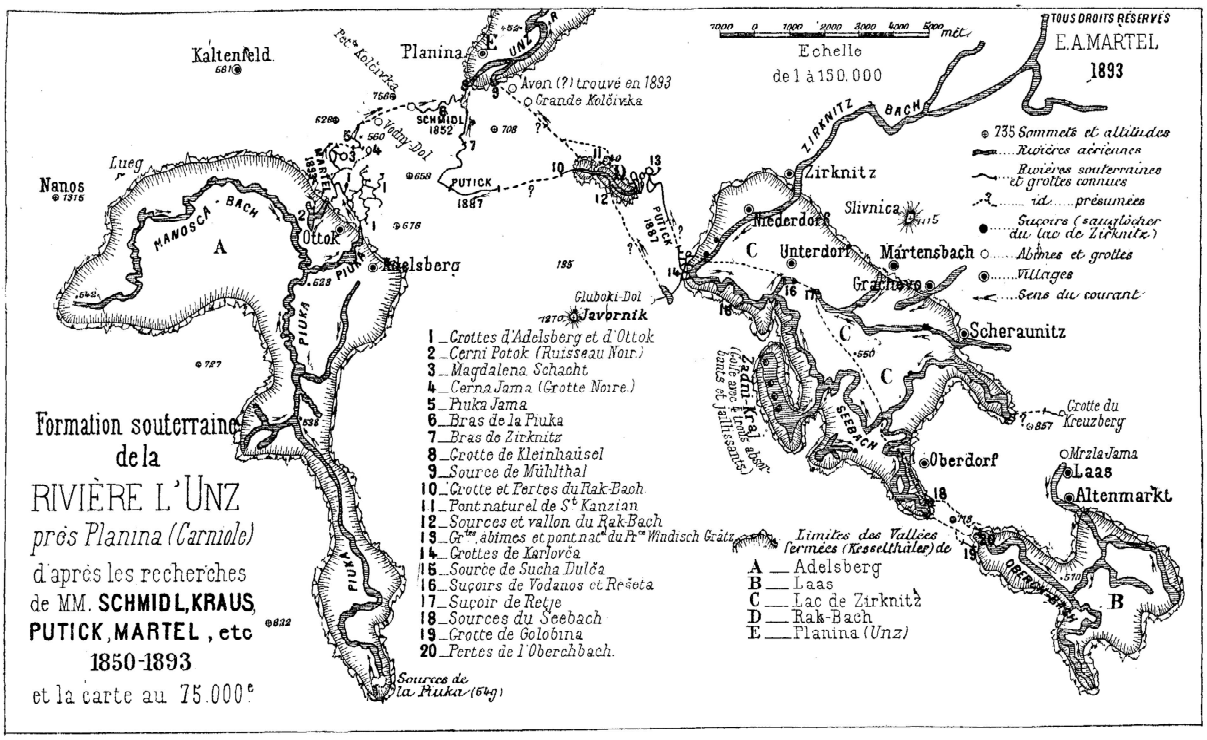

Fig. 1 A part of the Classical Karst: the catchment of the Unica River (modified after Martel, 1894), being a part of the catchment of the Ljubljanica River.

1.2 General definition and hydrology of a karst landscape

Today the word karst is a worldwide known term used to define a type of landscape made of rocks composed mostly of limestone ($CaCO_3$) or dolomite ($MgCO_3$), but also of gypsum ($CaSO_4$) such as the giant Gypsum caves of Western Ukraine (Klimchouk, 1996) or halite (NaCl) like the Russian hyperkarst of the Perm salt mine (Salomon, 2006). Those landscapes

share the particularity to present a high concentration of voids of different size and a tortuous geometry, as they are normally generated by the action of acid rainwater dissolving and enlarging them during the infiltration process.

This first geomorphologic and geographic definition can lead to a second more hydrogeologic definition which tends to consider karst landscapes as potential aquifers (Fig. 2), where the water can be stored or released depending on the hydrological conditions within the conduit network and its surrounding matrix.

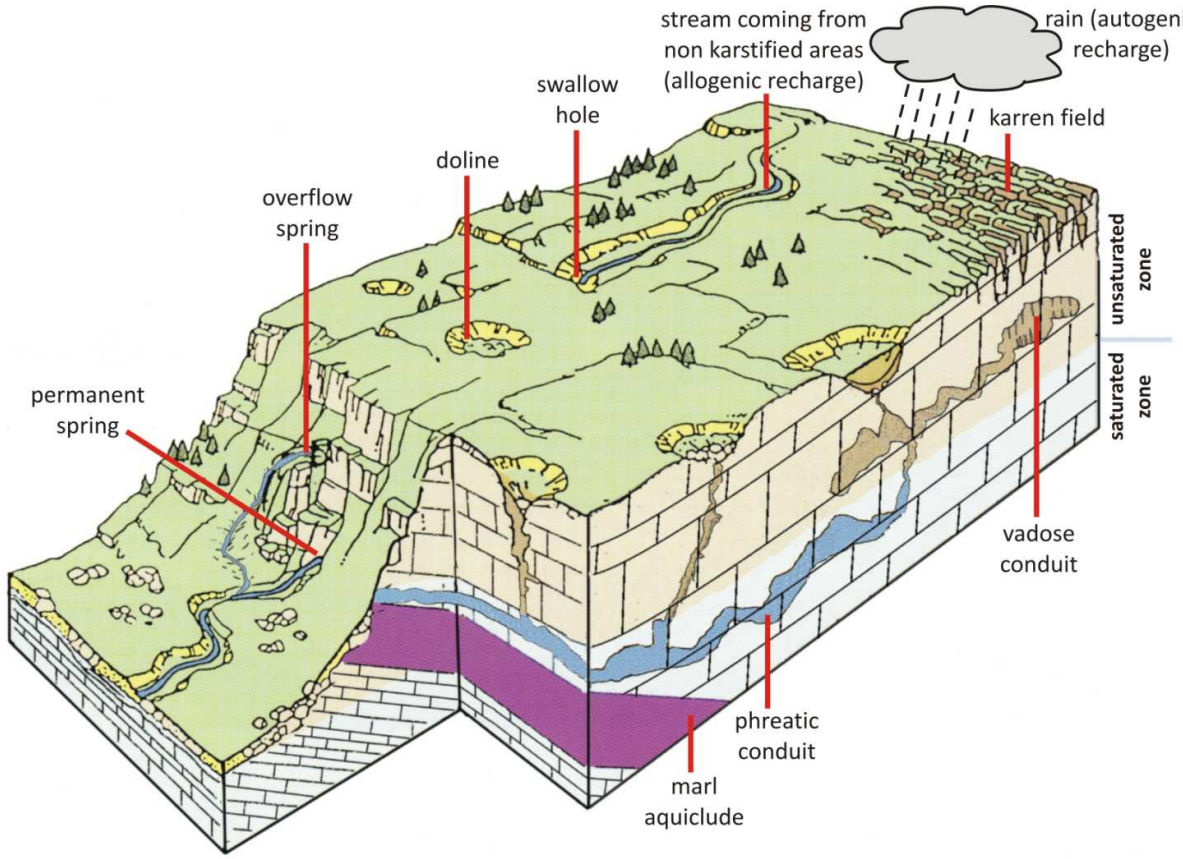

Fig. 2 Schematic view of a karst landscape including both saturated and unsaturated zones (modified from Filipponi, 2009).

Nevertheless, karst aquifers have to be distinguished from porous aquifers due to several particularities:

(i) due to the numerous voids with sizes varying several orders of magnitude and a tortuous geometry, their porosity can be described as a triple porosity comprising matrix, fracture and conduit porosity (Worthington, 2007). This is opposed to the conventional porous aquifers where the porosity mostly covers only one order of magnitude.

(ii) the development of these voids and their occurrence in the saturated and unsaturated zone creates a double infiltration capacity with two time scales (Marsaud, 1996): slow and diffuse infiltration of the rainwater in the fissures on top of the aquifer

(autogenic recharge); very rapid and localized infiltration of the water through the sinkholes, shafts and swallow holes (point source recharge). Oppositely, the porous aquifers have mostly a single diffuse infiltration capacity.

(iii) a double storage capacity (Atkinson and Smart, 1981): in the saturated zone the karst matrix offers an almost unlimited storage capacity and a long residence time of water, opposed to the limited storage capacity of the conduit network and its fast release of water (due to its high hydraulic conductivity). On the contrary, porous aquifers have only one type of storage and a rather slow release.

(iv) two different types of flow regimes; whereas the flow is laminar in the matrix, it can be either laminar or turbulent (depending on the value of the Reynolds number) in the conduits. Again, this is different from the porous aquifers where flow remains essentially laminar (Atkinson, 1977).

All this particularities are due to the physical nature of karst aquifers and can also be found in medias which are not made of limestone or dolomite and are not shaped by the action of rainwater acidity. The word Pseudokarst is then used to describe them (Ford and Williams, 2007). For example, mountain glaciers (frequently described by the term glaciokarst) present similar hydrological processes and follow the same physical laws as karst aquifers made of limestone (a third order porosity, a double storage capacity and a laminar/turbulent flow behaviour); but their network genesis evolves at a different (much shorter) time scale, mostly driven by the effect of water temperature. Aquifers of volcanic origin (vulcanokarst) belong also to pseudokarst because their vuggy porosity and their solidified lava tube network are sensibly similar to the organization of karstified limestone aquifers. In the following parts, the word karst will refers only to aquifers made of limestone or dolomite and their hydrology.

1.3 Interactions between karst and humans: a multi-aspects problem

1.3.1 Short historical context of karst-humans relationships

Karst and people interact with each other almost since the early days of humanity (Shen et al., 2013): during the prehistory, innumerable caves entrances developed in karst medias were used as shelters by the first hunters-gatherers and protected them against bad and cold weather or foreign aggressions. These caves participated also to their spiritual development and were sometimes used as object of devotion (Leroi-Gourhan and Michelson, 1986; Mithen, 1996). Many caves inhabited or visited by humans during Stone Age show numerous painting of the local fauna, and can provide a good indication of the past climate and the animal's diversity present on the surrounding of the cave at this time. As example, several of the most famous European painting caves such as Lascaux and Chauvet (France) or Altamira (Spain) can be cited (Bastian and Alabouvette, 2009; Bon et al., 2011).

Later, people profited from the natural advantages offered by the caves and their surrounding environment and used them as defense place to protect them against foreign aggressions. The

most famous examples can be found in Slovenia with the castles of Predjama (Fig. 3a) and Osp, or in Montenegro with the monastery of Ostrog. Even in the present times caves and underground settlement are still used has habitation by a non negligible percentage of population (in 1995 about 40 million people were reported to live in underground habitations in China, mostly build in loess; The UNESCO Courier, 1995). Troglodyte habitations can also be found overall around the world with famous examples in France (Fig. 3b), Turkey (Cappadocia), Italy, Vietnam, India or Morocco.

Fig. 3 (a) Picture of the castle of Predjama (literally "before the cave" in Slovenian), Slovenia. A small stream is vanishing in the Predjama cave system at the foot of the cliff. **(b)** Troglodyte house near the Grotte du Sorcier, south of France. Picture b was taken by the Wikipedia user Jebulon and is reproduced with permission.

During the past, karst areas were also exploited because of their natural wealth in diverse minerals and ores such as phosphates or bauxite. Very famous examples can be found in the regions of Quercy (south of France) and central Styria (Austria) where the phosphates deposits were exploited to produce fertilizers for agriculture, and were an important contribution to the local economy (Aguilar et al., 2007; Marchet, 1928). In the same way, numerous karst poljes and dolines were also used as pastry fields for the first ones and crop fields for the second ones in several European regions (for example since the Roman Empire in the Slovenian karst). All these strong interactions explain the close proximity of humans to karst areas and lead to the important problematic of water supply which will be treated in the following part.

1.3.2 Water supply

As pointed out by Williams and Fong (2011) about 13% of the emerged areas on earth are constituted of limestone, dolomite or gypsum and these areas represent about 25% of the available resources in groundwater. As example, a large part of the Alps is constituted of limestone and dolomite and almost all the coast around the Mediterranean Sea is karstified (Fig. 4).

As more than 768 million people around the world lacked on an improved water resource in 2011, (UNICEF, 2013), the huge reserves present in these aquifers are of extreme importance. In many countries, karst waters represent one of the major reservoirs of groundwater and even

sometimes the first. Countries like Slovenia or Austria take about 50% of their groundwater resources from karst aquifers (COST Action 64, 1995; Kralik, 2001). Moreover, many important European cities like Vienna (with the Hochschwab massif; Plan and Decker, 2006), Split (with the Jadro spring; Bonacci, 1987), Dubrovnik (Ombla spring; Bonacci, 1995), Montpellier (Lez spring; Fleury et al., 2007), or Angoulême (Touvre springs; Larocque et al., 1998) are supplied totally or partly by karst waters.

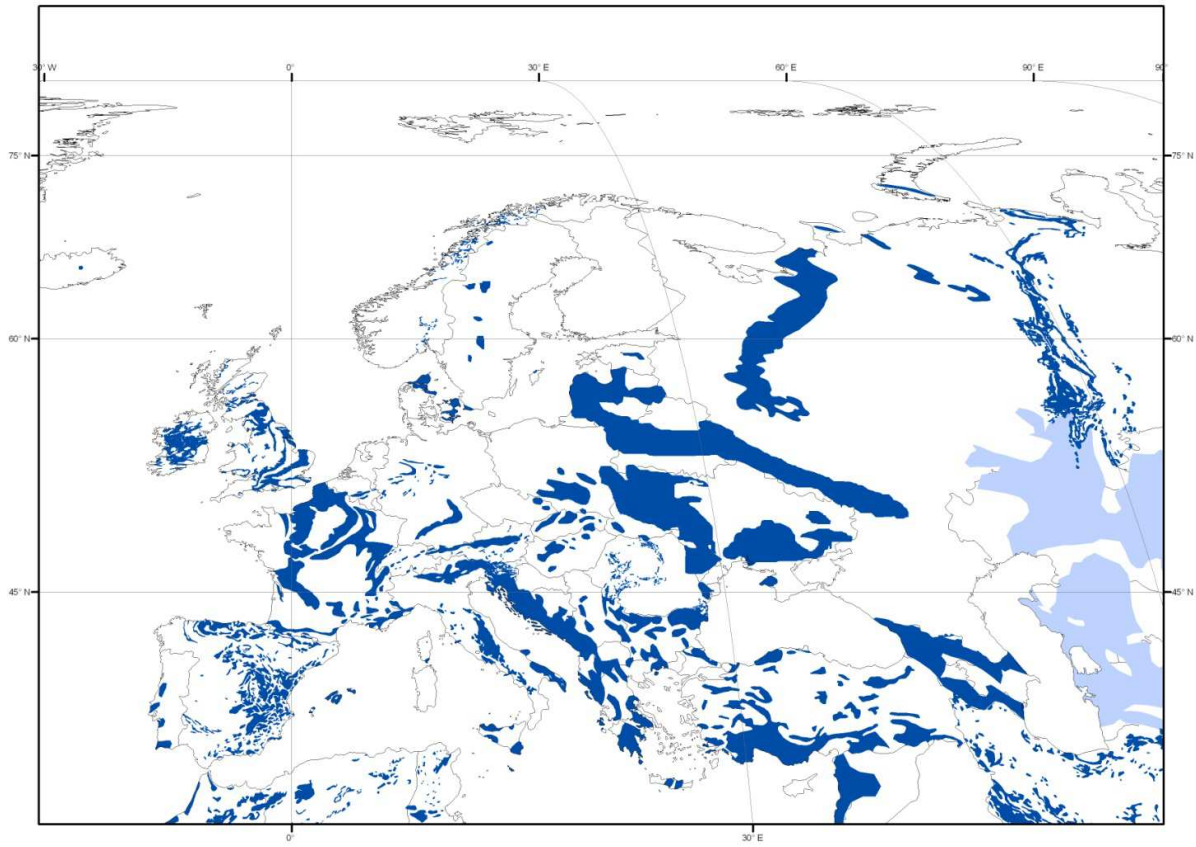

Fig. 4 Map representing all carbonate rock outcrops in Europe (Williams and Fong, 2011). Carbonate rock outcrops cover a surface of 21.8% of total Europe (excluding Russia and Iceland).

The importance of karst waters for water supply implies the need of an adapted management and protection policy of the available resources, which will be introduced in the next parts.

1.3.3 Protection of karst water resources and cave biodiversity

As karst aquifers are groundwater systems able to respond very quickly to a hydrological event, (the waters flowing through their conduits can have a very short travel time, reaching sometimes the velocity of several hundred meters per hour) they are very sensitive to chemical or bacterial contamination. Oppositely, due to the tortuous configuration of the conduit network, pollution may stay trapped in the aquifer for long period of time (LNAPL and DNAPLs are falling within this category; Vesper et al., 2001; Ghasemizadeh et al., 2012). This can be really problematic because the water of karst aquifers is a resource of primary importance for the people living around them. To minimize this risk and understand to which extent a karst aquifer is vulnerable to pollution hazards, several methods such as RISKE,

EPIK, or PaPRIKa (Dörfliger and Plagnes, 2009; Dörfliger and Zwahlen, 1998; Kavouri et al., 2011; Pételet-Giraud et al., 2000) were developed during the two last decades. These methods have the purpose to protect and prevent karsts aquifers from important contamination (for example from an oil leak of a tank). To do this, they use several evaluation criteria (like the size of the catchment, its geology, the importance of the human development on it and the location of the aquifer recharge areas) which help to define several protection perimeters for the aquifer. These perimeters evaluate the contamination risk in the investigated area and are of extreme importance for the local authorities, in order to make the appropriate decisions leading to a careful development near karst aquifer recharge areas.

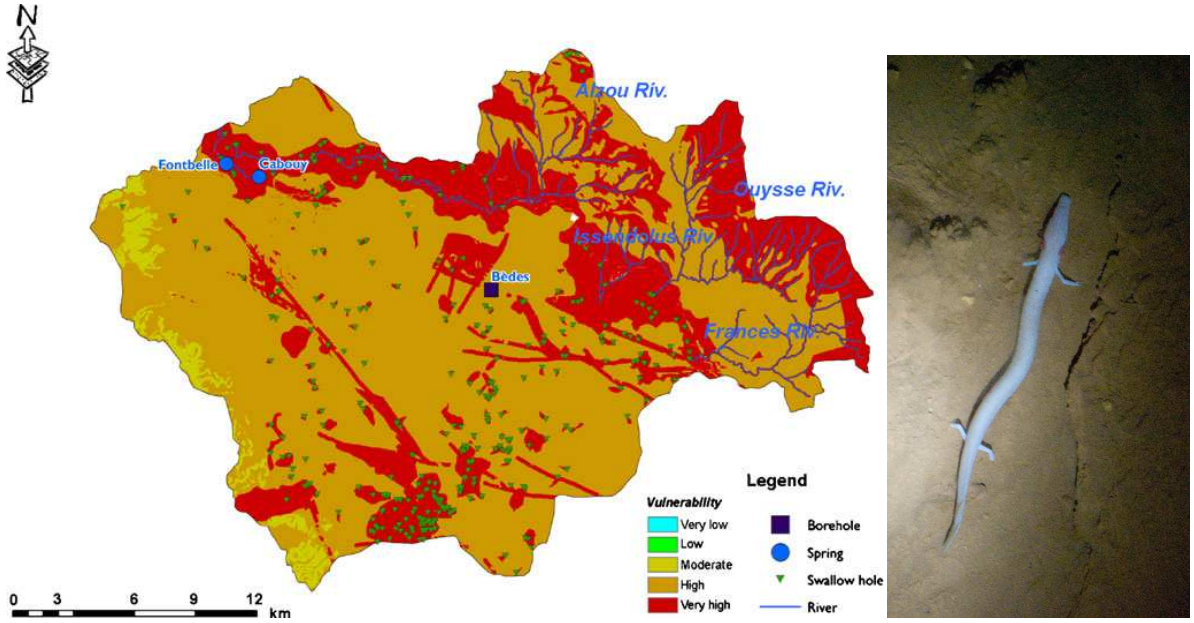

Fig. 5 Left: Intrinsic vulnerability map of the Ouysse karst system (France) evaluated with the PaPRIKa method (Kavouri et al., 2011). **Right:** picture of an Olm in its natural environment. Picture taken by the Wikipedia user Ranko Tomić and is reproduced with permission.

As karst aquifers need to be protected to preserve the quality of their waters from chemical and bacterial contamination, they also need to be protected because of the very rich biodiversity they host. Many troglodyte species have a biotope very limited geographically and are highly dependent of the water quality within the cave. One of the most famous example is the so called human fish or Olm (človeška ribica in Slovenian and Proteus anguinus in Latin) a cave salamander very sensitive to water quality, which is also the biggest vertebrae ever found in cave environment. As its living area is spatially very limited (located only in the northern and central parts of the Dinaric Karst) this animal can be very vulnerable to a potential degradation of the water quality (Pezdirc et al., 2011).

1.3.4 Protection of people and facilities against hazards

Another problem related to the interactions of karst and people arises from the hydrological behaviour of karst aquifers during flood hazards. Due to the large but limited-in-space storage capacity in their conduits, they can be subject to catastrophic flash flood events and cause important destructions of facilities and a high human death toll. This was the case in the city

of Nimes (France) in 1988 where the storage capacity of the karst aquifer was insufficient to buffer the intense precipitations and resulted in the inundation of a large part of the city, killing 9 people and causing more than 600 million Euros of damages (Maréchal et al., 2008). A similar flood event happened in Slovenia in September 2010 and flooded a great part of the country. This was one of the strongest floods reported in the whole history of Slovenia, with rain gauges recording a precipitation return period greater than 100 years in many places (Renko and Iršič-Žibert, 2011). An adapted monitoring system to forecast such hazards and give an alert to people in the right time is then needed (Llasat et al., 2010; Bailly-Comte et al., 2012).

Fig. 6 Example of a seasonal "normal" flood on the catchment of the Ljubljanica River (Slovenia): the Cerknica polje in June 2012 **(a)** and April 2013 **(b)**.

Besides extreme flood events, karst systems are still prone to periodic floods which are not so disastrous for people or facilities, but still prevent an optimal land use. This is the case for the so-called polje, fields which are flooded periodically one or two times per year and create an intermittent lake. Good examples can be found in the catchment of the Ljubljanica River (Slovenia), where the Cerknica and Planina polje are regularly flooded and transformed temporary in lakes (see Fig. 6). This prevents intensive agriculture and settlement development on their surface.

Oppositely to flood forecasting, management of karst waters is a very important issue in areas where (seasonal) hydrological stresses can occur, such as in most of the shoreline of the Mediterranean Sea. Then, a good estimation of the groundwater reserves of the aquifer is fundamental to have an idea of the maximum discharge which can be pumped during drought periods, without a complete depletion of the available resources (e.g. Polomčić et al., 2013).
As presented in this first part, the interactions between karst aquifers and humans are a complex multi-aspects problem, where the characterization and the understanding of the aquifer behaviour are two of the most important points. To do this, several techniques mostly based on comparison between available input and output (e.g. hydrograph and chemograph analysis) can be used (Bakalowicz, 2005; Kresic and Stevanovic, 2010; Pinault et al., 2001). Unfortunately, as only few percents of a karst aquifer is generally mapped (or recovered), there is a lack of methods able to go beyond the gap of the black box approach. Groundwater modelling is such a method and is particularly powerful to improve the general understanding of the aquifer processes, to make forecasting and to lead toward a careful management of the groundwater resources. In the next part a short review of the groundwater modelling techniques in karst aquifers is presented.

2. Groundwater modelling in karst aquifers

2.1 Purposes of groundwater modelling

To start from a first definition, a model is a simplified representation of the reality and can be made for different purposes (Anderson and Woessner, 1992):

(i) in a predictive way: the model is used to predict the future and has to be calibrated (Wagner et al., 2012; Panagopoulos, 2012).

(ii) in an interpretative way: the model is used as framework to study and understand the system dynamics and for aquifer characterization. It does not necessarily need to be calibrated (Ravbar et al., 2011; Mayaud et al., 2013; Wagner et al., 2013). Chapters 2, 3 and Appendix A are following this approach.

(iii) in a generic way: the model is used to analyze the flow in hypothetical systems and does not need to be calibrated (Hubinger and Birk, 2011; Reimann et al., 2011). Chapters 3 and 4 fall beyond this category.

In karst context, all these three different purposes are frequently encountered. To reach them, different types of groundwater models can be applied. The following part presents them concisely.

2.2 Modelling approaches: a short state of the art

After Rehrl and Birk (2010) groundwater models in karst terrains can be divided in two different main categories:

(i) the non-physically based models: these kind of models are also called global models or black-box models. As they are non-physically based, they present the advantage to require only few parameters to be calibrated (see example in Fig.7). Lumped-parameter models enter also in this category and can provide really good results to reproduce spring discharge. These models are recommended to make long term prediction or flood forecasting. For an example in the field of karst sciences, models like GR4J, GR2M (Le Moine et al., 2008; Moussu et al., 2011; Wagner et al., 2013) or Vensim© (Fleury et al., 2007) can be cited. Models using neural networks (Kong-Siou et al., 2011) are also in this category because they are non-physically based. A disadvantage of this modelling approach is that not all physical processes occurring within the karst aquifer (for example the duality between laminar and turbulent flow and the location of the conduits) are taken into account due to the few input parameters required by the models. Nevertheless, this approach can provide relevant results for aquifer characterization under certain circumstances. As an example, the use of a lumped-parameter model in a binary karst aquifer is presented in the Appendix A of this thesis (Wagner et al., 2013). In this paper, the authors use the GR2M model and are able to recognize that a change in the hydrological behaviour of a well investigated karst system was due to a change happening within the karst aquifer itself rather than a change happening outside of it. The role of sediment dynamics in the cave is pointed out to explain the change of hydrological behaviour of the karst system, rejecting then a change of meteorological conditions or of land use.

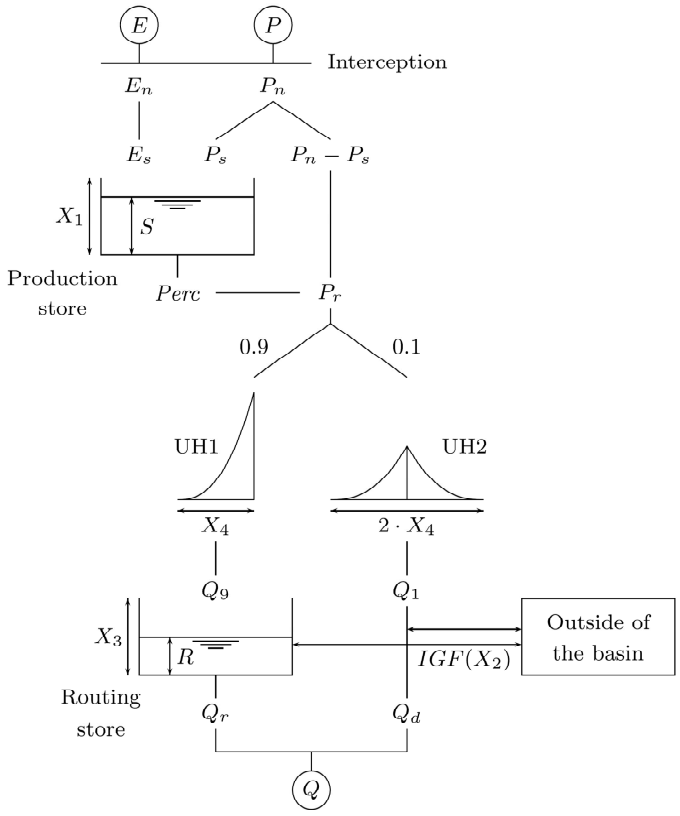

Fig. 7 Schematic representation of a lumped-parameter model (taken after Le Moine et al., 2008): the GR4J model (modèle hydrologique du Génie Rural à 4 paramètres au pas de temps Journalier).

(ii) oppositely, the physically based models try to approach the reality taking into account the most important physical and geometrical characteristics of the system. They first need the definition of a grid and the attribution of parameters values (e.g. hydraulic conductivity, specific storage) for each single element constituting it. The shape of the grid can be composed either of rectangular elements (finite differences), of elements of different shape (in this case the term finite elements is used) or of volumes of different form (finite volumes). Then, the groundwater equation is applied and solved numerically at each node of the whole grid and the groundwater flow field is computed. Software like MODFLOW (Harbaugh, 2005) FEFLOW (DHI-WASY GmbH, 2011) or MIKE SHE (Denmark Hydrology Institute, 2007) can be cited. These models are also called distributives models and are most frequently used for aquifer characterization (the interpretative and generic way fall in this category). Their great advantage is that they are able to integrate a particular feature present in the real system (like a karst conduit). Unfortunately, this can be also a disadvantage because a lot of information and field parameters which are frequently unknown or unavailable are needed as input. This complex implementation can lead to a higher computational effort than the lumped-parameter model approach.

A classification of the different types of distributed models frequently used in karst groundwater modelling was done by Teutsch and Sauter (1991) and by Sauter et al. (2006), and is described in the following (Fig. 8).

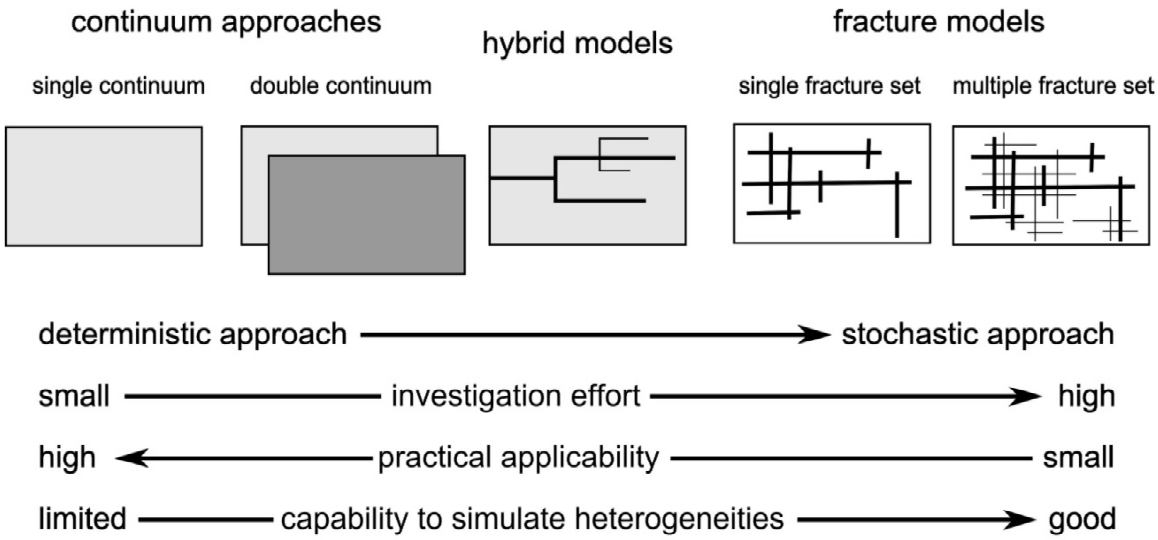

Fig. 8 The five different approaches used for distributive modelling in karst areas (taken from Reimann, 2012 according to Teutsch and Sauter, 1991).

The single and multiple fracture sets belong to the fracture models, and consist to represent a 1-D single or multiple fracture set within a low permeable matrix (Berkowitz, 2002). Flow and transport processes are only happening through the factures, following laminar or turbulent flow regimes. Due to the high number of parameters they require for their implementation, the practical applicability of those approaches is limited.

The hybrid model approach is one of the most frequently used in basic research for karst aquifer modelling. It combines a laminar matrix with a discretized conduit network where the flow in the conduits can be laminar or turbulent depending on the value of the Reynolds number. The flow exchange between the matrix and the conduit network is implemented by a lumped-parameter, which uses the head difference in the matrix and the conduit system. As example the works of Liedl et al. (2003) or Thrailkill (1974) can be cited. Until know, hybrid models were mostly used to apply the "generic" approach presented above and only a few studies applied them to real karst systems (Gallegos et al., 2013; Hill et al., 2010; Saller et al., 2013).

The double continuum approach combines two continuums together representing the matrix and the conduit system. This approach is able to consider laminar matrix flow and turbulent conduit flow. The two systems are connected via a linear exchange term (Sauter, 1992).

Finally, the single-continuum (or equivalent porous medium) approach is directly derived from conventional groundwater modelling in porous medias. This is the simplest of the five approaches, as it considers the whole karst system as a continuum and defines the hydrological heterogeneities (such as the karst matrix and the conduits) by creating contrast in hydraulic conductivity between them (Fig. 9a). Due to its really simple assumptions and easy implementation, this is the most frequently used approach for karst aquifer modelling of real systems. This type of model can be used either for prediction and groundwater management if the karst aquifer has boreholes or just simply as interpretative to understand the processes happening within the aquifer. As application examples, the papers of Budge et al. (2009), Mayaud et al. (2013, 2014 in press); Panagopoulos (2012), Polomčić et al. (2013), Ravbar et al. (2011), Scanlon et al. (2003) and Worthington (2009) can be cited.

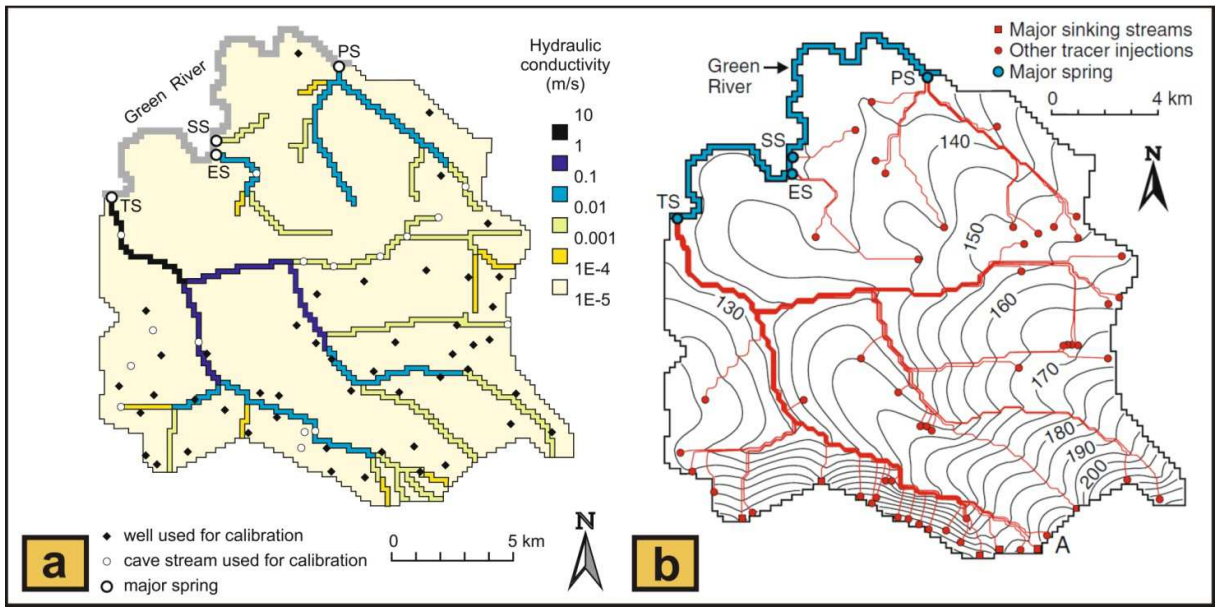

Fig.9 (a) Hydraulic conductivity contrasts between the matrix and the karst conduit in the Mammoth cave aquifer. **(b)** Computed water table and flow direction of the same area. This model was implemented with MODFLOW 96 in steady-state under laminar flow conditions (figure modified after Worthington, 2009).

Nevertheless, the single-continuum approach presents limitations compared to the other approaches. For example, the definition of the heterogeneities characterizing a given karst aquifer can be misled due to a lack of available field data (e.g. boreholes or conduit location). Moreover, those models were until recently only able to compute the groundwater flow field under laminar flow conditions, which was a strong limitation of their use (Worthington, 2009). Yet three MODFLOW packages allowing the computation of non-linear or turbulent flow with single-continuum models were recently developed (Mayaud et al., under review; Reimann et al., 2012; Shoemaker et al., 2008). One of these packages (Reimann et al., 2012) showed for a basic karst setting than single-continuum models considering turbulent flow are able to reproduce the same behaviour than hybrid models. This result is a strong argument in favor of the use of single-continuum models for karst aquifer modelling. Finally, the last developed package (Mayaud et al., under review) considers the implementation of the Forchheimer equation in MODFLOW and is presented in Chapter 4 of this work.

2.3 Purpose of this thesis

As the single-continuum approach is the most employed in research and by private companies, one important question concerns the relevance of its use instead of the use of a hybrid model or a fracture model, which both reproduce the flow processes occurring in karst aquifers more accurately. This PhD thesis has the purpose to investigate how far the single-continuum approach can be used for karst aquifer modelling, and to which extent it is able to reproduce the natural processes observed in real systems.

Therefore, the applicability of single-continuum models to reproduce the observed flow processes in real karst catchments will be investigated with practical field examples in Chapters 2 and 3.

Finally, Chapter 4 will introduce a new MODFLOW package allowing the simulation of non-linear flow within single-continuum models. First, the theory beyond the programming of the Forchheimer equation in MODFLOW is introduced, and then three benchmark models demonstrating the validity of the concept are presented. To check the ability of the package to compute non-linear flow in real karst systems, a more realistic example was directly taken from Chapter 2 will be shown.

CHAPTER II

UNDERSTANDING CHANGES IN THE HYDROLOGICAL BEHAVIOUR WITHIN A KARST AQUIFER (LURBACH SYSTEM, AUSTRIA)

Published in Carbonates and Evaporites as: *Mayaud et al., 2013. Understanding changes in the hydrological behaviour within a karst aquifer (Lurbach system, Austria). Carbonate Evaporite. doi: 10.1007/s13146-013-0172-3*

Abstract

A thorough data analysis combined with groundwater modelling was conducted in an Austrian binary karst aquifer to better understand changes in the hydrological behaviour observed at a karst spring. During a period of four years after a major flood event the spring hydrograph appears to be more damped with lower peak flow and higher baseflow than in the years before. The analysis of the hydrograph recession suggests that the observed hydrological change is caused by changes within the karst system rather than by varying hydro-meteorological conditions. The functioning of the aquifer and potential causes of the observed changes are further examined using the groundwater flow model MODFLOW. The simulation results suggest that a modification of hydraulic conductivity and storage within the conduit network, e.g. due to the plugging of the drainage conduits with sediments, may be the cause of the different behaviour. MODFLOW was able to reproduce the observed dynamics of spring flow, although it does not account for turbulent flow within karst conduits. Using a simplified model scenario it is demonstrated that the damping of the hydrograph is much stronger if turbulent conduit flow is taken into account. Thus, a turbulent flow model is needed to assess potential changes in the storage properties quantitatively.

Keywords: Binary karst aquifer - MODFLOW - Single-continuum model - Groundwater modelling - Laminar/turbulent flow - Hydrological behaviour

1. Introduction

Karst waters represent an important part of the water supply for the world's population (20-25%; Ford and Williams, 2007) but are known for their high vulnerability to chemical and bacterial contamination (e.g. Heinz et al., 2009) due to the pressure of urbanization and intensive agricultural use. To assess how changes within karst areas might influence the behaviour of karst springs a sound understanding of processes which govern flow through karst aquifers is needed. This work examines the hydrological behaviour of the Hammerbach karst spring in Austria, which appears to have changed after a storm event in August 2005. The purpose here is to improve our general understanding of flow processes within karst aquifers and especially to identify potential causes of the observed change within this spring catchment. To this end, hydrograph data from the karst spring are analysed and interpreted based on the existing knowledge from earlier investigations to develop a simplified conceptual aquifer model. The functioning of the aquifer and potential causes of the different changes in the hydrological behaviour are further examined using a process-based numerical groundwater flow model.

2. Field site

The investigation area is a binary karst system of 23 km^2 named Lurbach system and located in the Central Styrian Karst (Fig. 1a), about 20 km north of Graz (Styria, Austria). The upper part of the catchment is a 15 km^2 wide area of low permeable rocks (comprising mainly Quaternary sediments and Paleozoic schists), and is drained by the Lurbach stream in an East-West direction towards the Tanneben massif, a highly karstified limestone block with a sub-catchment size of 8 km^2. After the Lurbach stream reaches the limestone unit, it infiltrates along the streambed and finally disappears into a major sinkhole located some tens of meters behind the entrance of a big cave, the Lurgrotte (located at 633 m a.s.l.). Then, the water flows through the fissures and conduits of the limestone massif and resurges at the Schmelzbach outlet and the Hammerbach spring, which are both located at the western border of the catchment, at the foot of a 300 m high cliff called Peggauer Wand. The highest point within the catchment is the Fragnerberg in the North (1109 m a.s.l.; Fig. 1b) and the lowest is at the level of the Mur River (~400 m a.s.l.) at its western edge where the Hammerbach spring originates. The town of Semriach (709 m a.s.l.) is the main settlement in the area.

The Lurbach system is equipped with a measurement network well adapted to understand the karst processes. The discharge is measured at the Hammerbach spring and Schmelzbach outlet as well as the Lurbach prior to its disappearance into the ground: one gauge is located at the contact between the schists and the limestone and another one just in front of the Lurgrotte cave (Fig. 1c). However, not all of the measurement devices are operative at all times, mainly due to maintenance after flood events or general financial restrictions. As the Hammerbach discharge data are available on a continuous basis, it will be the focus of the modelling attempts presented below.

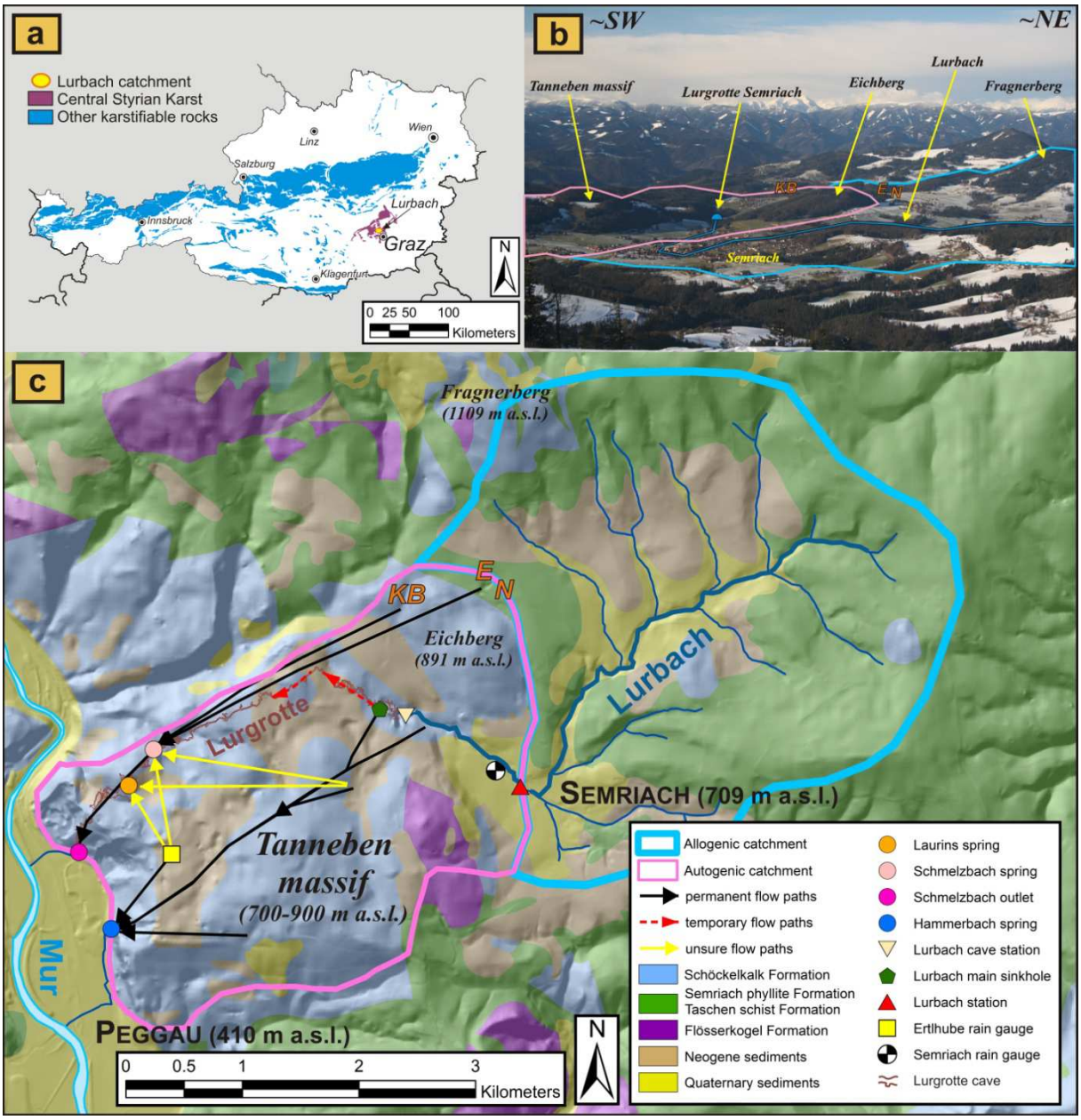

Fig. 1 Field site location. **(a)** Map showing the location of the Lurbach system in relation to the distribution of karst rocks in Austria (modified after Schubert, 2003); **(b)** View of the upper Lurbach catchment and the karstified area (the blue and pink polygons, respectively) taken from the summit of the Schöckl mountain (1445 m a.s.l.). Photo: M.Schneider & C.Aistleitner (used with permission); **(c)** Simplified geological map (modified after Geologische Bundesanstalt, 2005; Blatt 164-Graz) of the Lurbach catchment including the different subsurface flow paths (black, red and yellow arrows) inferred from results of tracer tests (the unsure flow paths were determined during a single tracer experiment with injection on top of the unsaturated zone and small recovery rates; Behrens et al., 1992), the measurement network and three minor sinkholes supplying the Schmelzbach spring (E = Eisgrube, N = Neudorferschwinde and KB = Katzenbachschwinde, respectively). The low permeable part (blue polygon) corresponds to the topographic catchment whereas the highly karstified part (pink polygon) was delineated taking into account results of tracers experiments. The boundary between the allogenic and the autogenic unit is based on the geological map.

Six rain gauges are located in the vicinity of the catchment and provide rainfall data (only the Ertlhube and Semriach rain gauges are visible in Fig. 1c). Temperature data are collected at a meteorological station located close to the Lurbach system, on the western side of the Mur valley (at an altitude of 610 m a.s.l.). Unfortunately, no water table data are available within

the limestone massif. Moreover, the conduit system draining towards the Hammerbach is not yet explored, as all attempts to access it failed up to the present. However, the Lurgrotte cave itself is a well explored partly water-active multi-level cave (e.g. Wagner et al., 2011) and shows relevant indications for the vadose/phreatic conditions inside parts of the Tanneben massif (Fig. 1c). Besides this, there are numerous other caves known in this region (more than 200 in the Tanneben massif). Yet their extents are rather small and they are generally plugged with sediments or collapse material preventing further exploration inside of the karst massif.

The Lurbach system is under a climate regime with low winter precipitation and is subject to heavy thunderstorm events during the summer (Harum and Stadler, 1992). The mean annual precipitation measured between 1965 and 2011 is 880 mm. The maximum precipitation value recorded in one day was 93.5 mm during the summer of 1975.

The subsurface drainage pattern of the Lurbach system changes depending on the hydrological conditions (Harum and Stadler, 1992):

(i) at low water conditions, the Lurbach discharge becomes very small and sometimes intermittent (the minimum discharge measured at the Lurbach station is ~5-10 l/s) along the streambed between the upstream gauge of the Lurbach and the cave entrance (some sinkholes become visible along the stream bank). Then, the Hammerbach and Schmelzbach systems are totally separated, significantly fed by infiltration of the autogenic waters of the Tanneben massif and by a small cave-spring called Laurins spring (see in Fig. 1c) for the Schmelzbach.

(ii) at normal water conditions, the Lurbach disappears into the Lurgrotte and resurges mainly at the Hammerbach spring, whereas the Schmelzbach is only supplied by the autogenic recharge through the Tanneben massif, by the Laurins spring, and by three small sinkholes (E, N and KB; Fig. 1b&c) located in the NE boundary of the karstified area.

(iii) at medium to high water conditions, an overflow from the Hammerbach system to the Schmelzbach system is observed. Harum and Stadler (1992) showed that when the Hammerbach spring discharge increases to more than ~200 l/s, a part of the Lurbach water flows towards the Schmelzbach system.

(iv) at flood conditions the Lurbach is subject to catastrophic flood events (the maximum discharge measured at the Lurbach station exceeded 10 m^3/s) and the Lurgrotte cave system itself acts as the main drainage system (Fig. 1c). Then the Hammerbach system cannot drain more than ~2 m^3/s, whereas the Schmelzbach outlet receives the most part of the Lurbach water and can reach peak discharges up to 10 m^3/s and more. These flash floods caused sometimes the outage of measurement devices at the Schmelzbach outlet and within the active accessible cave stream. Then, redistribution of sediments and plugging of sinkholes and cave passages are regularly reported (Harum and Stadler 1992, p. 39).

3. Data analysis

The Hammerbach spring hydrograph between 1998 and 2010 (Fig. 2a) exhibits a changed behaviour after a major flood event in August 2005. From then onward, the spring response appears to be more damped and the peak discharge did not exceed 400 l/s over a period of about 4 years. Moreover, the baseflow appears to have increased. In contrast, precipitation appeared to be rather unchanged. Unfortunately, there is not enough discharge data of the Schmelzbach spring to identify potential changes in its discharge behaviour. Since June 2009, several floods due to intense storm events indicate that the Hammerbach has recovered to its previous flashy behaviour.

When plotting cumulative frequency curves of 3-year periods of the Hammerbach discharge from 1965 to 2010 (Fig. 2b) the curve from 2006 to 2008 (the bold solid black line) reveals a rather damped discharge behaviour with a lower maximum and a higher minimum compared to the other curves. If the year 2009 is included in the curve from the previous 3 years, the resulting bold dashed black curve is more similar to the curves prior to 2005. This observation confirms that the hydrological behaviour of the Hammerbach spring from 2006 to 2008 differs from that of the years before and after that time period.

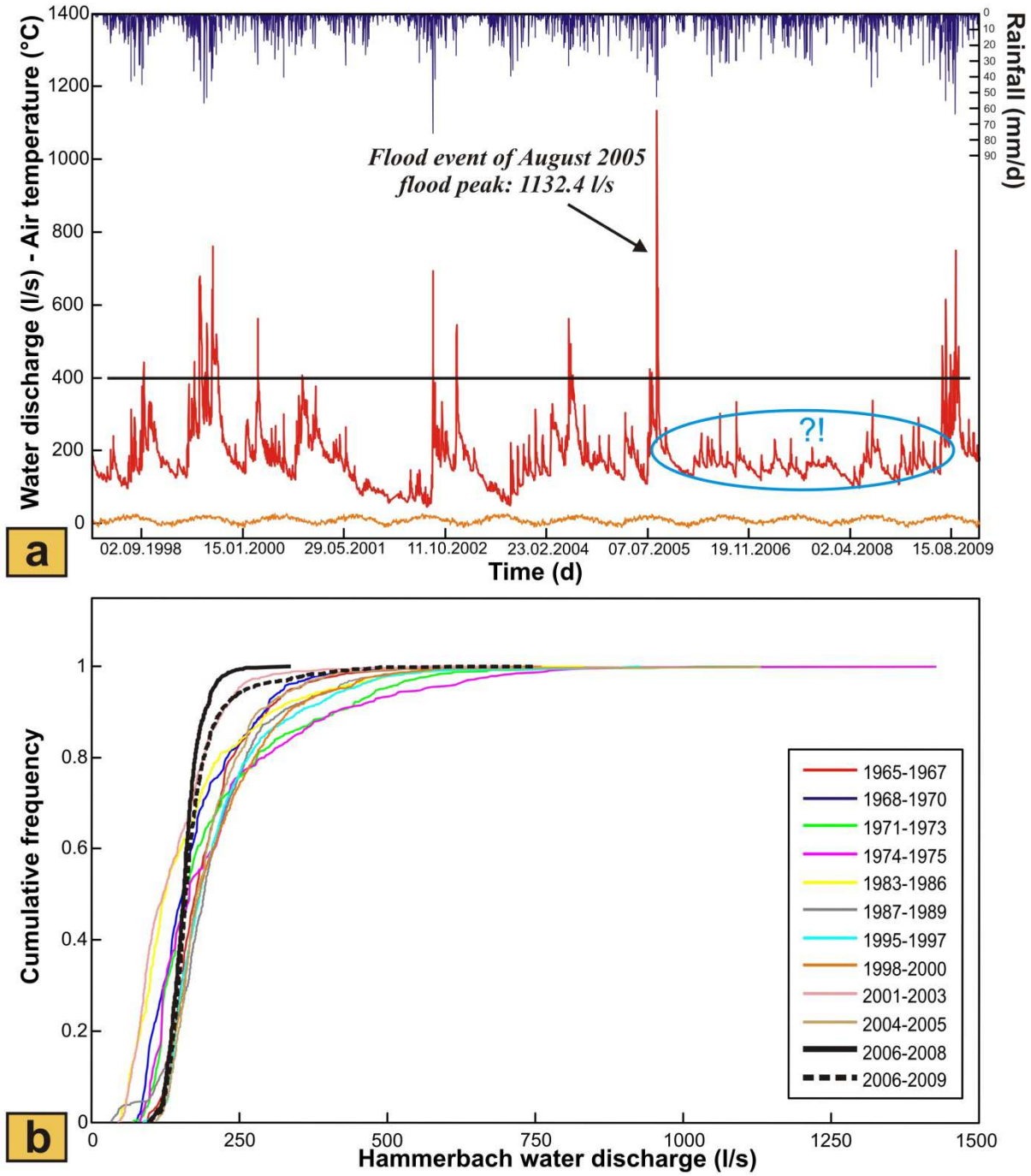

Fig. 2 Hammerbach spring data. **(a)** Hammerbach daily discharge (red line), precipitation (blue bars) and air temperature (orange line) data from 1998 to 2010. Black line: discharge of 400 l/s, blue circle: changed behaviour from August 2005 to June 2009. Precipitation data are the computed average of the six stations located in the region; the temperature data are taken from a station located on the western side of the Mur valley; **(b)** Cumulative frequency curves of the Hammerbach discharge from 1965 to 2010. The bold solid black line represents the changed behaviour between 2006 and end 2008, whereas the bold dashed black curve represents the period from 2006 to 2009 including the return to the previous drainage behaviour of the Hammerbach spring.

The Hammerbach master recession curves shown in Fig. 3 confirm the hypothesis of a different hydrological behaviour between August 2005 and June 2009. The recession behaviour of the period 1965-2005 is clearly different from that of the period 2005-2008. The return to the pre-2005 behaviour is illustrated by the violet curve from 2005 to 2009, which is

closer to the recession curves from 1965 to 2005. The same result was found when master recession curves of 3-year periods between 1965 and 2005 were compared to that of the period 2005-2008. This is shown in the inset of Fig. 3, where a similar trend is observable when looking at the exponent and the coefficient of a power law fit of the master recession curves of 3-year periods before 2005, whereas the period between 2006 and 2009 (surrounded by the red circle) is clearly different. As master recessions curves provide information about the aquifer structure (Kresic and Bonacci, 2010, p. 134), these results suggest that the observed hydrological change is caused by changes within the binary karst catchment rather than by varying meteorological conditions. Since we are also not aware of any significant changes in land use, deforestation and/or housing, which may potentially have influenced the flow regime of the Lurbach stream in the upper part of the catchment, it is an obvious idea to assume that changes occurred within the karst aquifer of the Tanneben massif. Although a sediment barrage in the Lurbach stream is dredged from time to time where some sinkholes are reported, it appears unlikely that this may have caused a change in the hydrological behaviour over a period of 4 years.

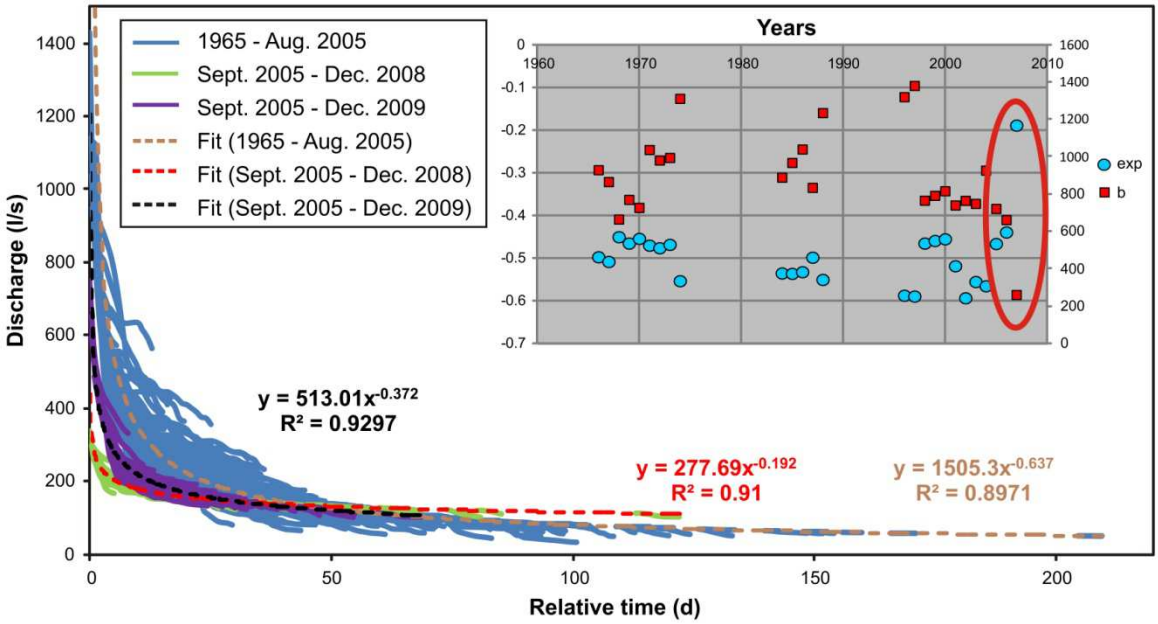

Fig. 3 Master recession curves of the Hammerbach between 1965 and 2010. The changed recession behaviour within the period from 2005 to 2009 is evident. Inset: coefficient and exponent of a power law fit of the master recession curves for time periods of three years. The change after 2005 is highlighted by the jump of the constant and exponent. Master recession curves were computed with the method according to Posavec et al. (2006).

A possible explanation of the observed hydrological change is a change in the karst drainage system due to the flood event of August 2005. Potentially an aggradation of sediments in the Hammerbach conduit network caused a decrease of the hydraulic conductivity and/or changes in the storage properties. This is a plausible process, as sediment redistributions are common in karst aquifers (e.g. Farrant and Smart, 2011) and are noticed regularly in the accessible parts of the cave system after stronger rainfall events (Kübeck et al., 2013). The apparent return to the former behaviour may be explained by the re-excavation of the sediments previously plugging conduit sections during the major storm events of summer 2009. Results

from a tracer experiment in December 2008 (Oswald, 2009) further indicate that the above-mentioned overflow from the Hammerbach system to the Schmelzbach may occur at a lower Hammerbach discharge than earlier reported by Harum and Stadler (1992). In addition, the transit times for this particular tracer experiment were almost 60 hours (Oswald, 2009), whereas tracer experiments conducted prior to August 2005 show transit times of less than 40 hours at comparable discharge rates (Behrens et al., 1992). This too might be explained by the plugging of infiltration sinkholes and flow paths by sediments or tree lumps, caused by the major flood event of August 2005.

4. Modelling

Karst aquifers are known for their large but organized heterogeneities, which can be conceptualized as a dual flow system consisting of a highly conductive network of solution conduits that is embedded in the less conductive fissured carbonate rock (e.g. Kiraly, 1998). These dual flow characteristics are responsible for intrinsic difficulties in modelling groundwater flow in karst terrains. An overview of modelling approaches that have been proposed to overcome these difficulties is provided by Rehrl and Birk (2010). One approach frequently employed for generic investigations into flow and transport processes in karst aquifers are hybrid models, which couple a pipe flow model representing the network of solution conduits to a continuum model representing the fissured rock (Teutsch and Sauter, 1991). Applying hybrid models to real karst aquifers, however, is highly challenging, since adequate information about the geometric and hydraulic properties of the conduit system are rarely available. Therefore, single-continuum groundwater flow models such as MODFLOW (Harbaugh et al., 2000) are frequently employed for these purposes (e.g. Ravbar et al., 2011; Worthington, 2009). The flow calculation in this type of model typically is based on Darcy's law, thus assuming only laminar flow conditions. Reimann et al. (2011) demonstrated that spring hydrographs simulated with MODFLOW may differ significantly from those obtained with a hybrid model that accounts for turbulent flow in solution conduits. Yet results obtained with an extension to MODFLOW that accounts for turbulent flow were found to be in agreement with those from the hybrid model. In this work MODFLOW is employed considering first only laminar flow. Subsequently, it is attempted to apply a recently developed turbulent-flow package for MODFLOW (Shoemaker et al., 2008).

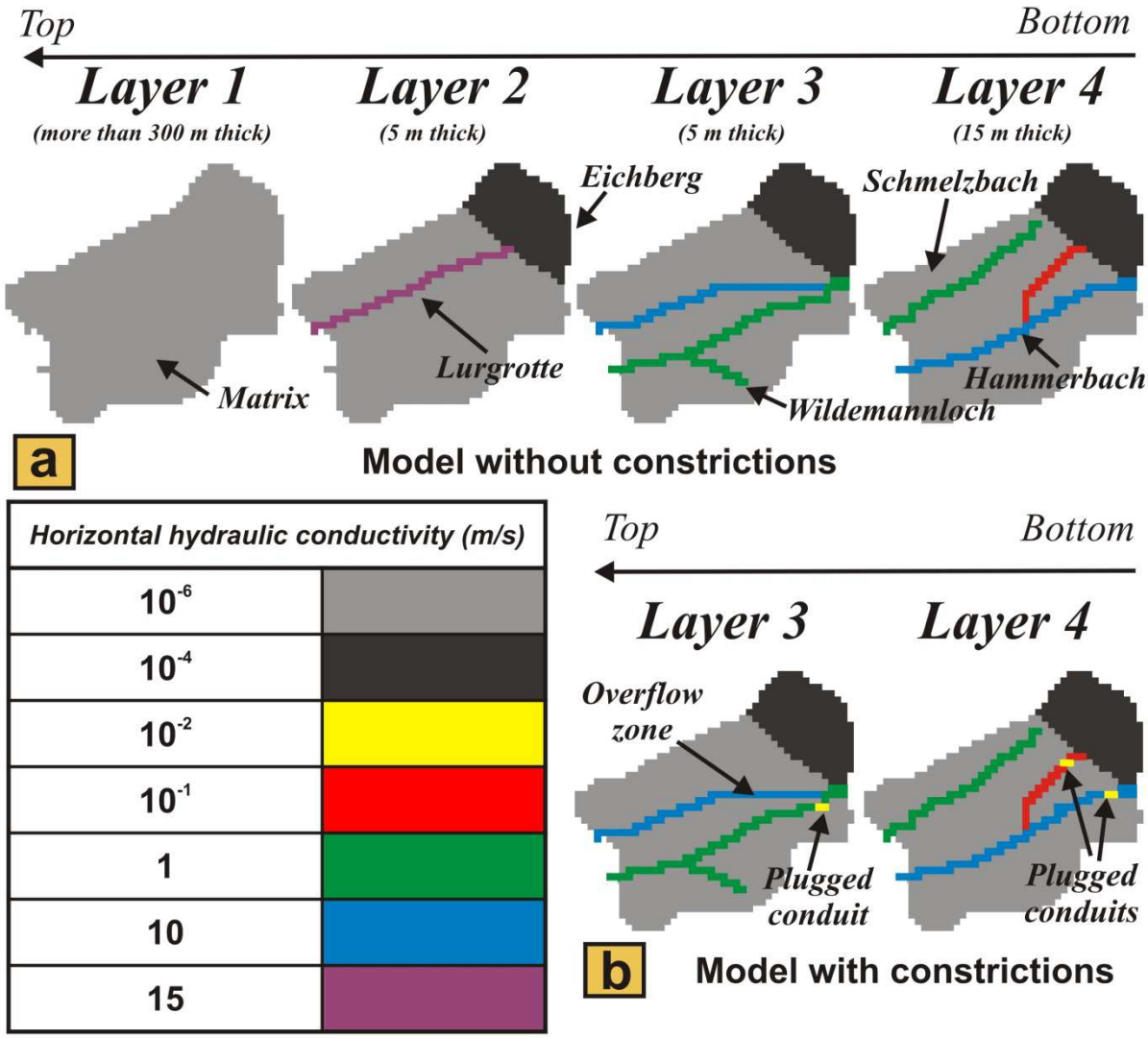

Fig. 4 Model setup. Comparison of the horizontal hydraulic conductivities and the geometry between the model without constrictions **(a)** and the model with constrictions **(b)**. The plugged conduits are represented in yellow in **(b)**. With these two model setups it is attempted to reproduce the pre-event 4a and post-event 4b drainage behaviour of the Lurbach system. The specific storage of the matrix was set to 10^{-5} m^{-1} for the two models whereas it was given 0 in the conduit for the unplugged case and 0.5 m^{-1} to the constrictions of the plugged case. The vertical conductivity was set to 10^{-4} m/s for the whole model range, except where the Lurbach allogenic input is added, where a high value of 10 m/s was defined in order to simulate the sinkholes.

4.1 Laminar flow

The design of the numerical model is based on the conceptual understanding of the Lurbach system described above. The model is a simplified Lurbach system representing only the autogenic sub-catchment and consists of four layers that differ in thickness and horizontal hydraulic conductivity (Fig. 4a) to capture the complexity of the multi-level cave system. The catchment is made up of a low conductivity matrix (light grey and dark grey in Fig.4) whereas the highly conductive flow paths introduced in the layer 2 to 4 represent the Lurgrotte cave and the assumed Hammerbach conduit system. The structure of the conduit system was designed to account for the behaviour of the Lurbach system described in Harum and Stadler (1992): during low water conditions the lower layer (layer 4) drains most of the allogenic

recharge and both Hammerbach and Schmelzbach systems are separated. When the allogenic input rises above the drainage capacity of the layer 4, the layer 3 begins to drain and the overflow towards the Schmelzbach aquifer is activated. The layer 2 becomes prominent during strong storm events and allows water to flow through the upper levels of the Lurgrotte cave system (see Kübeck et al., 2013). The uppermost layer represents the more than 300 m thick karst matrix of the Tanneben massif which might serve as further storage component if extreme floods are considered (high historical floods reported in Benischke et al. (1994) indicate that part of the Semriach basin was flooded in 1812 and 1827).

Three steady-state model scenarios were designed using autogenic recharge based on the formula of Turc (e.g. Gray, 1970), the minimum, mean and maximum annual precipitation depths, respectively, and a mean annual air temperature (7.4°C) reported in Harum and Stadler (1992). Correspondingly, the lowest, mean and highest Lurbach discharges reported by Harum and Stadler (1992) were used as concentrated allogenic recharge. The allogenic recharge was given as localised input where the Hammerbach and Schmelzbach conduits begin (at the border between the Eichberg zone and the matrix zone in Fig 4) and along the Lurbach riverbed with emphasis on the conduits draining the Hammerbach system. The autogenic recharge was given as a constant flux rate (in m/s) within the entire model domain. The three steady-state models were calibrated to the lowest, mean and highest discharges at the Hammerbach spring and Schmelzbach outlet by adjusting the hydraulic conductivity of the low-permeability matrix and the highly conductive flow paths. These simulations gave reasonable results (Mayaud, 2010) and confidence into the model setup, especially concerning the aforementioned intercatchment flow and its dependence on the hydrological conditions. The resulting model was subsequently employed for transient simulations to reproduce the Hammerbach spring hydrograph of the flood event of August 2005 (Fig. 2a). This event was chosen because of its nearly undisturbed long-term recession, because the discharge peak reached almost the Hammerbach filling capacity, and because it is likely the last strong event prior to the change in the system behaviour. Unfortunately no Lurbach data is available for this period. Thus, only the autogenic recharge was computed using daily precipitation data minus 50% evaporation rate, whereas the concentrated allogenic recharge component was adjusted in the model calibration. For the transient simulations the specific yield of the matrix was set to 0.01 in the whole unconfined aquifer whereas the specific storage was defined as 0 in the conduits and 10^{-5} m^{-1} in the matrix.

Fig. 5 shows the simulated (dashed red line) compared to the measured (solid blue line) discharge of the Hammerbach. The simulation matches the observed discharge behaviour reasonably well and makes the assumptions of the model setup a plausible option (admittedly not the only one). To examine potential effects of sediment aggradations that may have caused the plugging of conduits within the Hammerbach system the hydraulic conductivity of some conduit cells was lowered (see Fig. 4b). The resulting flow constrictions cause an increase of the water table and of the hydraulic gradient within the conduits, thus forcing more water to flow towards the Schmelzbach network. As a consequence the Hammerbach peak discharge is lower in these scenarios compared to the scenario without constriction (Fig. 5). This is qualitatively similar to the behaviour of the Hammerbach spring hydrograph after the flood event of August 2005 (Fig. 2a). It is evident that the constricted conduit sections prevent a

part of the Lurbach water from flowing immediately towards the Hammerbach spring. Thus, the water flows more frequently towards the Schmelzbach drainage network and explains the damped discharge behaviour presented in the previous paragraphs. This is in accordance with a tracer experiment in 2008 where overflow to the Schmelzbach system was already observed at ~135 l/s (Oswald, 2009) compared to the previously reported threshold of ~200 l/s (Behrens et al., 1992).

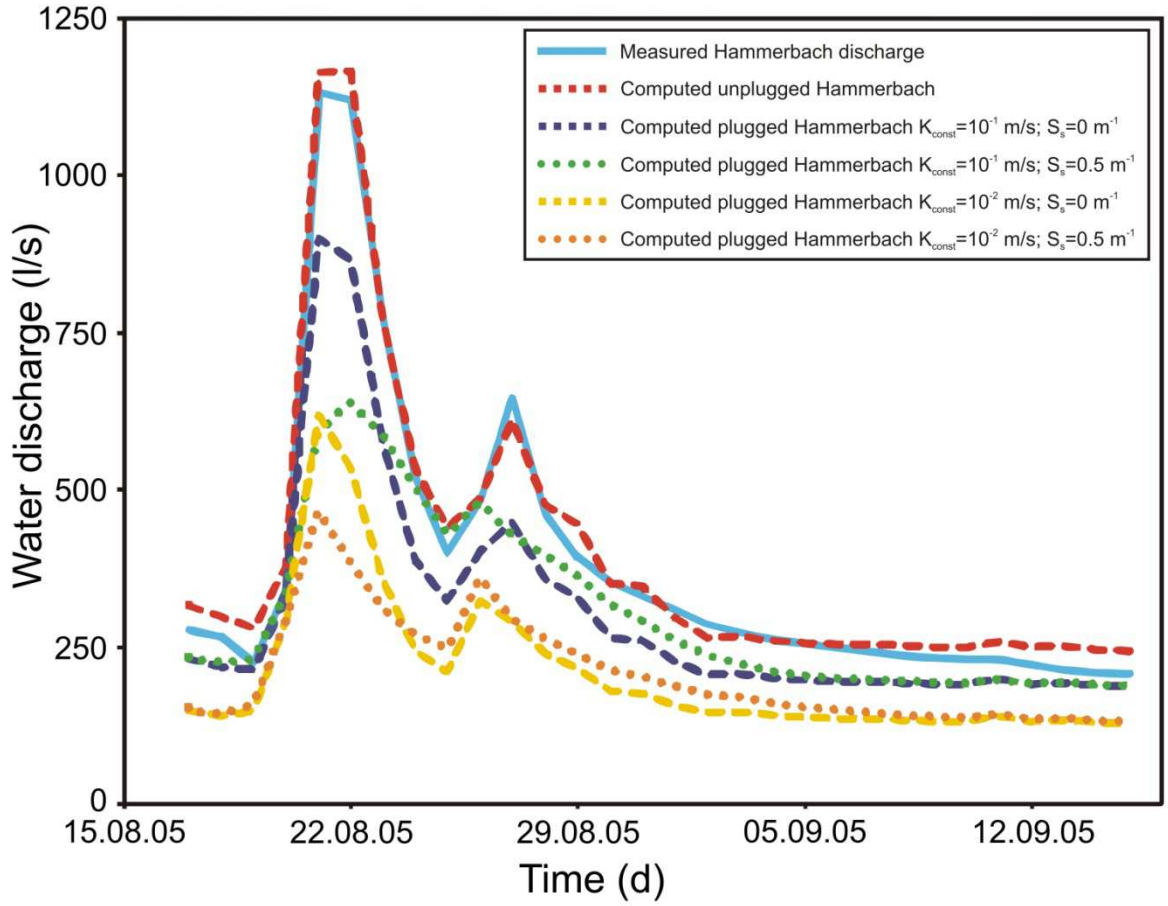

Fig. 5 Measured and simulated Hammerbach discharge for the flood event of August 2005 without and with constrictions and sediment storage in the conduit network (see the location of constrictions in Fig. 4b). The violet curve represents the discharge when constrictions with hydraulic conductivity of 10^{-1} m/s are assigned, the yellow curve when constrictions with hydraulic conductivity of 10^{-2} m/s are assigned. The green and orange curves represent the response when a high specific storage value of 0.5 m^{-1} (compared to the value of 0 given for the previous cases) is given to the constrictions.

However, the observed increase in the baseflow is not reproduced by the simple assumption of constrictions with lower hydraulic conductivity. A potential explanation to this increase is that the aggradation of the sediments may not only have changed the hydraulic conductivity but also the storage properties of the Hammerbach aquifer. To examine if changes of the storage properties related to the sediments in the constrictions may have caused the increase of the baseflow observed after the major flood event in 2005, a simple hypothesis was considered by assigning high values of storativity to the conduit constriction (storativity was set to zero before). Results are presented in Fig. 5 (dotted green and orange lines) and show that the baseflow of the Hammerbach is increased if the storativity in the constriction is

increased. Then, the peak flow is more damped compared to the scenarios without change in the storativity. Thus changes in the storativity might account for the second observed characteristic of the Hammerbach behaviour between August 2005 and June 2009.

4.2 Turbulent flow

As flow in such a mature karst aquifer is likely to be locally (i.e., in the karst conduits) turbulent, it was an obvious objective to integrate turbulent flow into the modelling approach. The program used for this purpose was the Conduit Flow Process (CFP) for MODFLOW developed by Shoemaker et al. (2008). Only a simplified one-layer model was realized with CFP due to convergence problems; more complex multi-level models are subject of ongoing modelling attempts. The geometry of the model aquifer had to remain simple and comprised only a square catchment with one conduit representing the Hammerbach system (see Fig. 6a). The spring response to an artificial event was computed taking into account turbulent flow and compared with a standard MODFLOW approach (laminar flow only). The results (Fig. 6b) show an agreement with the previous results of Fig. 5 with an increase of the baseflow correlated to an increase of the storativity in the constrictions. It is important to note that the damping is much stronger in the model scenarios that account for turbulent conduit flow than in those ignoring turbulent flow, which is in accordance with the findings by Reimann et al. (2011). These authors showed that the hydraulic gradient in the conduits is higher if turbulent flow is taken into account. As a result, the conduit hydraulic heads are higher in the model accounting for turbulent flow than in a purely laminar flow model. Thus, flow from the matrix to the conduit is more strongly reduced in the turbulent flow model, which causes an increase of storage in the fissured matrix that is not considered in the laminar model. Therefore, turbulent flow needs to be considered to be able to quantitatively assess storage effects in such a karst system.

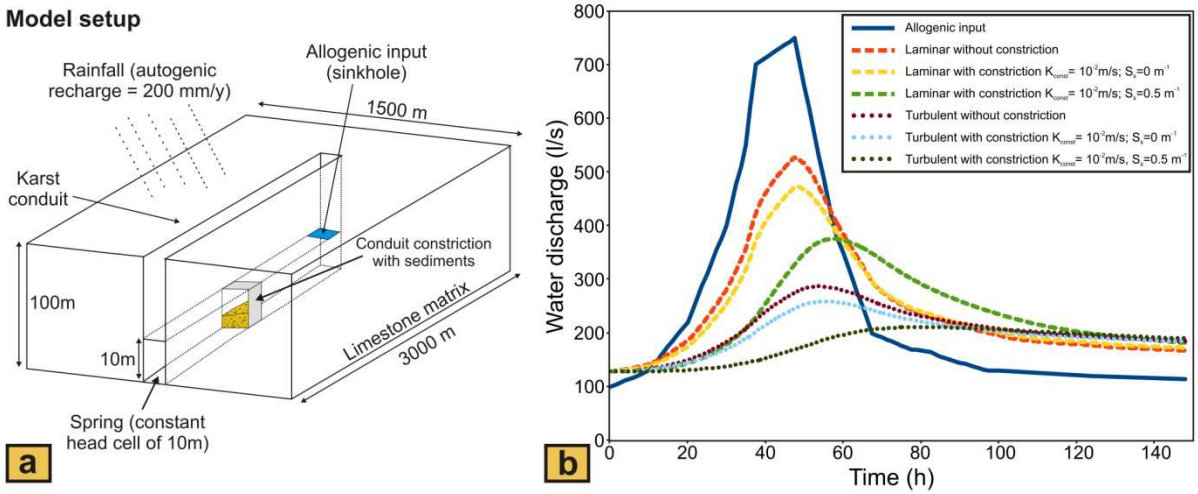

Fig. 6 Comparison of laminar and turbulent flow conditions of the simplified model setup. **(a)** Model setup including the geometrical assumptions and the boundary conditions. **(b)** Changes in spring discharge considering and neglecting turbulent flow conditions within the conduit. Moreover, the influence of constrictions within the conduit is considered by changing conductivity and specific storage of the constriction. The red, yellow and green dashed curves are the responses neglecting turbulent flow whereas the dotted purple, light-blue and dark-green curves represent the spring responses taking turbulent flow into consideration.

5. Discussion

A change of hydrological behaviour was observed at the Hammerbach spring during a period of nearly 4 years. This change resulted in a damped behaviour of the peak flow combined with an increase in the baseflow. The analysis of discharge data using cumulative frequency and master recession curves combined with previously reported tracer experiment results suggest that the change is caused by processes within the karst system rather than by climatic and/or anthropogenic factors. Based on field investigations it is suggested that sediments may constrict and/or plug karstic conduits and lead to the damped discharge behaviour observed at the spring. A simplified distributive groundwater model was built based on the current conceptual understanding of the system in order to investigate if conduit constrictions and sediment plugging in karstic conduits may cause changes in the spring response similar to those identified from the field observations. The simulation results are in accordance with the aforementioned hypotheses: the modification of the hydraulic conductivity and the specific storage in the karstic conduit led to a more damped discharge at the spring.

It should be noted, however, that the design and calibration of the groundwater model is highly non-unique because of the scarcity of data. Thus, the model should be viewed as an interpretative (Anderson and Woessner, 1992, p.4) model that is aimed at improving the conceptual understanding of the hydrogeological system at the field site but not as a predictive model. For the latter purpose, a parsimonious lumped-parameter rainfall-runoff model appears to be more appropriate. When applying such a model to simulate the Hammerbach spring Wagner et al. (2013) found that it was unable to reproduce the observed change in the discharge behaviour with parameter sets identified from other time periods. Within the 4 years period that is characterized by the damped discharge behaviour a reasonable model fit was obtained only by an increased overflow towards the neighbouring sub-catchment of the Schmelzbach aquifer and an increased storage capacity in the aquifer itself. This is in agreement with the findings from the data analysis and groundwater modelling presented here, which suggest that changes of hydraulic properties rather than climatic factors are responsible for the observed hydrological change.

6. Conclusions

Data analysis reveals a change in the hydrological behaviour of the Lurbach system after a storm event in August 2005 until June 2009. The spring response appears to be more damped and the baseflow higher than before, which is probably related to the aggradation of sediments in conduit sections during the storm event in 2005. Using the distributive groundwater flow model MODFLOW the changed behaviour of the Hammerbach spring was qualitatively reproduced by incorporating sections of low conductivity and high storage in highly conductive flow paths representing the conduit network (to mimic plugged conduit sections). Thus, the single-continuum model MODFLOW was found to be able to reproduce the transient behaviour observed at the spring. This model, however, does not account for turbulent flow in karst conduits. A MODFLOW package that considers turbulent flow in the continuum model (CFP) was employed to assess potential effects of turbulence on the

transient flow behaviour. Results from a highly simplified model scenario demonstrate that the storage in the fissured matrix is underestimated if turbulent flow is ignored. The implementation of turbulent flow in a more realistic model setting is the subject of future work.

Acknowledgements

This project was supported by the Austrian Science Fund (FWF): L 576-N21 and the Austrian Academy of Sciences (ÖAW) Project: Global models of spring catchments. The authors thank K. Lompe, G. Winkler, T. Reimann, S. Oswald and the owners of the Lurgrotte Peggau and Semriach for the fruitful discussions. The Hydrographische Dienst Steiermark is thanked for providing the meteorological data. Comments on the manuscript by two anonymous reviewers are gratefully acknowledged.

CHAPTER III

SINGLE EVENT TIME SERIES ANALYSIS IN A BINARY KARST CATCHMENT EVALUATED USING A GROUNDWATER MODEL (LURBACH SYSTEM, AUSTRIA)

Accepted for publication by Journal of Hydrology as: *Mayaud et al., 2014. Single event time series analysis in a binary karst catchment evaluated using a groundwater model (Lurbach system, Austria). doi: 10.1016/j.jhydrol.2014.02.024*

Abstract

The Lurbach karst system (Styria, Austria) is drained by two major springs and replenished by both autogenic recharge from the karst massif itself and a sinking stream that originates in low permeable schists (allogenic recharge). Detailed data from two events recorded during a tracer experiment in 2008 demonstrate that an overflow from one of the sub-catchments to the other is activated if the discharge of the main spring exceeds a certain threshold. Time series analysis (autocorrelation & cross-correlation) was applied to examine to what extent the various available methods support the identification of the transient inter-catchment flow observed in this binary karst system. As inter-catchment flow is found to be intermittent, the evaluation was focused on single events. In order to support the interpretation of the results from the time series analysis a simplified groundwater flow model was built using MODFLOW. The groundwater model is based on the current conceptual understanding of the karst system and represents a synthetic karst aquifer for which the same methods were applied. Using the wetting capability package of MODFLOW, the model simulated an overflow similar to what has been observed during the tracer experiment. Various intensities of allogenic recharge were employed to generate synthetic discharge data for the time series analysis. In addition, geometric and hydraulic properties of the karst system were varied in several model scenarios. This approach helps to identify effects of allogenic recharge and aquifer properties in the results from the time series analysis. Comparing the results from the time series analysis of the observed data with those of the synthetic data a good agreement was found. For instance, the cross-correlograms show similar patterns with respect to time lags and maximum cross-correlation coefficients if appropriate hydraulic parameters are assigned to the groundwater model. The comparable behaviour of the real and the synthetic system allow to deduce that similar aquifer properties are relevant in both systems. In particular, the heterogeneity of aquifer parameters appears to be a controlling factor. Moreover, the location of the overflow connecting the sub-catchments of the two springs is found to be of primary importance, regarding the occurrence of inter-catchment flow. This further supports our current understanding of an overflow zone located in the upper part of the Lurbach karst aquifer. Thus, time series analysis of single events can potentially be used to characterize transient inter-catchment flow behaviour of karst systems.

Keywords: Binary karst aquifer - Single event - Overflow behaviour - Time series analysis - MODFLOW - Single-continuum model

1. Introduction

Karst aquifers are of primary importance for supplying drinking water to nearly 25% of the world's population (Ford and Williams, 2007), but their significant reserves are highly vulnerable to contamination and to industrial or intensive agricultural land use. Because karst is a highly heterogeneous environment comprising aperture diameters varying over more than five orders of magnitude (from fracture openings less than 1 mm in the limestone matrix to conduits of more than 10 m width in large caves) there is a need to develop and improve existing tools helping to better understand the processes governing the hydrodynamic behaviour of karst systems. As not more than a few percent of a karst aquifer are generally mapped (or explored), it can be defined as grey/black-box system, where the input is routed through to the output without a direct observation of the water transfer. Thus, indirect methods of characterization have been developed to obtain a maximum of information from the karst systems. They are mostly focused on the comparison between the available input and output data and include hydrograph and chemograph analyses using discharge, specific electric conductivity, water temperature, chemical parameters, isotopes and tracer experiments (e.g., Bakalowicz, 2005; Geyer et al., 2013; Kresic and Stevanovic, 2010; Pinault et al., 2001; Rehrl and Birk, 2010).

Time series analysis are signal processing methods belonging to this category, and are mostly used to improve the understanding of the hydrological behaviour of karst systems. Mangin (1984) was the first to apply them to the field of karst hydrology. He compared the autocorrelation and power spectral density functions of the discharge of three Pyrenean karst aquifers under the same climatic conditions and deduced that their different responses were due to different degrees of karstification and storage capacities. Larocque et al. (1998) extended the analysis to a broader dataset (piezometric level, water discharge at the inlet and outlet, precipitation, specific electrical conductivity and water temperature) combined with new methods such as cross-correlation, cross-spectral density, coherence function, gain and phase functions, and proved their usefulness for the purpose of water management. Panagopoulos and Lambrakis (2006) applied time series analysis to two Greek karst aquifers well-known for their different karstification and found that the different results were in agreement with the differences in karstification. More recently Bailly-Comte et al. (2008) applied these methods to a small Mediterranean karst system and highlighted the interactions between the karst aquifer and an overflow river. Kovačič (2010) applied autocorrelation, cross-correlation, power spectral density and coherence function to the complex Unica river catchment and improved the understanding of its hydrodynamic behaviour, allowing the differentiation of flow paths using two datasets of different time scale. Time series analysis were also successfully used by Amraoui et al. (2003), Bailly-Comte et al. (2011), Bouchaou et al. (2002), Jemcov and Petrič, (2010), Genthon et al. (2005) and Massei et al. (2006) using a broader dataset (rainfall, specific electric conductivity, turbidity, water temperature) and different methods (e.g. spectral and wavelet analyses).

Until now, time series analysis were mostly applied to time-periods covering a period of one year or more (Eisenlohr et al., 1997; Kovačič, 2010; Larocque et al., 1998; Mangin, 1984;

Panagopoulos and Lambrakis, 2006). Only a few studies (e.g. Bailly-Comte et al., 2008; Budge and Sharp, 2009; Covington et al., 2009; Covington et al., 2012; Valdes et al., 2006) applied the methods at a very short -or single event time scale to provide information about the hydrodynamic behaviour of a karst system for short periods. Indeed, as opposed to long-term time series analysis, which is recommended to provide information about the "average" aquifer behaviour/properties (Kovačič, 2010; Panagopoulos and Lambrakis, 2006), single event analysis has the potential to show how the system reacts at the scale of a single event only (Bailly Comte et al., 2008; Covington et al., 2009; Covington et al., 2012; Valdes et al., 2006). This is of primary importance, because karst aquifers are highly dynamic non-linear systems whose behaviour may evolve or vary temporarily depending on the hydrological conditions within the system (Mayaud et al., 2013; Wagner et al., 2013).

As demonstrated by the examples cited above, time series analysis has been frequently applied to karst catchments. Although the results from these applications were found to be in qualitative agreement with field observations, it has only rarely been attempted to verify the interpretation more quantitatively by applying the methods to synthetic catchments represented by a numerical model, where aquifer properties and hydrological stresses are known in detail. This approach was followed by Eisenlohr et al. (1997) who evaluated the results from times series analysis using a numerical groundwater flow model. These authors concluded that the results were not only dependent on the system geometry but also on the frequency and type (allogenic vs. autogenic) of the recharge events and on their intensity. In addition, an inappropriate length of the analysed time series may cause errors in the interpretation. Jeannin and Sauter (1998) concluded that these methods were inappropriate without knowledge of the investigated area to characterize the underground geometry of karst aquifers. Nevertheless, Larocque et al. (2000) applied successfully autocorrelation and cross-correlation analysis to numerical data of a groundwater model representing the Larochefoucault karst aquifer (France). Later, Budge and Sharp (2009) applied short term cross-correlation analysis to a simplified synthetic MODFLOW catchment in order to develop a conceptual understanding of the Barton springs-Edwards aquifer. Their results showed that the cross-correlation was dependent on the input data but also on the geometrical properties of the aquifer.

The purpose of this paper is to improve the interpretation of time series analysis at the scale of single events in karst catchments that are characterized by the existence of a localized recharge component from a sinking stream and by temporarily varying drainage pattern due to the overflow from one spring catchment to another. This involves the need to investigate how physical characteristics of the karst system are reflected in the results from the time series analysis. To this end, two methods, autocorrelation and cross-correlation, are applied to a well investigated field site, the Lurbach karst system (Austria), where an overflow from one sub-catchment to another one is reported by numerous tracer experiments, and to a synthetic karst catchment represented by a numerical groundwater flow model, which accounts for the most relevant features of the field site in a simplified manner.

2. Approach

The following subsection (2.1) provides a brief introduction into the two time series analysis methods that are examined in this paper. These methods are evaluated in parallel using both a field site and a synthetic karst catchment represented by a numerical groundwater flow model, which are both described in the subsequent subsections 2.2 and 2.3, respectively. If the time series analysis of the synthetic and the field case yield comparable results, similar aquifer properties and geometries of the overflow section present in the model can be deduced for the Lurbach system.

2.1 Methods

2.1.1 Autocorrelation

The autocorrelation function examines how a value depends on the preceding values over a period of time. This function is represented with a correlogram. The slope of the correlogram is determined by the response of the system to an event. If the event has only a short-term influence on the response of the karst system, the slope of the correlogram will decrease steeply and quickly. In contrast, if the system is influenced by an event for a long time, the slope of the correlogram will decrease slowly. Generally the length of the influence of an event is given by the "memory effect" which is according to Mangin (1984) the lag number when *r(k)* reaches the value of 0.2. The formula for autocorrelation is (Larocque et al., 1998; Mangin, 1984):

$$r(k) = \frac{C(k)}{C(0)} \tag{1}$$

with

$$C(k) = \frac{1}{n}\sum_{t=1}^{n-k}(x_t - \bar{x})(x_{t+k} - \bar{x}) \tag{2}$$

where *k* is the time lag and varies from 0 to *m*. According to Mangin (1984) *m* has to be taken as 1/3 of the length of the whole dataset to avoid stability problems.

Applied at a single event or short time scale, autocorrelation has the potential to allow an estimation of the inertia of the system (Valdes et al., 2006). Then, the memory effect shows how the karst conduits react to the event, and cannot be compared to memory effects resulting from analysis of a long time series.

2.1.2 Cross-correlation

Cross-correlation is used to determine the relationship between two variables x and y. In the case of karst hydrology they are mostly input-output relationships as for discharge-discharge, rainfall-discharge or water level-discharge. The cross-correlation is represented by a cross-correlogram, which has a positive and a negative part. A peak in the positive part means that

the input signal has an influence on the output signal. If the cross-correlogram is symmetrical then the two signals respond at the same time. The maximum amplitude and the lag value of the cross-correlogram provide information about the delay which indicates the time of the pressure pulse transfer into the aquifer. If the input signal is a random process, then the cross-correlation function has the form of the impulse response of the system. According to Larocque et al. (1998) the formula for cross-correlation is:

$$r_{xy}(k) = \frac{C_{xy(k)}}{\sigma_x \sigma_y} \tag{3}$$

with

$$C_{xy}(k) = \frac{1}{n}\sum_{t=1}^{n-k}(x_t - \bar{x})(y_{t+k} - \bar{y}) \tag{4}$$

where σ_x and σ_y are the standard deviations of the two time series.

Applied at a single event scale, the cross-correlation shows how the energy is transferred and modified from the input to the output during a flood (Bailly Comte et al., 2008; Covington et al., 2009) and represents the impulse response of the system.

2.2 Field site

The area under investigation is a binary karst catchment of 23 km² named Lurbach system, located about 15 km north of Graz (Styria, Austria) and belongs to the Central Styrian Karst (Fig. 1). The upper part of the catchment comprises an area of about 15 km^2 essentially composed of Paleozoic schists, and is drained by the Lurbach stream in an E-W direction towards the lower part, which is an 8 km^2 highly karstified unit. After passing the contact schist-limestone, the stream infiltrates along the streambed at a length of some hundred meters and finally disappears into a major sinkhole located right after the entrance of a big cave, the Lurgrotte (entrance at 633 m a.s.l.). Then, the water flows through the conduits and fissures of the limestone massif and resurges at the Schmelzbach outlet and the Hammerbach spring, both located in the valley of the Mur River on the western side of the catchment. The altitude of the whole area ranges between 1.109 m a.s.l. on the top of the Fragnerberg mountain (Fig. 1) and approximately 400 m a.s.l. at the bottom of the Mur valley close to the location of the Hammerbach spring.

The Lurbach system is subject to a climate regime with low winter precipitation (approximately 50 days of snow cover per year) and frequent heavy thunderstorms during the summer (Harum and Stadler, 1992). The mean annual precipitation recorded from 1965 to 2010 at the station of Semriach (Fig. 1) is 880 mm. The maximum precipitation value was recorded at the same station during the summer 1975 with 93.5 mm rain in one day.

As it is regularly reported for karst aquifers, the behaviour of the Lurbach system varies strongly according to its different hydrological conditions (Harum and Stadler, 1992):

(i) at low and medium water conditions, the allogenic Lurbach waters (mean annual discharge of 141 l/s) supply only the Hammerbach spring (mean annual discharge of 193 l/s). The Schmelzbach outlet drains only autogenic recharge from the limestone massif and has a mean annual discharge of 79 l/s. Thus, both Hammerbach and Schmelzbach sub-systems are then totally separated.

(ii) when the Hammerbach discharge increases above a threshold discharge (about 200 l/s according to Behrens et al., 1992) an overflow from the Hammerbach sub-system to the Schmelzbach sub-system occurs.

(iii) at high water conditions the Lurbach stream can reach a maximum discharge of more than 10 m^3/s and the whole system is subject to catastrophic flood events. Then, the Lurbach flows directly through the Lurgrotte cave, toward the Schmelzbach, which becomes the main outlet of the karst aquifer and can reach peak discharges up to 10 m^3/s, whereas the Hammerbach spring shows a limited discharge capacity and cannot drain more than 2 m^3/s.

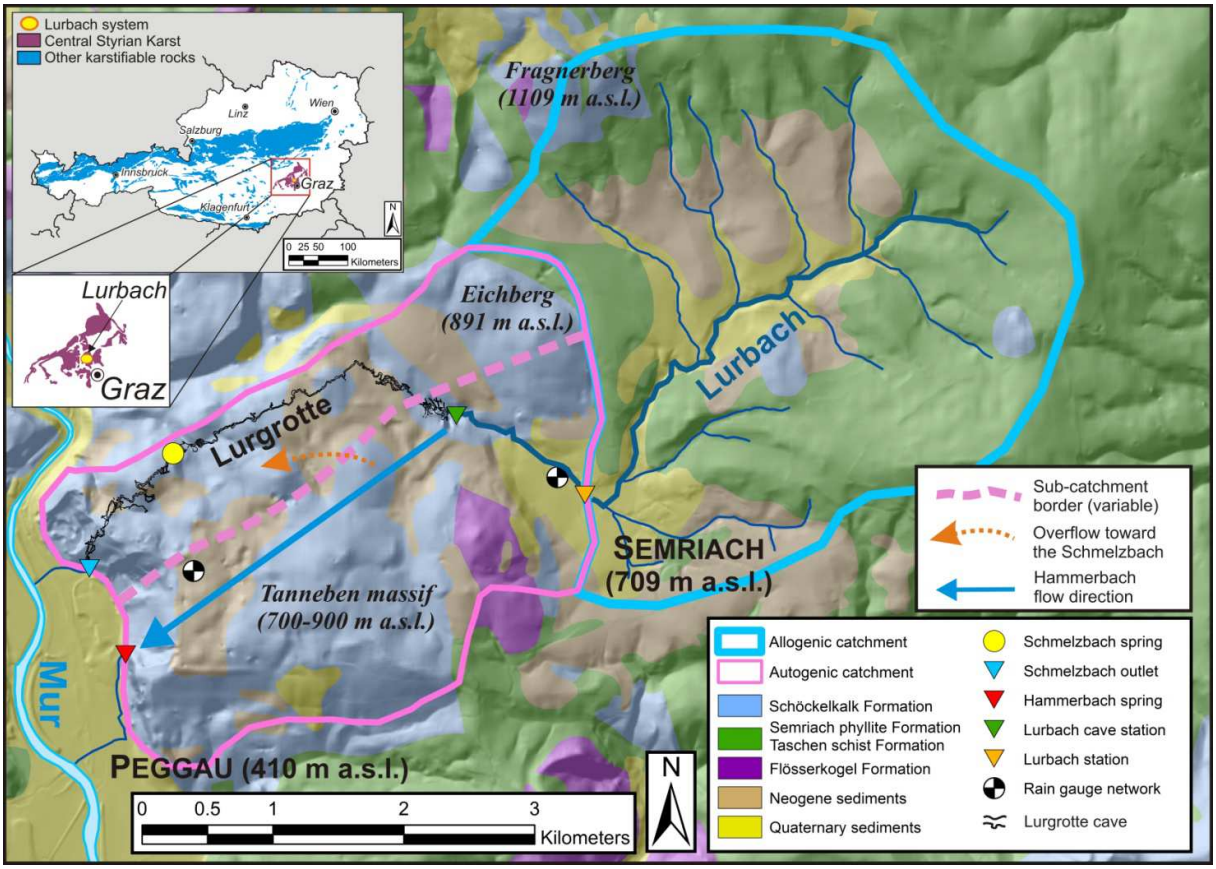

Fig. 1 Simplified geological map (modified after Geologische Bundesanstalt, 2005; sheet 164-Graz) of the Lurbach system including approximate flow directions and the monitoring network. The low permeable part (allogenic catchment) corresponds to the topographic catchment whereas the highly karstified part (autogenic catchment) was delineated taking into account results of numerous tracer experiments (Behrens et al., 1992). The boundary between the allogenic and the autogenic units is based on the geological map. The boundary between the Hammerbach and the Schmelzbach sub-catchments is variable depending on the hydrological conditions within the autogenic catchment. Insets: location of the Lurbach system in the Central Styrian Karst and the distribution of karst rocks in Austria (modified after Schubert, 2003).

The Lurbach karst aquifer has undergone a complex speleological development: on the one hand the Lurgrotte (see Fig. 1) is a well-explored about 3 km long multi-level cave (Wagner et al., 2011). On the other hand, the Hammerbach conduit network is totally unexplored as all attempts to access it failed up to the present. The overflow between the Hammerbach and the Schmelzbach sub-systems is documented only by indirect observation of numerous tracer experiments (Behrens et al., 1992; Kübeck et al., 2013). Moreover, as no boreholes are available in the study area, there is a lack of information concerning the extent and local position of a phreatic zone within the karst massif. The only available information regarding phreatic conditions in the karst aquifer were derived from speleological observations in the cave Lurgrotte itself and by geomorphological observations of several dry caves located in the Tanneben massif (with more than 200 known smaller inactive caves).

The last field campaign in the Lurbach system was conducted from the 28th November 2008 to the 30th December 2008). At the beginning of this time period, a tracer experiment had been carried out (Oswald, 2009). One kilogram of uranine (Uranin AP; AppliChem GmbH, Germany) was continuously injected into the Lurbach stream at the contact between schist and limestone (marked as Lurbach station in Fig. 1) from the 28th November 2008 at 14:11 to the 29th November 2008 00:35. The water levels were recorded at the stations Lurbach cave, Hammerbach spring and Schmelzbach outlet with a frequency of 30 seconds, whereas the Lurbach station was recorded at a frequency of 5 minutes. Then, they were converted to discharge rates using control measurements. Precipitation and air temperature were recorded at a 5-minute interval at the Ertlhube meteorological station (located at 763 m a.s.l.) on top of the Tanneben karst massif (Fig. 1). During the observation period, two hydrological events occurred. The results from this tracer experiment provide insight into the overflow behaviour from the Hammerbach sub-catchment to the Schmelzbach sub-catchment, which will be taken into account when interpreting the results from the time series analysis.

2.3 Synthetic karst catchment

In order to evaluate the interpretation of results from single event time series analysis, the groundwater flow model MODFLOW-2005 (Harbaugh, 2005) is used to implement a simplified hypothetical karst setting similar to the Lurbach system. Since the model is applied to a karst setting, it is an obvious idea to employ the Conduit Flow Process (CFP; Shoemaker et al. 2008) for MODFLOW-2005 to account for turbulent flow conditions. However, neither CFP mode 1 (hybrid approach) nor CFP mode 2 (continuum approach) were found to be capable of simulating the rewetting and falling dry of cells representing the transient overflow from the Hammerbach to the Schmelzbach sub-system in the given model setting. Yet, it is important to note that in this work the model is intended to provide general insight into the dependency of the results from the time series analysis on the physical characteristics of a generic type of karst catchment. Thus, similar to the MODFLOW models presented by Ravbar et al. (2011) and Mayaud et al. (2013), the purpose is to represent the natural processes in a simplified manner rather than to provide a quantitative representation of the actual field site. For this purpose, using MODFLOW-2005 without CFP appears to be adequate, as it allows a robust, approximate representation of the overflow dynamics.

The general approach here is to apply single event auto- and cross-correlation to a synthetic catchment and to examine how far the results are similar to or different from those obtained for the Lurbach system. As the model parameters are all known, the differences found in the auto- and cross-correlation of the various scenarios can be clearly attributed to a controlling parameter. Thus, this approach helps to interpret the results from the real system. In addition to a general evaluation of the applied time series analysis methods, this will also improve the current understanding of the Lurbach system.

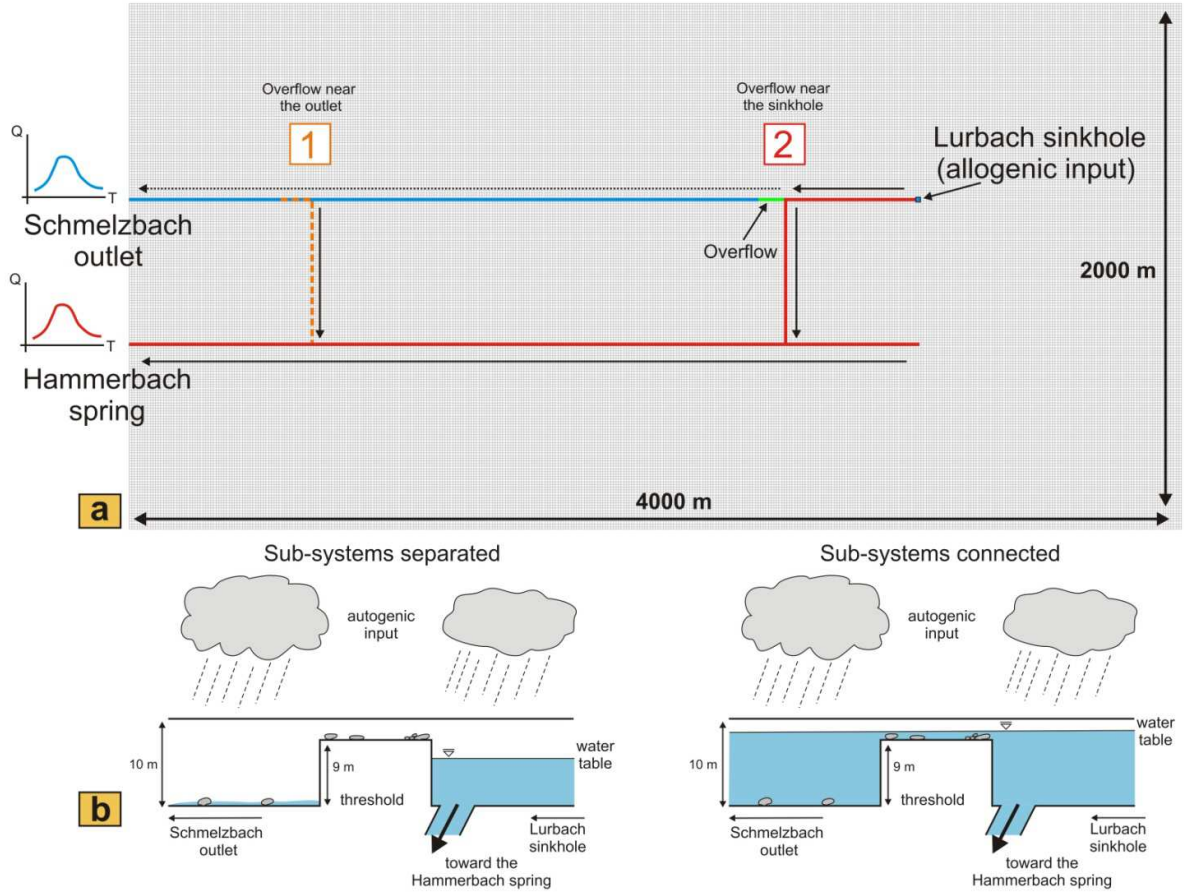

Fig. 2 Model setup. **(a)** Geometry of the MODFLOW model. The allogenic input is implemented using the Well package of MODFLOW in one cell representing the Lurbach sinkhole. The two different assumptions regarding the connection between the Hammerbach sub-catchment and the Schmelzbach sub-catchment are respectively indicated. If an overflow location close to the sinkhole is considered (case 2), the solid arrows indicate the flow toward the Hammerbach when the overflow is inactive, the dotted arrow the autogenic flow toward the Schmelzbach. **(b)** Schematic illustration of the functioning of the overflow in the MODFLOW model. When the water table is below the level of the threshold both Hammerbach and Schmelzbach sub-systems are separated (left). Then, the Schmelzbach is only supplied by autogenic waters from the limestone massif, whereas the Hammerbach drains all water coming from the sinking Lurbach stream. When the water table rises above the threshold, the overflow is activated and the two sub-systems are connected (right). Then, both Schmelzbach outlet and Hammerbach spring drain allogenic water from the Lurbach sinkhole and share a large part of their respective catchments together.

The model setting is composed of a single unconfined layer with a dimension of 8 km^2 (4 km * 2 km), which provides a simplified, hypothetical representation of the autogenic part of the Lurbach system (Fig. 2a). The mesh size is set constant to 10 m * 10 m. The Lurbach

allogenic input is introduced at a single point (Fig. 2a) using the Well package of MODFLOW, whereas autogenic recharge is given as a constant flux over the whole area. The model was built using the single-continuum approach (Sauter et al., 2006; Teutsch and Sauter, 1991) with two parallel cell lines of high hydraulic conductivity (representing the Schmelzbach and Hammerbach conduits) embedded in a low permeable matrix (see Fig. 2a). The conduit length was set to 3 km for each of the two conduits and is supposed to be close to the real length of the Schmelzbach and Hammerbach network sections (Behrens et al., 1992). The two outlets of the conduits were defined as constant head cells (to simulate the karstic springs) with a two meters difference of relative altitude (the Hammerbach spring being lower than the Schmelzbach outlet) and a linear distance of 550 m to each other. Similarly, the two conduits are connected to each other by a conduit of 550 m length with an overflow located after the first junction (Fig. 2b).

Two different assumptions with regard to the geographical location of the overflow are presented here (Fig. 2a). First, the overflow is located near the Schmelzbach outlet, whereas in the second case it is located close to the Lurbach sinkhole. These two extreme locations were chosen in order to obtain the maximum difference in the hydrological behaviour of the springs. The overflow was simulated by elevating a hundred meter stretch of the bottom of the Schmelzbach conduit located just after the connection between the Hammerbach and Schmelzbach sub-systems (Fig. 2b). Within this part of the Schmelzbach conduit, the bottom of the cells was elevated by 9 m relative to the other model cells, such that flow through the conduit occurs only if a threshold water level is exceeded. The initial water table was defined below the overflow level to allow a separation of the two sub-systems at the beginning of the simulation. Then, the Wetting-Capability package of MODFLOW was used to allow rewetting of these cells and thus an activation of the overflow depending on the position of the water table (Fig. 2b). This implies that after a first stress period computed in steady-state the model simulation was transient with 384 stress periods of the same length (30 minutes), making a total simulation of 192 hours. For both locations of the overflow between the two sub-systems, the values of constant head at the two outlets were adjusted such that the hydraulic gradient between the overflow and the Schmelzbach outlet remained approximately equal. First, the Schmelzbach and the Hammerbach catchment were assumed to consist of a homogeneous matrix and conduit system with one value of conductivity (1 m/s) in the conduits, one value in the matrix (10^{-5} m/s) and a constant specific yield for both matrix and conduit (0.01). Then, differences in the hydraulic conductivity and specific yield of the karstic conduits connecting to the two springs inferred from field observations were introduced, to account for heterogeneities of the two sub-systems.

3. Results

3.1 Field site

During the one-month period shown in Fig. 3a, two precipitation events of different intensities occurred. The first was short and showed the stronger amplitude (maximum intensity of 5.75 mm per hour at the Ertlhube rain gauge) but the lower cumulative rainfall of 12.9 mm from

the 30th November 2008 to the 2nd December 2008; the second had lower intensity (rainfall maximum of 2.6 mm per hour) but extended over a larger time span, resulting in a higher cumulative rainfall of 42.7 mm from the 10th December 2008 to 13th December 2008. Interestingly, no precipitation in form of snow was observed within this period. During these two events the air temperature recorded at the same station stayed mostly between 0 °C and 5 °C, although negatives temperatures were also reported for short periods.

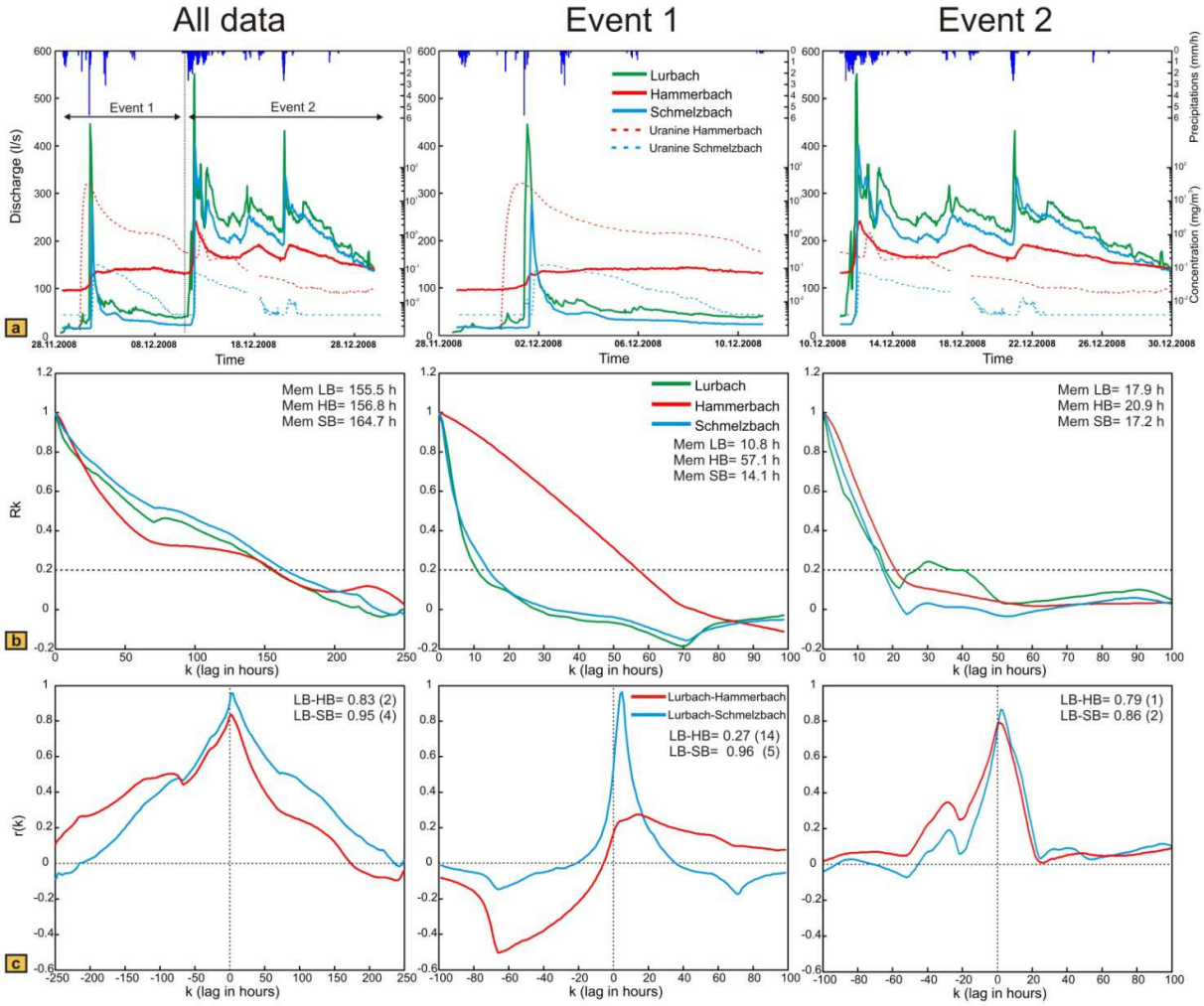

Fig. 3 Field data. **(a)** Discharge recorded at the stations Lurbach cave, Hammerbach spring and Schmelzbach outlet; semi log-scale plot of uranine concentrations at Hammerbach spring and Schmelzbach outlet in December 2008 for the whole period and the two events separated. Vertical bars: hourly precipitation recorded at the Ertlhube rain gauge. **(b)** Autocorrelation functions and memory effects of the discharge at Lurbach cave (LB), Hammerbach spring (HB) and Schmelzbach outlet (SB) for the whole period and the two events separately; the lags are given in hours. **(c)** Cross-correlation functions (amplitude and lags) between Lurbach cave-Hammerbach spring (LB-HB) and Lurbach cave-Schmelzbach outlet (LB-SB) for the whole period and the two events separately; the lags are given in hours.

The two precipitation events led to two hydrological events showing different spring responses (the first with a low baseflow, the second with a higher baseflow) recorded at the discharge gauging stations. The raw data of the gauging stations Lurbach cave, Hammerbach spring, Schmelzbach outlet and the precipitation data were transformed in hourly data in order to have an hourly scale for the time series analysis. A gap of approximately 30 hours in the discharge dataset from the gauging stations Lurbach cave, Hammerbach spring and

Schmelzbach outlet was filled with white noise based on the discharge recorded at Lurbach station which was complete.

The discharge and uranine concentrations show that a large part of the tracer was recorded at the Hammerbach spring a few hours before the first event was recorded at the station Lurbach cave (Fig. 3). Within this time period, no uranine was detected at the Schmelzbach outlet. This indicates that the Lurbach water was drained only toward the Hammerbach spring before the hydrological event. After the beginning of the first event, the tracer was still mainly recovered at the Hammerbach spring, and the breakthrough curve showed an undisturbed tailing. However, some small quantities of uranine were also recorded at the Schmelzbach outlet. This suggests that the overflow towards the Schmelzbach sub-system was activated due to the increasing water table during the event. An interesting observation is that the overflow seemed to happen at lower discharge than the value of 200 l/s reported in Behrens et al. (1992), which agrees with the findings of Mayaud et al. (2013) and Wagner et al. (2013) that the Hammerbach spring exhibits a changed hydrological behaviour since a major flood event happened in 2005. The shapes of the hydrographs further support the assumption of an activation of the overflow from the Hammerbach to the Schmelzbach sub-system because the hydrograph of the Schmelzbach appears to be similar to the hydrograph of the Lurbach, whereas the Hammerbach spring shows a damped response to this event and seems to drain mostly water from the aquifer storage.

Despite the lower maximum intensity of precipitation during the second event, the Hammerbach responds stronger to the resulting recharge pulse possibly due to the higher total amount of precipitation, which leads to an increase of the water table and the hydraulic gradient within the aquifer. The shape of the Schmelzbach hydrograph still appears to be almost identical to that of the Lurbach hydrograph. Uranine is still found in larger quantities at the Hammerbach spring but the concentration recorded at the Schmelzbach outlet responds faster than the Hammerbach to the recharge event. This suggests higher flow velocities and thus probably higher hydraulic conductivity of the Lurbach-Schmelzbach flow path and is in agreement with the assumption that the Schmelzbach still drained most of the Lurbach water during the second event when the overflow was already activated. The higher quantity of tracer recovered at the Hammerbach during the second event might be explained by a remobilization of uranine that was still stored within the Hammerbach sub-catchment down-gradient from the overflow.

Auto- and cross-correlations were computed for the three gauging stations Lurbach cave, Hammerbach spring and Schmelzbach outlet using the time series of the whole period (from the 28th November 2008 to the 30th December 2008 on the left hand side on Fig. 3), and for the two events separately (see Fig. 3 on the middle and right hand side). The two different events were defined taking into account the precipitation distribution and the baseflow discharge rather than the occurrence of discharge peaks. This allows the clear definition of two different periods: a first one with low baseflow (from the 28th November 2008 to the 11th December 2008) followed by a second one with a higher baseflow (from the 11th December 2008 to the 30th December 2008, respectively). As can be seen by comparing the results of

auto- and cross-correlation of event 1 and event 2, the system behaviour varied strongly during the period. During the first hydrological event, the Hammerbach autocorrelation indicates a damped behaviour with a longer memory effect compared to the Lurbach and Schmelzbach autocorrelations. In contrast, the autocorrelation of the Schmelzbach is similar to that of the Lurbach. Correspondingly, the cross-correlation Lurbach cave-Schmelzbach outlet is higher in amplitude and shows a shorter lag time than the cross-correlation Lurbach cave-Hammerbach. This supports the idea that most of the Lurbach event-water was drained towards the Schmelzbach system after the overflow had been activated during the first event. The damped discharge of the Hammerbach is potentially explained by a larger storage capacity within this sub-catchment (Behrens et al., 1992).

When looking at the second event, the results from the time series analysis show a different trend: the Hammerbach autocorrelation function is very similar to those of the Lurbach and Schmelzbach. More specifically, the memory effect apparent in the autocorrelation of Lurbach and Schmelzbach (17.9 and 17.2 hours in either case) is still similar to that of the first event (10.8 hours and 14.1 hours, respectively), whereas in the case of the Hammerbach it is clearly reduced from 57.1 hours in the first event to 20.9 hours in the second. This suggests that the aquifer storage of the Hammerbach sub-catchment is not able to attenuate the flood pulse of the second event to the same extent as in event 1, possibly because additional conduit pathways are activated at higher water levels (Kübeck et al., 2013). This further indicates that at this time, the Lurbach water pulse is transmitted toward the Hammerbach and Schmelzbach spring at a similar time-scale and that the two sub-catchments have more similar drainage behaviour compared to event 1. This is also supported by the finding that the cross-correlation between Lurbach-Hammerbach and Lurbach-Schmelzbach at this time shows the same pattern (r_{xy} values of 0.79 and 0.86 with lags from 1 to 2 hours respectively, opposed to r_{xy} values of 0.27 and 0.96 with lags of 14 and 5 hours during the first event), which shows that the two sub-systems behave similar. Obviously, the different and varying behaviour of the Hammerbach and Schmelzbach sub-catchments for these two particular events cannot be inferred from the autocorrelation and cross-correlation of the complete discharge dataset. In particular, the different behaviour of Hammerbach and Schmelzbach during event 1 is not apparent if the events are not separated in the analysis (Fig. 3b and 3c, first column), as both springs then show similar memory effects (156 hours for the Hammerbach, 164 hours for the Schmelzbach) and similar cross-correlations with the Lurbach (0.83 amplitude and 2 hours delay for the Hammerbach opposed to 0.95 in amplitude and 4 hours delay for the Schmelzbach). Thus, single event analysis proves useful in this particular example, as it allows distinguishing the change of the global behaviour of the Hammerbach sub-catchment during the two events.

3.2 Synthetic karst catchment

3.2.1 Homogeneous cases

Fig. 4 shows the modelling results of the synthetic karst catchment for the overflow located close to the Schmelzbach outlet (case 1 in Fig. 2a) and the overflow located near the Lurbach

sinkhole (case 2 in Fig. 2a). The aquifer is unconfined and conduits and matrix are homogeneous, i.e. with the previously mentioned constant values of hydraulic conductivity and specific yield. In order to reproduce a hydrological situation similar to that occurring during the tracer experiment, two artificial allogenic recharge events were defined. The intensity of the allogenic input (Lurbach discharge) was increased from a first to a second event roughly by a factor of two (Fig. 4) in order to see the influence of event intensity on the overflow and discharge characteristics. Autogenic recharge remained constant during the whole simulation.

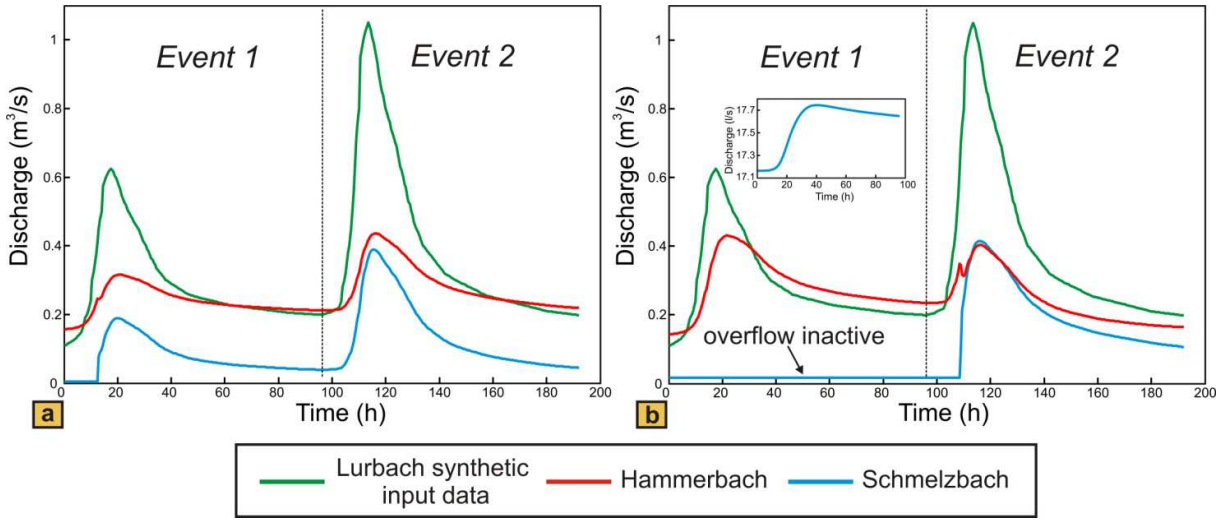

Fig. 4 Results from the groundwater flow model: Simulated discharge response of Hammerbach and Schmelzbach due to two recharge events of different intensity. **(a)** Overflow located close to the Schmelzbach outlet (case 1 in Fig. 2a); **(b)** overflow located near the Lurbach sinkhole (case 2 in Fig. 2a). The inset shows that some minor matrix flow happens from the Hammerbach sub-catchment to the Schmelzbach sub-catchment during the first event. Hydraulic conductivity, specific yield, and porosity are identical in the two model setups and homogeneous within matrix and conduit system.

The comparison of the resulting responses of the synthetic Schmelzbach and Hammerbach hydrographs reveals an activation of the overflow similar to the observation at the field site: in the case of the overflow near the outlet (Fig. 4a) the Schmelzbach hydrograph stays at a constant value over a period of approximately 12.5 hours during the first event when the Hammerbach has already started to respond to the Lurbach flood pulse by an increase in discharge. In the case of the overflow near the sinkhole (Fig. 4b), the Schmelzbach does not respond to the first Lurbach flood pulse, and responds later than the Hammerbach during the second event (after 108.5 hours). Evidently, the intensity of the first event is too weak to activate the overflow in the case where it is located near the sinkhole (Fig. 4b). Yet, it should be noted that a slight increase in Schmelzbach discharge (see inset in Fig 4.b) is caused by the pressure propagation within the low-permeability matrix flow. It is further noteworthy that the peak discharge of the Schmelzbach slightly exceeds that of the Hammerbach for the second event when the overflow is located near the sinkhole (Fig. 4b), while it stays below in the case with the overflow near the Schmelzbach outlet (Fig. 4a). Likewise the baseflow of the Schmelzbach remains higher with the overflow near the sinkhole than with the overflow near the outlet. These observations are explained by the size of the autogenic sub-catchment of the Schmelzbach, which increases with increasing distance of the overflow from the outlet. Thus,

the location of the overflow in the groundwater model is found to be of primary importance.

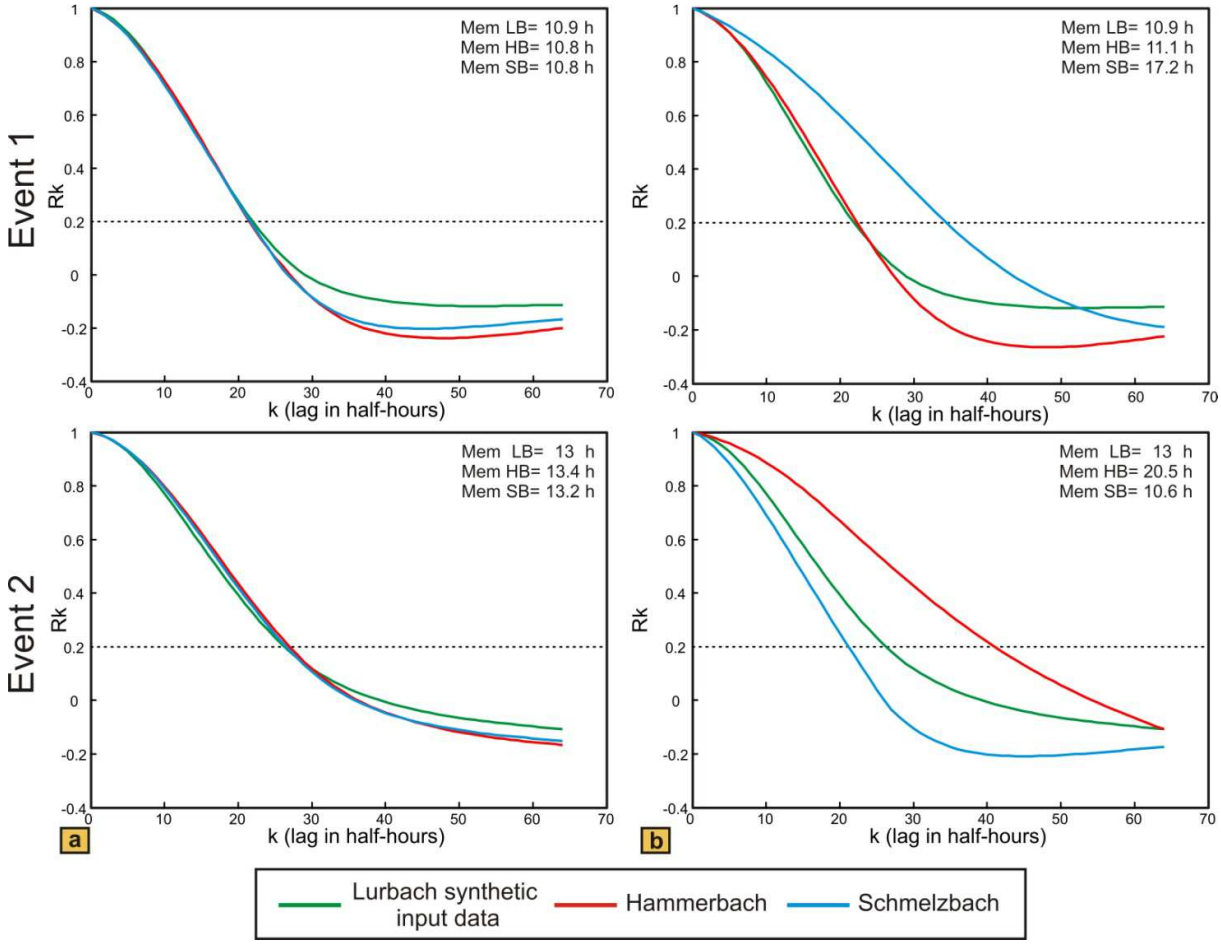

Fig. 5 Autocorrelation functions of the simulated Lurbach (LB), Hammerbach (HB) and Schmelzbach (SB) discharges presented in Fig. 4 for the two separated events; **(a)** overflow near the outlet, **(b)** overflow near the sinkhole. Here the lags are given in half hours. Memory effects are given in hours.

The autocorrelation of the hydrographs of the two models is presented in Fig. 5. With the overflow located near the outlet (Fig. 5a) the values of the memory effect for the Hammerbach and Schmelzbach are identical for both events and the values obtained for the first and the second event are similar (approximately 10.8 hours during the first event; nearly 13 hours during the second event). Contrary, the model with the overflow located near the sinkhole (Fig. 5b) shows different memory effects for Hammerbach and Schmelzbach and the memory effect is found to be different for the two events. The result from the first event can be explained by the inactivity of the overflow: almost all Lurbach allogenic water is drained towards the Hammerbach spring, whereas the Schmelzbach outlet is supplied only by a constant flux of autogenic water and a small amount of Lurbach water transferred through the matrix (see Inset in Fig. 4b). As a consequence, the memory effect for the Schmelzbach is higher than that for the Hammerbach. During the second event both Hammerbach and Schmelzbach are supplied by allogenic water from the Lurbach but still have different memory effects (11.1 hours during the first event and 20.5 hours during the second for the Hammerbach; 17.2 hours during the first event and 10.6 hours during the second for the Schmelzbach). As opposed to the first event the Schmelzbach responds faster (lower memory effect) than the Hammerbach. This is due to the sudden activation of the overflow forcing a

high proportion of Lurbach water to flow towards the Schmelzbach system. Similarly, the memory effect of the real Schmelzbach was found to be lower than that of the real Hammerbach when the overflow was activated in the first event observed at the field site (see event 1 in Fig. 3b). The above findings thus demonstrate that the memory effect is influenced by the overflow. Yet, it should be noted that differences in the memory effects of different events can also be caused by different input signals, which suggests that the interpretation of the memory effect in a setting with strongly varying input signals is not straightforward and should be supported by additional evidence from other methods.

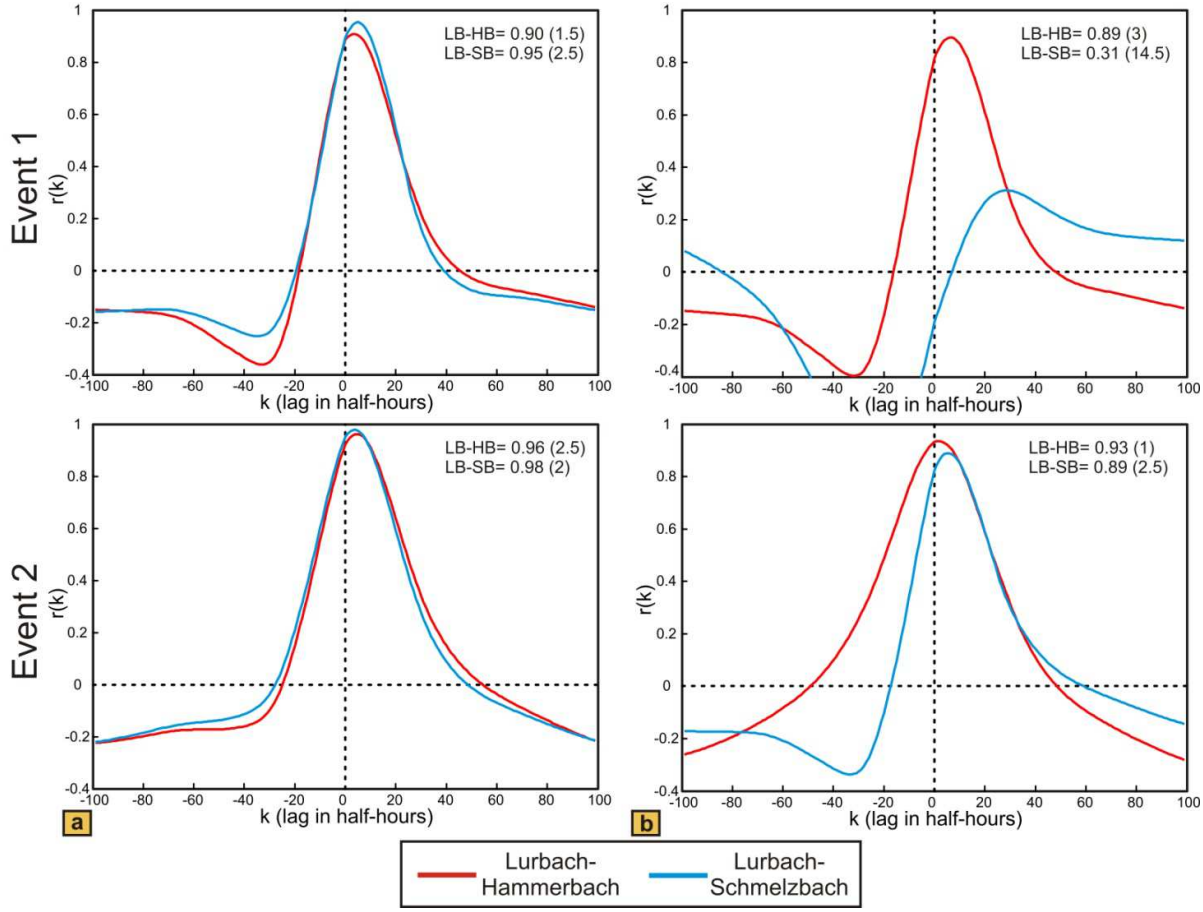

Fig. 6 Cross-correlation functions of the simulated Lurbach-Hammerbach (LB-HB) and Lurbach-Schmelzbach (LB-SB) discharges presented in Fig. 4 for the two separated events; **(a)** overflow near the outlet, **(b)** overflow near the sinkhole. Here the lags are given in half hours. Cross-correlation results are given in hours.

Single event cross-correlation results obtained with the two model set-ups are shown in Fig. 6. Corresponding to the results from the autocorrelation, the Lurbach-Hammerbach and Lurbach-Schmelzbach cross-correlation functions are similar in both events (more than 0.90 in amplitude for all cases) if the overflow is located near the outlet (Fig. 6a). In contrast, the model with the overflow near the sinkhole (Fig. 6b) shows a lower cross-correlation amplitude for the Lurbach-Schmelzbach during the first event when the overflow is not activated and a higher amplitude reaching almost the Lurbach-Hammerbach cross-correlation during the second event. Yet even during the second event the amplitude of the Lurbach-Hammerbach cross-correlation is higher than that of the Lurbach-Schmelzbach cross-correlation. In addition, the maximum of the lag time of the Lurbach-Schmelzbach cross-

correlation is larger than that of the Lurbach-Hammerbach cross-correlation (14.5 hours opposed to 3 hours during the first event and 2.5 hours to 1 hour during the second event). These findings are explained by the activation of the overflow during the second event, which causes a delayed response of the Schmelzbach relative to the Hammerbach. This is in striking contrast to the observation at the field site, where the real Lurbach-Schmelzbach cross-correlation exhibits a higher amplitude and lower lag time than the real Lurbach-Hammerbach cross-correlation when the overflow is activated (see event 1 in Fig. 3c). Thus, the autocorrelation of the observed hydrograph and that obtained with the model where the overflow is close to the sinkhole show some similarity (memory effect of Schmelzbach lower than that of Hammerbach when the overflow is activated), but the cross-correlation from the first event at the field site clearly suggests a more attenuated and damped response of the Hammerbach than that obtained with the model. In the above considered model scenarios the matrix and the conduit system were assumed to be homogeneous. As karst aquifers are highly heterogeneous an important question is how heterogeneities may influence the numerical spring response and the resulting shape of the auto- and cross-correlation functions. This is considered in the following sub-section.

3.2.2 Heterogeneous cases

As the Schmelzbach system is assumed to be higher karstified than the Hammerbach system (Behrens et al., 1992), heterogeneities were introduced in the groundwater model by increasing the conduit hydraulic conductivity from 1 m/s to 1.2 m/s from the overflow location to the Schmelzbach outlet. Moreover, as the Hammerbach is reported to have the higher aquifer storage (Behrens et al., 1992), the value of specific yield of the conduit cells within this sub-catchment was consequently increased from 0.01 to 0.5.

Fig. 7 presents a comparison of hydrographs, auto- and cross-correlation functions between the heterogeneous case (dashed lines) and the homogeneous one (solid lines) for the overflow located near the outlet (Fig. 7a) and the overflow located near the sinkhole (Fig. 7b). Auto- and cross-correlation are shown only for the second event. For both geometries the Hammerbach hydrograph is evidently more damped in the heterogeneous than in the homogeneous case. In addition, the Hammerbach response in the heterogeneous model appears to be delayed compared to the homogeneous case if the overflow is located near the sinkhole (but not when the overflow is near the outlet). Another important result in the heterogeneous model with the overflow near the sinkhole is the activation of the overflow during the first event (after 14 hours) whereas it remained inactive for the homogeneous case. This result is consistent with the lower value of 12.5 hours found for the overflow located near the outlet.

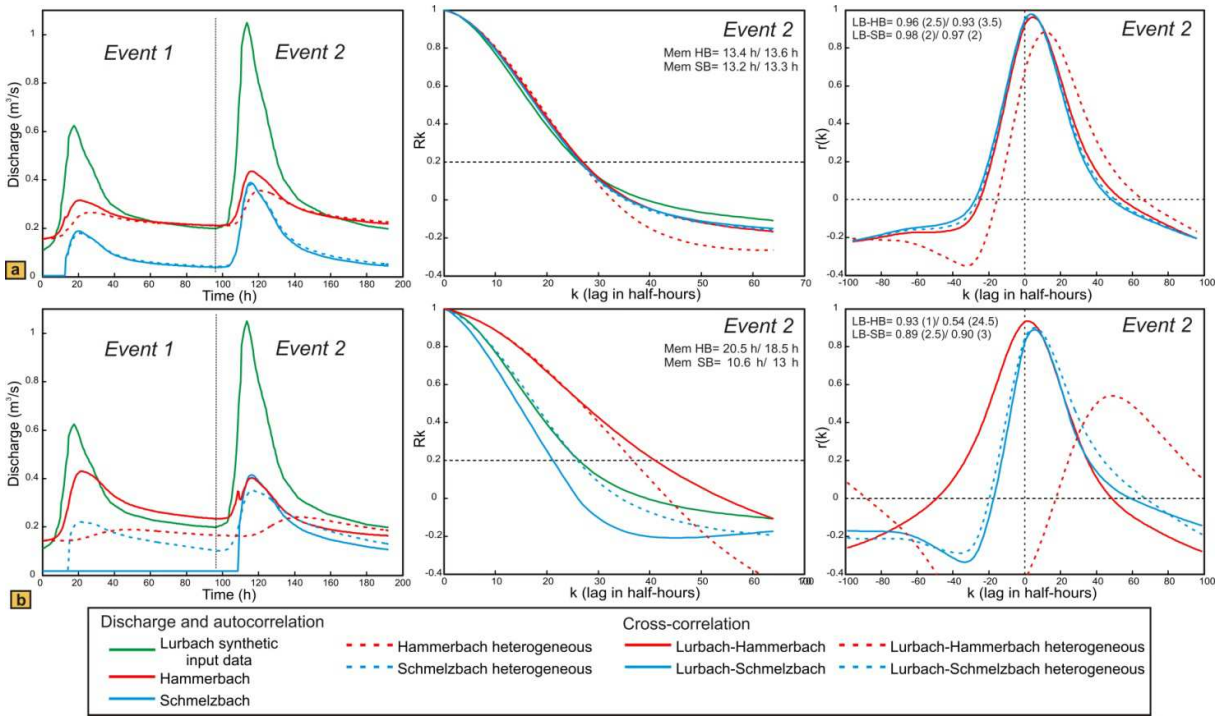

Fig. 7 Comparison of discharge, auto- and cross-correlation from the homogeneous model (solid lines) and the heterogeneous one (dashed lines); **(a)** overflow near the outlet, **(b)** overflow near the sinkhole. While matrix and conduit parameters of the Schmelzbach and Hammerbach sub-catchments are identical in the homogeneous model, the hydraulic conductivity of the Schmelzbach conduit and the specific yield in the Hammerbach conduit were increased in the heterogeneous model. Auto- and cross-correlation are shown for the second event only. Here the lags are given in half hours. Hourly auto- and cross-correlation results are indicated for the homogeneous and the heterogeneous model, respectively.

The autocorrelation for the model with the overflow located near the outlet shows almost no influence of the heterogeneities and yields similar memory effects for Hammerbach and Schmelzbach than those of the homogeneous case. Contrary, the model with an overflow located near the sinkhole shows different memory effects for the Hammerbach and the Schmelzbach and the values differ from those of the homogenous case (18.5 and 13 hours as opposed to 20.5 and 10.6 hours for the homogeneous case).

The results of the cross-correlation analysis correspond to those of the autocorrelation: the heterogeneous model with the overflow located near the outlet has cross-correlograms similar (Lurbach-Schmelzbach) or slightly damped and delayed (Lurbach-Hammerbach) compared to the homogeneous case. Evidently, the heterogeneity has little influence on the spring response if the overflow is close to the outlet. In this case the greater part of the aquifer is upstream of the overflow and thus shared by the two springs, while there is only a small part downstream of the overflow with two separate heterogeneous sub-catchments. In contrast, the model with the overflow located near the sinkhole is strongly influenced by the heterogeneities: the Lurbach-Hammerbach cross-correlation is clearly damped, whereas the Lurbach-Schmelzbach cross-correlation is only slightly changed. Thus, the Schmelzbach is the main outlet of the system and has a more flashy behaviour than the Hammerbach, which corresponds well with the field observations and further supports a location of the overflow in the upper part of the aquifer.

Results from the aforementioned tracer experiment (Fig. 3a) also suggest an overflow location close to the sinkhole: since most of the tracer was recovered at the Hammerbach spring and even in the time period when the overflow was active only a small amount of tracer was detected in the Schmelzbach, the overwhelming majority of tracer must have passed the overflow location at the time when the overflow became active. In agreement with the results of the single event time series analysis these findings support an overflow location within the upper part of the Lurbach aquifer.

4. Conclusion

Single event time series analysis was combined with a groundwater model to examine how the inter-catchment flow in a karst aquifer varies during a period of one month and how this is reflected in the results from the time series analysis. Auto- and cross-correlation of the observed data differ for the two events considered here, thus showing the necessity to make a single event analysis rather than an analysis of the whole dataset. The numerical model implemented with MODFLOW was able to reproduce the general overflow behaviour observed in the Lurbach system. Results of auto- and cross-correlation of the numerical model showed that aquifer heterogeneities and the overflow location were of primary importance. The model with an overflow located near the outlet was found to be relatively insensitive to a variation of hydraulic parameters. Contrary, the model with an overflow located near the sinkhole showed a high sensitivity to heterogeneities and was selected as the most probable option to better reproduce the observed behaviour of the Lurbach system. Results from the model with the overflow near the sinkhole and heterogeneous aquifer parameters were found to be in good agreement with the field observations. Thus, in agreement with evidence from tracer tests an overflow location in the upper part of the aquifer rather than in the lower part is suggested. In summary, single event time series analysis was found to be useful for characterizing transient inter-catchment flow and aquifer properties (overflow location, aquifer heterogeneity) controlling the spring responses to recharge in this karst catchment. Yet, it is important to note that results from time series analysis need to be complemented by other aquifer characterization techniques to interpret them in terms of flow processes and aquifer properties. In this work, tracer testing and groundwater modelling proved useful for this purpose.

Acknowledgements

This project was supported by the Austrian Science Fund (FWF): L 576-N21 and the Austrian Academy of Sciences (ÖAW) Project: Global models of spring catchments. The authors would like to thank Gerfried Winkler and Stefan Oswald for the fruitful discussions and the owners of the Lurgrotte Peggau and Semriach for the access to the cave. The Hydrographische Dienst Steiermark is thanked for providing the meteorological data. Comments on the manuscript by three anonymous reviewers are gratefully acknowledged.

CHAPTER IV

NON-LINEAR FLOW PROCESS (NLFP): A NEW PACKAGE TO COMPUTE NON-LINEAR FLOW IN MODFLOW

Submitted to Groundwater as Methods Note: *Mayaud et al., (under review) Non-Linear Flow Process (NLFP): a new package to compute non-linear flow in MODFLOW.*

Abstract

A new MODFLOW package (Non-Linear Flow Process; NLFP) simulating non-linear flow following the Forchheimer equation was developed and implemented in MODLFOW-2005. The package is based on an iterative modification of the conductance calculated and used by MODFLOW to obtain an effective Forchheimer conductance. The method was successfully tested using different layer types, boundaries conditions, and solvers as well as the wetting capability of MODFLOW. The correct implementation is demonstrated using three different benchmark scenarios for which analytical solutions are available. A scenario considering transient flow in a more realistic setting and a larger model grid demonstrates that NLFP performances well under more complex conditions, although it converges moderately slower than the standard MODFLOW depending on the non-linearity of flow. Thus, this new tool opens a field of opportunities to groundwater flow simulation with MODFLOW, especially for core sample simulation or vuggy karstified aquifers as well as for non-linear flow in vicinity of pumping wells.

Keywords: Forcheimer equation - non-linear flow - MODFLOW - Karst - benchmark

1. Introduction

Groundwater flow in porous aquifers is mostly considered to be laminar and thus described by Darcy's law (Darcy, 1856), i.e., by a linear relationship between specific discharge and hydraulic gradient. However, in some cases where the observed flow behaviour is non-linear, Darcy's law is found to be inadequate (Kuniansky et al., 2008; Scanlon et al., 2003). As widely used groundwater modelling software packages such as MODFLOW-2005 (Harbaugh, 2005) are generally based on Darcy's law, there is a lack of tools accounting for such non-linear flow behaviour through porous media or karst aquifers. The Conduit Flow Process (CFP) released by the USGS (Shoemaker et al., 2008) was the first MODFLOW package that allowed the use of a non-linear (turbulent) flow equation in MODFLOW. This package offers two different modes that can also be combined: the first mode is based on a hybrid approach coupling to MODFLOW a discrete pipe network where flow can be laminar or turbulent (Liedl et al., 2003); the second mode is intended for porous or vuggy karstified aquifers and allows turbulent flow simulations in preferential flow layers, where a non-linear flow law is used if the specific discharge exceeds a given threshold (Kuniansky et al., 2008). Reimann et al. (2011, 2012) modified and extended CFP mode 2 to enable the use of different non-linear flow laws.

The aforementioned packages are based on an approach where a switch from the linear Darcy law to the non-linear equation occurs when the Reynolds number (calculated from the specific discharge and a user-specified diameter of the flow pathways) exceeds a threshold defined by the user. But in contrast to the flow in a single conduit, the wide spectrum of conduit sizes present in real aquifers should leads to a more smooth transition from laminar to turbulent flow. A parameter study based on laboratory experiments using core samples of a vuggy Floridian aquifer suggests that an approach where Darcy's law is entirely replaced by the non-linear Forchheimer equation might be more appropriate than a sharp transition from laminar to turbulent flow (Chin et al., 2009). The purpose of this methods note is to present such an approach and its implementation into a new package that allows the simulation of non-linear Forchheimer flow in MODFLOW. This package is not only intended for karst aquifers but can also be employed in porous aquifers where non-linear flow occurs close to pumping wells (e.g. Forchheimer, 1901; Halford, 2000; Wen et al., 2011). The background theory and the limitations of the package are presented in the first part of the paper. Then, three benchmarks tests showing the validity of NLFP are described in the second part. Finally, one additional example comparing NLFP to CFP mode 2 in a more realistic context is shown in the third part.

2. Background and theory

The Forchheimer equation (Chin et al., 2009; Forchheimer, 1901) extends the linear Darcy law by a quadratic term:

$$i = aq + bq^2 \tag{1}$$

where i is the hydraulic gradient [-], q is the specific discharge [LT^{-1}], a [TL^{-1}] and b [TL^{-1}]^2 are the Forchheimer parameters. It reproduces Darcy's law in the limit of small discharges q where a is the inverse of the hydraulic conductivity K_0 [LT^{-1}]:

$$K_0 = \frac{1}{a} \tag{2}$$

In return, it turns into a quadratic flow law in the limit of large discharge. In general, Equation (1) can be transformed to Darcy's law with a discharge-dependent hydraulic conductivity [LT^{-1}]:

$$q = K_F i \tag{3}$$

where

$$K_F = \frac{1}{a + bq} = \frac{K_0}{1 + q\frac{b}{a}} \tag{4}$$

is the effective Forchheimer hydraulic conductivity [LT^{-1}].

As MODFLOW uses conductance instead of hydraulic conductivity to compute flow, equation (4) has to be written in terms of conductance too. The linear conductance [L^2T^{-1}] is calculated by MODFLOW using the distance Δl [L] and the area of the flow cross-section A [L^2] between two nodes:

$$C_0 = \frac{K_0 A}{\Delta l} \tag{5}$$

In analogy, the Forchheimer conductance [L^2T^{-1}] can be defined as:

$$C_F = \frac{C_0}{1 + q\frac{b}{a}} \tag{6}$$

Since the Forchheimer conductance is dependent on the specific discharge it must be calculated iteratively by a fixed point scheme. Analogous to the treatment of unconfined flow in MODFLOW, the conductance is updated in each iteration step based on reconstructing the specific discharge from the Forchheimer conductance and the hydraulic gradient of the previous iteration step:

$$C_F^{new} = \frac{C_0}{1 + \left(\frac{C_F^{old}}{C_0} K_0 \frac{\Delta h^{old}}{\Delta l}\frac{b}{a}\right)} \tag{7}$$

Here C_F^{new} and C_F^{old} denote the Forchheimer conductances [L^2T^{-1}] at the new and the previous iteration step, and Δh^{old} [-] the head difference between two nodes from the previous iteration step, respectively.

Thus, Equation (7) is used to modify the conductance in MODFLOW at each iteration. A sketch of the NLFP algorithm and its implementation in MODFLOW-2005 is shown in Figure 1. The computation of C_F^{new} occurs only after the read and prepare procedure, where the input data are read and boundary conditions, layer type and no-flow cells are identified. As a being the inverse of the hydraulic conductivity K_0 is already available, NLFP requires only the ratio *b/a* as input parameter from the user; typical values of *b/a* for various materials are provided, e.g., by Chin et al. (2009), Sidiropoulou et al. (2007) or Zheng et al. (2006). Setting *b/a* zero corresponds to using the standard Darcy equation. It is noteworthy that in contrast to the Conduit Flow Process, where the parameters controlling the non-linear flow are constant within each layer, different values of *b/a* can be specified for each cell with NLFP. In addition to this aquifer parameter, a criterion for convergence of the Forchheimer conductance can be specified by the user, as it was found that under certain conditions the hydraulic heads in MODFLOW converged while the Forchheimer conductance would still change if the iteration was continued.

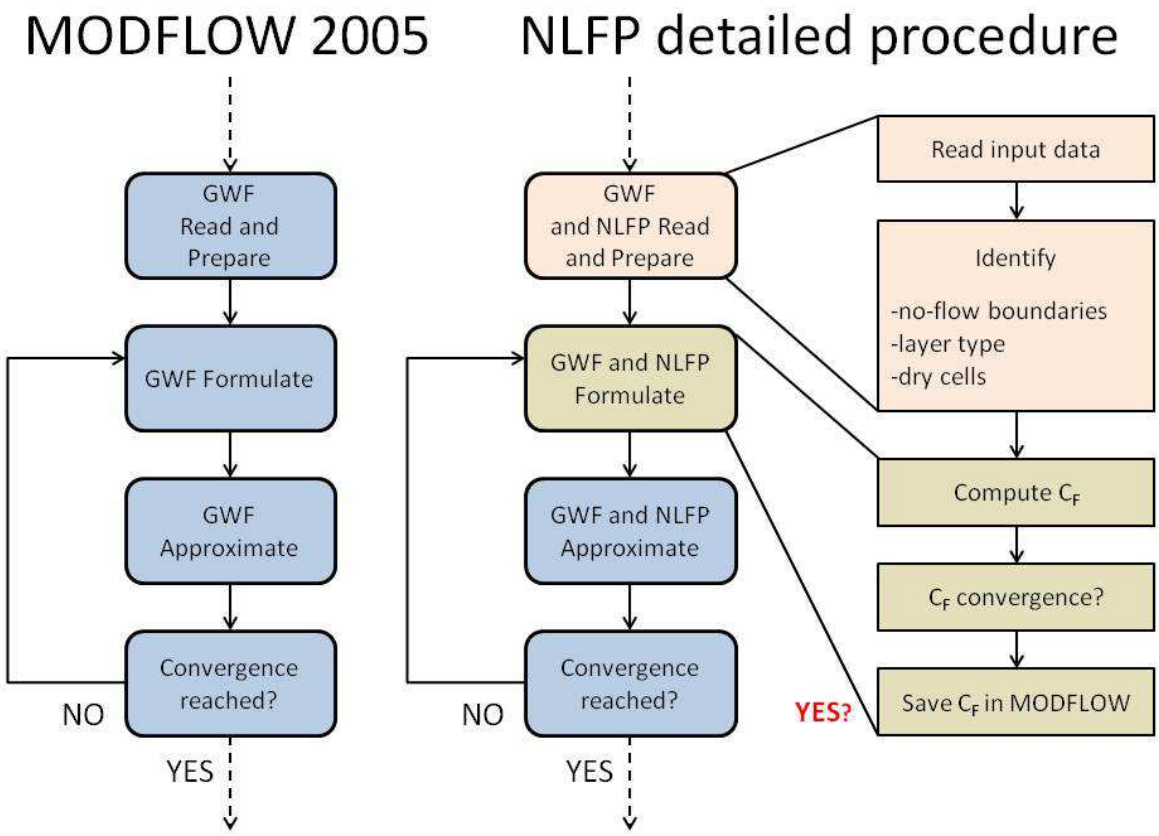

Fig. 1 Extract of MODFLOW 2005 flow chart (Harbaugh, 2005) and modified flow chart showing implementation of NLFP.

At present, the NLFP package can be used only with the Block Centered Flow package (BCF). An adaptation to the Layer Flow Package (LPF) will be subject of future work. NLFP was successfully tested with the three solvers DE45, SIP, and PCG2; the latter showed the fastest convergence for the test runs.
NLFP supports the use of deactivated cells (when IBOUND is set to 0) within the model. The package is also compatible with each of the four existing MODFLOW layer types (strictly confined, strictly unconfined, unconfined with constant/variable transmissivity). The use of wetting capability option is also possible. The NLFP package was written in a single file and compiled with the last available version of CFP (which can be found on the USGS website). The source code can be downloaded at: http://www.uni-graz.at/steffen.birk/research.html. A separate compilation with the last version of MODFLOW-2005 is also possible but was not tested until now.

3. Benchmark tests

In order to verify the correct implementation and functioning of the Forchheimer equation in the NLFP source code, three benchmark scenarios are considered.

3.1 First test: specified flow in a confined aquifer

The first model is composed of 1 row and 11 columns. The size of the cells is constant 10 m by 10 m; the thickness of the single confined layer is also 10 m. The hydraulic conductivity is set to $K_0 = 1/a = 1$ m.s^{-1} and $b/a = 0.25$ s.m^{-1}. On the left boundary, a constant head is set to 11 m, while on the right boundary a constant discharge is specified using the WELL package of MODFLOW. The discharge is varied from 10^{-6} m^3/s to 10^3 m^3/s in subsequent steady-state simulations. This scenario allows a straightforward comparison of the hydraulic gradient calculated by NLFP with that obtained directly from the Forchheimer equation (Equation 1). As can be seen from Figure 2 NLFP agrees well with the Forchheimer equation over a wide range of hydraulic gradients. For low hydraulic gradients the Forchheimer equation approaches the linear Darcy law, whereas at high hydraulic gradients the non-linear term of the Forchheimer equation dominates and thus the graph approaches a power law with an exponent of 2. The latter corresponds to well-known turbulent flow laws such as the Darcy-Weisbach equation.

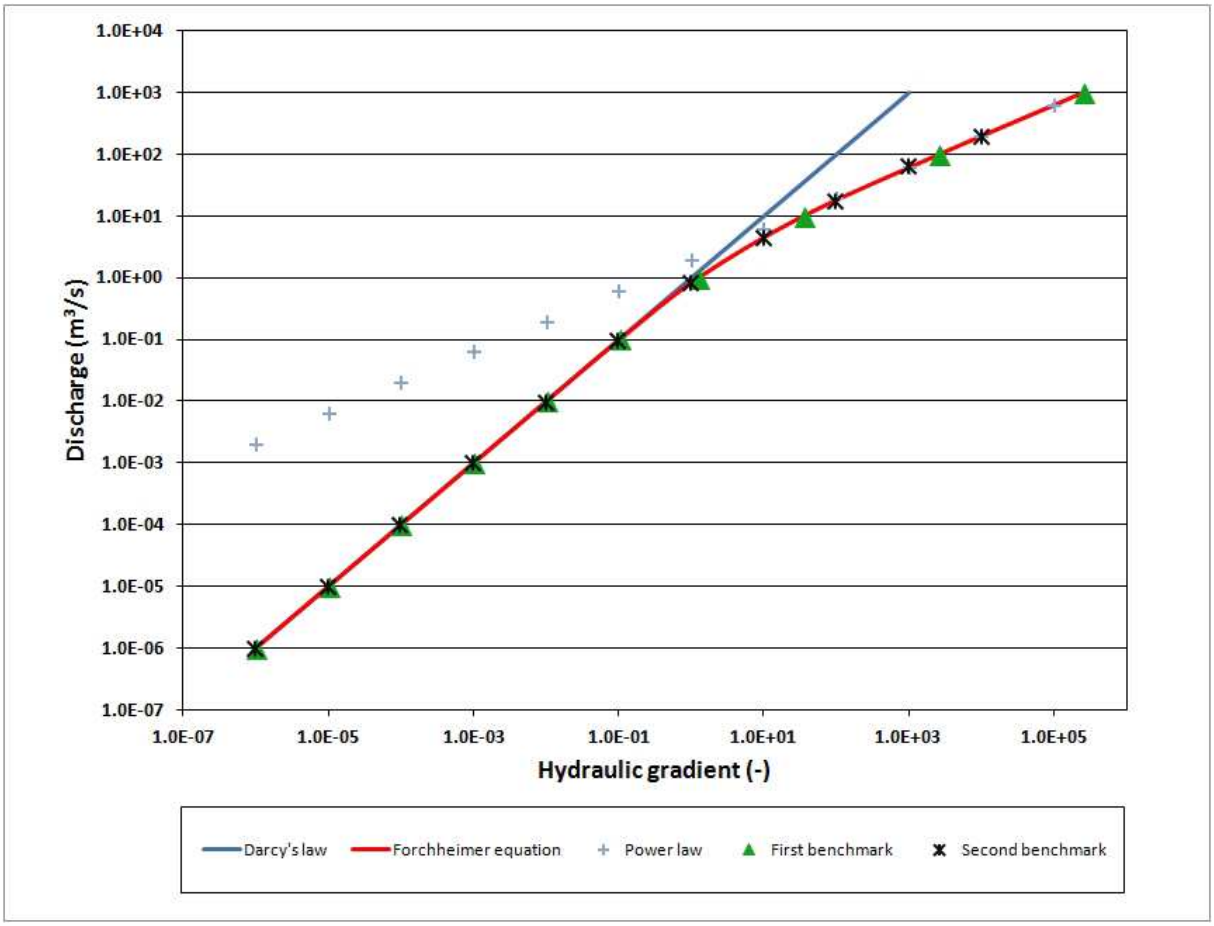

Fig. 2 Discharge versus hydraulic gradient of the two confined benchmark models. Simulation results of the first test case are represented with triangles, those of the second test case with stars. The power law was represented with an exponent of 2.

3.2 Second test: fixed gradient in a confined aquifer

The second test example comprises a single row of 11 confined cells with a constant head defined at both the left and the right boundary. The size of the cells is 1 m width by 10 m length; the thickness of the single confined layer is also 1 m. The hydraulic parameters are identical to the previous scenario. A sequence of steady-state simulations is conducted varying the hydraulic gradient by several orders of magnitude. Figure 2 shows the results computed by NLFP compared with those obtained from the Forchheimer equation (Equation 1) solved for the discharge (Moutsopoulos et al., 2005):

$$q = \frac{-a + \sqrt{a^2 + 4bi}}{2b} \tag{9}$$

Similar to the first benchmark model, NLFP is found to agree well with the Forchheimer equation under conditions ranging from linear flow following the Darcy equation to non-linear flow where the second term of the Forchheimer equation dominates. These findings show that NLFP behaves correctly regarding to the Forchheimer equation for confined flow.

3.3 Third test: specified discharge in an unconfined aquifer

To check if NLFP computes non-linear flow for unconfined conditions correctly, a corresponding analytical solution is derived. To simplify the problem, only one-dimensional steady-state flow is considered. The boundary conditions correspond to those of the first test case, i.e. a constant head $h(0) = h_0$ at one boundary and a specified discharge at the other.
Conservation of mass requires:

$$hq = Q = const \tag{10}$$

with the hydraulic head h [L] referring to the aquifer base as a datum level and Q the discharge per width [L^2T^{-1}].
Combining Equations (1) and (10) we obtain:

$$\frac{\partial h}{\partial x} = \frac{aQ}{h} + \frac{bQ^2}{h^2} \tag{11}$$

The integration of Equation (11) using the polynomial division leads to:

$$x + const = \int \frac{h}{aQ} - \frac{b}{a^2} + \frac{b^2 Q}{a^3 h + a^2 bQ}\, dh \tag{12}$$

Adjusting the constant of integration to satisfy the constant-head boundary condition finally gives the analytical solution:

$$x = \frac{h^2 - h_0^2}{2aQ} - \frac{b(h - h_0)}{a^2} + \frac{b^2 Q}{a^3} ln \frac{h + \frac{bQ}{a}}{h_0 + \frac{bQ}{a}} \quad (13)$$

where x [L] is the distance from the constant-head boundary h_0 at which the hydraulic head h is obtained. Note that although this equation cannot explicitly be solved for h, it can be used for a graphical evaluation of the numerically calculated hydraulic head distribution.

The analytical solution provided by Equation (13) and the respective numerical results are shown in Figure 3 for three different values of b/a and a specified discharge of 10 m^3/s. As can be seen NLFP with $b/a = 0$ (represented by squares in Figure 3) is able to reproduce the water table obtained with the Darcy equation (bold curve in Figure 3). The NLFP package also shows good agreement with the analytical solution for a value of b/a = 0.25 $s.m^{-1}$. Finally, the analytical solution of the Forchheimer equation with b/a = 20.25 $s.m^{-1}$ (represented by circles) is shown. As can be seen, the MODFLOW model does not match the analytical solution anymore under these conditions. The reason for the deviation from the analytical solution, however, is an inappropriate discretization of the model. If the cell size is reduced from 10 m to 1 m the numerical model (represented by triangles) agrees well with the analytical solution. This proves that the numerical implementation is correct and demonstrates that an appropriate model discretization is important when non-linear Forchheimer flow is calculated under unconfined conditions.

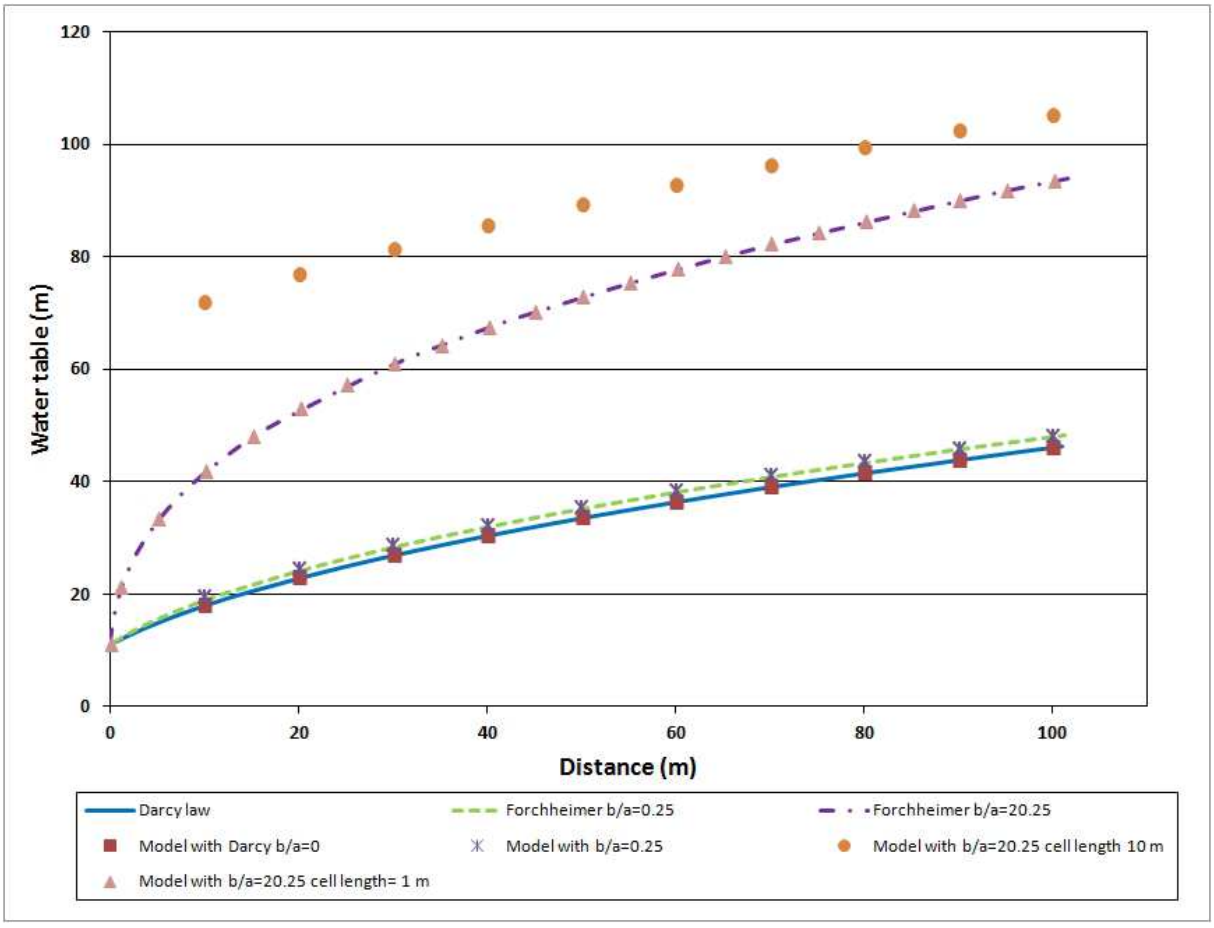

Fig. 3 Comparison of the analytical solution of the Forchheimer equation in an unconfined aquifer to the result of the numerical NLFP model.

In summary, the three benchmark tests show that the NLFP package is able to simulate Forchheimer flow under both confined and unconfined conditions. However, the scenarios considered above are highly simplified. The performance of NLFP in a more complex case thus is considered in the next part.

4. Application example

The computational performance of the NLFP package was examined using a more realistic scenario taken from Mayaud et al. (2013). The selected catchment is 3 km long and 1.5 km wide. The model domain is discretized in 44700 cells of constant size (10 m by 10 m) and represents a simplified confined karst system that is drained by a single conduit (length 2300 m). The simulation comprises 83 stress periods representing a recharge event of in total 150 hours. A first steady-state stress period is used to define the initial conditions for the subsequent transient simulation. The model scenario was implemented to investigate how far a conduit constriction (represented by reducing the hydraulic conductivity of individual model cells within a sequence of highly conductive cells) can influence the discharge behaviour of a karst spring (for more details see Mayaud et al., 2013). The value of b/a was varied from 0 to 500.25 $s.m^{-1}$ in subsequent model runs. The model always converged and the computation time varied from 61 s for linear flow simulated with the standard MODFLOW-2005 to 91 s for NLFP with b/a = 500.25 $s.m^{-1}$. The resulting spring hydrographs are shown in Figure 4 together with those obtained using the standard (laminar) MODFLOW and MODFLOW-CFP mode 2 (Shoemaker et al. 2008). NLFP showed an increasingly damped response of the simulated spring discharge, which is similar to the behaviour of CFP mode 2 described by Mayaud et al. (2013).

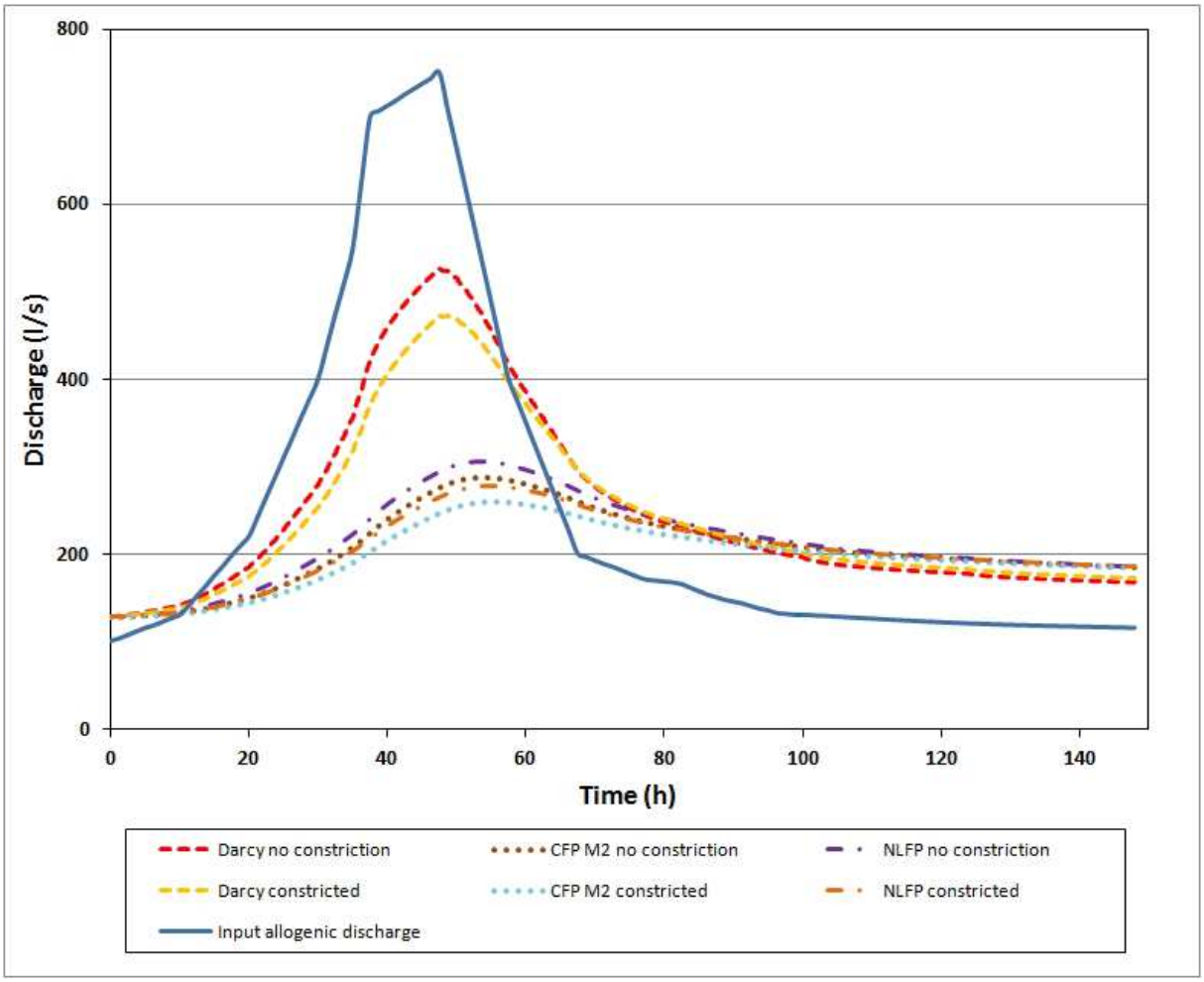

Fig. 4 Numerical discharge due to an artificial recharge event of a hypothetical karst catchment computed by MODFLOW 2005, CFP Mode 2 and NLFP (b/a = 500.25 s.m^{-1}). See Mayaud et al. (2013) for more details on the model scenario and the results obtained with MODFLOW 2005 and CFP Mode 2.

5. Conclusion

A new MODFLOW package (Non-Linear Flow Process; NLFP) computing non-linear Forchheimer flow was developed and implemented in MODFLOW-2005. The approach is based on an iterative modification of the conductance provided by MODFLOW. The package requires only one additional aquifer parameter and an additional convergence criterion to check the convergence of the Forchheimer conductance. NLFP was tested in three benchmark scenarios and found to compare favorably with the corresponding analytical solutions both under confined and unconfined conditions. The package was also successfully applied to a more realistic setting with a larger grid. Depending on the choice of the Forchheimer parameter b/a which determines the non-linearity of the equation, NLFP was found to converge only moderately slower than the standard MODFLOW in the scenarios considered. Thus, this new tool opens a new field of modelling opportunities related to non-linear flow, e.g., in (vuggy) karstified aquifers or in the vicinity of pumping wells.

Acknowledgments

This project was supported by the Austrian Science Fund (FWF): L 576-N21. The authors would like to thank W.B. Shoemaker, G. Winkler and T. Wagner for the fruitful discussions.

CHAPTER V

OVERALL CONCLUSIONS

As each chapter of this thesis has its own conclusion, the following section summarizes the essential results of this work.

The purpose of this PhD thesis was to investigate to which extent single-continuum models are able to reproduce flow processes observed in karst aquifers. To this end, several examples show how single-continuum models can be employed for karst aquifer modelling in order to improve our understanding of the aquifer functioning, contributing thus to the aquifer characterization. Results of this thesis further demonstrate that the model application has to be integrated in a broader investigation approach that includes other methods such as recession analysis (Chapter 2), time series analysis (Chapter 3), or conceptual lumped-parameter modelling (Appendix A; Wagner et al., 2013). The experiences from these applications of existing single-continuum models further suggested the need for an improved implementation of a non-linear flow package, which is provided by the newly developed NLFP package (based on the Forchheimer law) presented in Chapter 4.

In detail, the previous chapters lead to the following conclusions:

(i) Chapter 1 presents the current problematic related to karst aquifers (water quality, extreme events forecasting as well as aquifer characterization). This part introduces the current employed approaches for karst aquifer modelling and explains why a general need for a better understanding of modelling of karst aquifers is essential.

(ii) Chapter 2 provides an example that single-continuum models are able to reproduce the general flow behaviour observed at a karst spring and that they can be employed to improve our understanding of the functioning of karst aquifers. In this particular case, the model was used to examine the potential cause of an observed change in the hydrograph response to recharge events of a binary karst system. The results support the hypothesis of a change of the properties of the conduit system within this karst aquifer, possibly due to sediment redistribution after a major flood event. This demonstrates the advantage of single-continuum models: on the one hand, they are able to account for geometrical features and their position within a catchment (as opposed to global models); on the other hand, they are easier to implement compared to hybrid or fracture models.

(iii) Chapter 3 also shows the usefulness of single-continuum models to mimic flow processes observed within karst aquifers. Indeed, the transient inter-catchment flow behaviour reported from the Lurbach system was successfully reproduced for different model settings. Moreover, the combination of the single-continuum approach with statistical methods (here time series analysis) helped to improve the understanding of the overflow. Since hybrid or fracture models until now are not able to simulate such an overflow process this is a promising result, which further supports the use of the single-continuum approach, as such overflow processes are frequently encountered in karst systems.

(iv) Chapter 4 supports the integration of turbulent or non-linear flow processes within single-continuum models to reproduce appropriately the flow dynamics observed within karst aquifers. As Chapters 2 and 3 described the limitations of the two previously existing turbulent flow packages (e.g. problems with the rewetting package or with inactive cells), it was a need to develop another package allowing a broader use of non-linear flow with single-continuum models. The Non-Linear Flow Process package (NLFP) was developed based on the non-linear Forchheimer flow law. The computation of turbulent flow for three benchmark scenarios and a large more realistic karst setting proved to be successful and encourage further use of this approach.

These results lead to several future research topics as the direct consequence of this work. All of them are listed below and have the potential to further improve the common use of single-continuum models in karst aquifers (compared to hybrid or fracture models).

(i) turbulent and non-linear flow modelling should be further developed and applied to a greater number of real karst systems. A promising research topic is the integration of transport simulations using single-continuum models under turbulent flow conditions.

(ii) the use of different synergetic methods (e.g. tracer tests data/time series analysis, as in chapters 2 and 3) with single-continuum model has to be generalized as it allows to improve the understanding of flow processes and reduces the equifinality of the model results.

(iii) the development of several guidelines for groundwater modelling in karst terrains is also a potential promising topic. These guidelines should serve as case study and help other users (i.e. practical appliers such as students or private companies) with similar modelling purposes.

APPENDICES

APPENDIX A

EIN BESSERES VERSTÄNDNIS DES LURBACH-KARSTSYSTEMS DURCH EIN KONZEPTIONELLES NIEDERSCHLAGS-ABFLUSS-MODELL

A BETTER UNDERSTANDING OF THE LURBACH KARST SYSTEM VIA A CONCEPTIONAL RAINFALL-RUNOFF MODEL

Published in Grundwasser as: *Wagner et al., 2013. Ein besseres Verständnis des Lurbach-Karstsystems durch ein konzeptionelles Niederschlags-Abfluss-Modell. Grundwasser, 18(4), 225-235. doi: 10.1007/s00767-013-0234-4.*

Zusammenfassung

Am Beispiel des Lurbach-Systems (Österreich) wird untersucht, inwieweit ein parameterarmes globales Niederschlags-Abfluss-Modell in einem komplexen Karstsystem anwendbar ist. Trotz geringer Anzahl an freien Modellparametern sind Abflusssimulationen über einen Zeitraum von sieben Jahren in zufriedenstellender Übereinstimmung mit den beobachteten Abflüssen. In der darauffolgenden rund vierjährigen Zeitperiode ist das Modell jedoch nur unter Verwendung stark veränderter Parameter in der Lage, das beobachtete Abflussverhalten nachzuvollziehen. Die kalibrierten Parameterwerte zeigen, dass in diesem Zeitraum der Abfluss zu benachbarten Einzugsgebieten und die Kapazität des Boden- oder Gebietsspeichers stark erhöht sind. Dies ist in Einklang mit Auswertungen von Markierungsversuchen und Trockenwetterfalllinien, die auf Änderungen der Eigenschaften des Quelleinzugsgebiets vermutlich durch Sedimentumlagerungen bei einem Starkniederschlagsereignis hindeuten. Solche dynamischen Prozesse können in Niederschlags-Abfluss-Modellen (noch) kaum berücksichtigt werden und bedingen daher erhebliche Prognoseunsicherheiten. Das vorgestellte Beispiel zeigt jedoch, dass ein parameterarmes hydrologisches Modell zur Charakterisierung von Quelleinzugsgebieten beitragen kann.

Abstract

A parsimonious lumped-parameter rainfall-runoff model was tested to determine if it could be used to appropriately represent a karst hydrological system, the Lurbach system in Austria. Simulated and observed hydrographs of spring discharge were favorably simulated for a time period of seven years in spite of the small number of free parameters. Following this period the four year discharge records were only reproducible using strongly different parameter values. Results suggest during this period overflow to neighboring catchments and the capacity of production or routing store have strongly increased. This relationship is also observed in tracer test and baseflow recession data sets and is attributed to the likely redistributions of sediments. Such dynamic processes are rarely accounted for in rainfall-runoff models, and may cause severe prediction uncertainties. However, in the Lurbach system a parsimonious hydrological model was used successfully to characterize changes in hydrological conditions.

Keywords: Karst - Rainfall-runoff model - Lumped-parameter - Groundwater exchange - Spring catchment - Sediment redistribution

1. Einleitung

Karstquellen tragen wesentlich zur Trinkwasserversorgung bei. Das Verständnis des Abflussverhaltens und die Bewertung der Vulnerabilität solcher Quellen sind daher wichtig. Für derartige hydrologische Fragestellungen könnten grundsätzlich physikalisch-basierte, distributive Modelle verwendet werden. Dabei ist allerdings die oft begrenzte Datengrundlage problematisch. Häufig sind nur Niederschlag, Lufttemperatur und Abfluss verfügbar (z. B. Jakeman & Hornberger 1993). Alternativ bieten sich parameterarme, globale („lumped-parameter“) Niederschlags- Abfluss-Modelle (N-A-Modelle) an. Diese Modelle finden ihre primäre Verwendung, um Niederschlagsereignisse und deren Auswirkungen auf das Abflussverhalten von Oberflächengewässern abbilden zu können (Perrin et al. 2001, Mouelhi et al. 2006), sind aber auch für Karstsysteme von Interesse, da meist die räumliche Lage und Geometrie der hochdurchlässigen Karsthohlräume und deren Interaktion mit der geklüfteten Gesteinsmatrix nur unzureichend bekannt sind (Rehrl & Birk 2010). Es wird zwar das (teilweise) Fehlen des physikalischen Hintergrundes dieser Modelle beanstandet (Abbott et al. 1986), zugleich aber auch eingesehen, dass eine für physikalisch-basierte distributive Modelle ausreichende hydrogeologische Charakterisierung sehr aufwendig ist und selbst dann das Problem besteht, dass die gemessenen kleinskaligen Werte in effektive Werte der Modellzellen umgerechnet werden müssen (z. B. Gupta et al. 2005). Ein distributives Modell wäre kaum eindeutig zu kalibrieren bzw. validieren, da es zu viele Unbekannte gibt, die aus dem Informationsgehalt von Niederschlag, Temperatur und Abfluss alleine nicht eindeutig zu bestimmen sind. Selbst globale Modelle leiden unter dem Prinzip der Zielgleichheit (Beven 1993). Modellansätze mit einer geringen Anzahl an Parametern können jedoch auf effiziente Art und Weise die Transformation von Niederschlag zu Abfluss abbilden (Perrin et al. 2001). Nach der Kalibrierung und Validierung solcher Modelle können die Parameterwerte im Hinblick auf die physikalische Relevanz interpretiert werden und somit potenziell einen Beitrag zur Charakterisierung des Einzugsgebietes leisten (Mouelhi et al. 2006). In Bezug auf die Anwendung in Karsteinzugsgebieten kommen Jeannin & Sauter (1998) jedoch zur Erkenntnis, dass globale Modelle zwar zum besseren Verständnis der Karst-Hydrodynamik beitragen können und zur Interpolation (Lücken füllen) und Extrapolation (Prognose) von Abflüssen nützlich sind, jedoch wenig zur Charakterisierung des Quelleinzugsgebietes geeignet sind. Globale N-A-Modelle zum besseren Verständnis bzw. zur Charakterisierung von Karst-Grundwassersystemen konnten jedoch mehrfach erfolgreich eingesetzt werden (z. B. Fleury et al. 2007, Geyer et al. 2008, Butscher & Huggenberger 2008, Hartmann et al. 2012). Am Beispiel des binären Lurbach-Karstsystems soll hier diskutiert werden, ob ein parameterarmes N-A-Modell für Prognosezwecke herangezogen werden kann und inwieweit es helfen kann, das konzeptionelle Verständnis des Karstgrundwasserleiters zu verbessern und damit zur Charakterisierung des Quelleinzugsgebietes beizutragen. Von besonderem Interesse ist, inwieweit eine augenscheinlich abrupte Änderung der Abflusscharakteristik der untersuchten Quelle nach einem Hochwasserereignis durch das verwendete Modell nachvollzogen werden kann.

2. Das Lurbach-System

Das Lurbach-System (LBS) ist ein binäres Karstsystem (d. h. Oberflächenabfluss aus einem nicht verkarsteten Teil des Einzugsgebietes speist über Schlucklöcher das Karstsystem) im Mittelsteirischen Karst des Grazer Paläozoikums etwa 15 km nördlich von Graz (Österreich; Abb. 1). Das Gebiet kann generell in das stark verkarstete Tannebenkarstplateau (~8 km^2) und das geringer durchlässige Semriacher Becken (~15 km^2) eingeteilt werden (Behrens et al. 1992). Das Semriacher Becken wird vom Lurbach (Abb. 1) in westlicher Richtung entwässert.

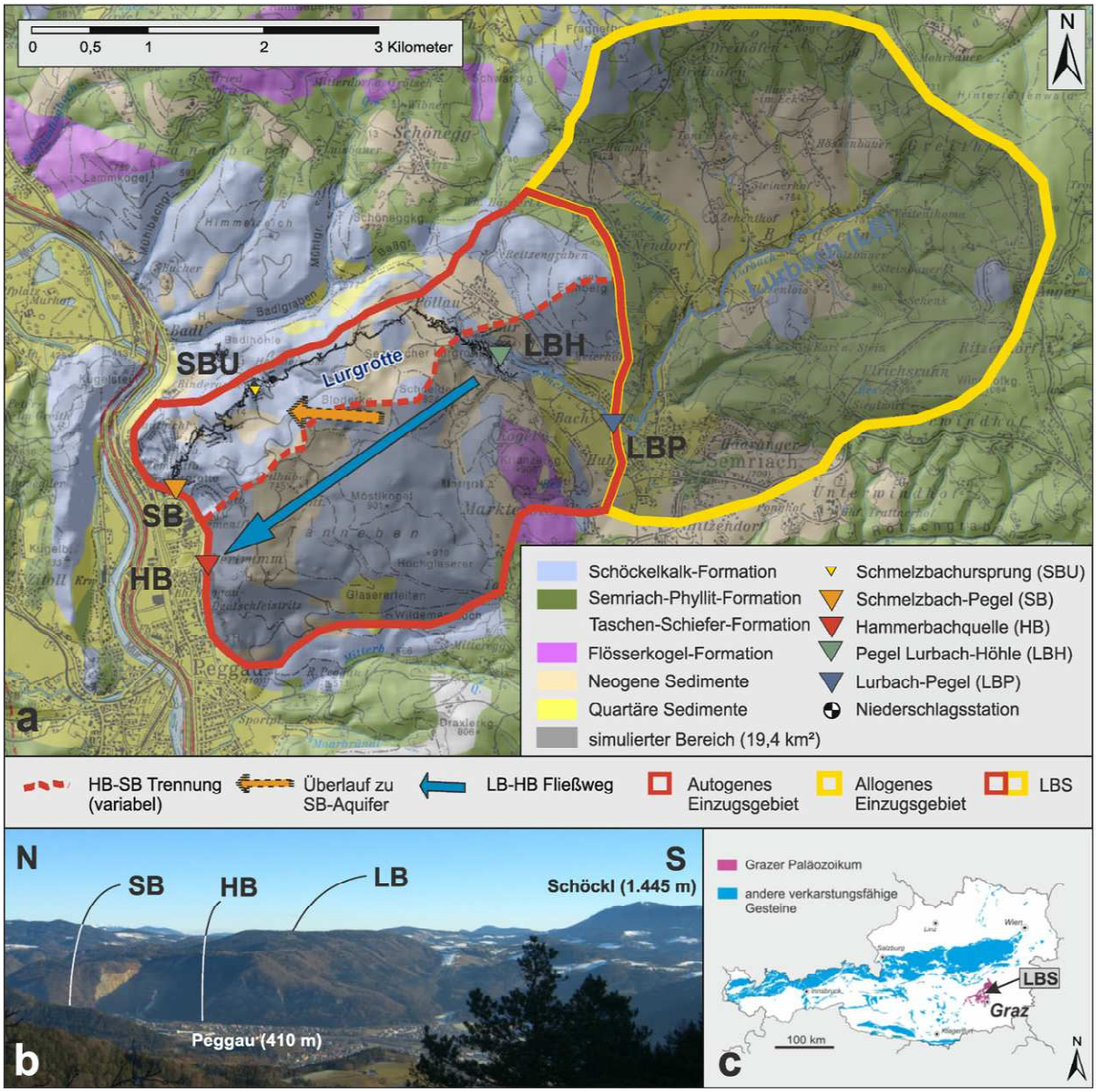

Abb. 1 Das Lurbachsystem. **(a)** Geologische Karte (basierend auf Geologische Bundesanstalt 2005; Blatt 164-Graz). Rotes Polygon: Karststock der Tanneben; gelbes Polygon: Einzugsgebiet des Lurbaches. Rot gestrichelte Linie: Hammerbach- und Schmelzbach-Aquifer bei Niedrigwasser (schematisch). **(b)** Die Peggauer Wand bzw. der Westabfall des Tannebenmassivs gesehen vom Gamskogel (859 m Seehöhe) aus. **(c)** Lage des Mittelsteirischen Karsts und des Lurbachsystems (LBS) (modifiziert nach Schubert 2003).

Der Lurbach verliert nach Übertreten der Schiefer-Kalk-Grenze Wasser in den Untergrund, bis er kurz nach dem Eintritt in die Lurgrotte in einem nicht weiter begehbaren Abschnitt zur Gänze verschwindet. Die Verbindungen zwischen Lurbachschwinde und den Quellen des Hammerbaches und des Schmelzbaches (HB u. SB; Abb. 1) auf der westlichen Seite des Tannebenstocks sind durch Markierungsversuche bestätigt (Behrens et al. 1992, Oswald 2009). Die Hammerbachquelle stellt unter Niedrigwasserbedingungen den einzigen Austritt des versickernden Lurbachwassers dar. Ihr Einzugsgebiet umfasst etwas weniger als 20 km^2 (Abb. 1a). Erst bei stärkerer Wasserführung der Hammerbachquelle (~200 l/s; Behrens et al. 1992) wird ein anteilhafter Austritt von Lurbachwasser am Schmelzbach beobachtet. Bei Starkniederschlägen kann zeitweise auch das Höhlensystem der Lurgrotte selbst als Fließweg genutzt werden. Aufgrund speläologischer Untersuchungen ist bekannt, dass diese Bereiche des LBS durch ein mehrstufiges Höhlensystem charakterisiert sind (Behrens et al. 1992, Wagner et al. 2010). Im Detail sind die Fließwege zwischen Lurbach und Hammerbachquelle nicht bekannt (erste Ansätze siehe Kübeck et al. 2013), jedoch sind hochdurchlässige, phreatische Röhrensysteme anzunehmen.

Für das Gesamteinzugsgebiet liegen langjährige Datensätze der Schüttung der Hammerbachquelle sowie Niederschlag und Lufttemperatur im Gebiet vor. Abflussdaten des Lurbaches (LBP – Lurbach-Pegel; LBH – Lurbach-Höhle) sowie des Schmelzbaches liegen nur für kurze Zeiträume vor. Eine Niederschlagsstation befindet sich in der Ortschaft Semriach und einige weitere in unmittelbarer Nähe des Einzugsgebietes. Eine innerhalb des Einzugsgebiets auf dem Tannebenplateau bei der Ertlhube (Abb. 1) gelegene Station wurde aufgrund großer Datenlücken nicht berücksichtigt. Ferner sind auch keine Grundwasserstände bekannt, da im Gesamteinzugsgebiet keine verwertbaren Bohrungen vorhanden sind. Folglich steht für das N-A-Modell nur die Schüttung der Hammerbachquelle sowie Niederschlag und Lufttemperatur zur Verfügung. Im Untersuchungsgebiet sind im Zeitbereich der Analyse (1998–2009) keine wesentlichen Änderungen der Landnutzung oder Bodenbeschaffenheit bekannt. Eine Sedimentsperre oberhalb der Lurgrotte wird jedoch gelegentlich ausgebaggert und kann somit die Versickerung entlang des Lurbaches beeinflussen. Der verkarstete Bereich des Tannebenmassivs ist dicht bewaldet und ein Großteil des Semriacher Beckens dient seit jeher der landwirtschaftlichen Nutzung. Schnee hat in diesem Einzugsgebiet aufgrund der geringen und kurzzeitigen Schneedecke zwar nur eine untergeordnete Bedeutung, jedoch sind Schneeschmelzereignisse im Frühjahr ausgeprägt genug, um diese mit zu berücksichtigen.

3. Niederschlags-Abfluss-Modellierung

Das konzeptionelle, globale N-A-Modell GR2M (Mouelhi et al. 2006) ist ein Wasserbilanzmodell mit monatlichem Zeitschritt. Das Modell benötigt Niederschlag und potenzielle Evapotranspiration (PET) als Eingangsgrößen sowie eine gemessene Abflussganglinie für die Modellkalibrierung. Da nur Niederschlag und Lufttemperatur direkt zur Verfügung stehen, wurde die PET nach Oudin et al. (2005) berechnet. Hierbei gehen neben der Lufttemperatur auch die geographische Lage des Einzugsgebietes und die Jahreszeit mit ein (um die extraterrestrische Sonnenstrahlung zu berechnen). Um die Effekte von festem Niederschlag, Schneespeicherung und Schneeschmelze aufgrund sich ändernder

Lufttemperatur zu berücksichtigen, wurde ein Schneemodell nach Xu et al. (1996) verwendet. Somit werden die PET und die Schneespeicherung entsprechend der bestehenden Datengrundlage nur mithilfe der Lufttemperatur beschrieben. Dieser vereinfachende Ansatz ist gerade bei nur eingeschränkt vorhandenen Messdaten etwa in alpinen Einzugsgebieten interessant.

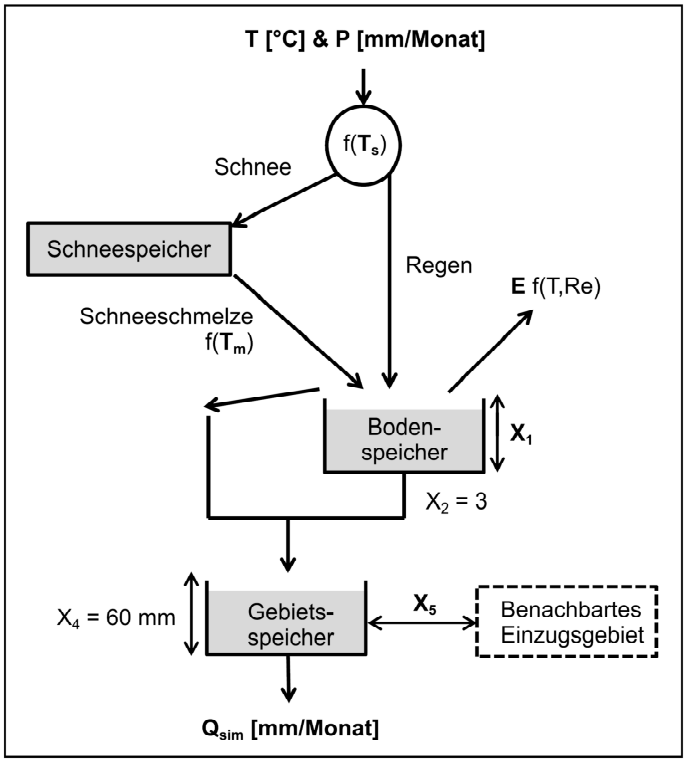

Abb. 2 Schematische Darstellung des N-A-Modells. *T*, *P* = gemessene Temperatur und Niederschlagshöhe; *E* = aktuelle Evapotranspiration; *Re* = extraterrestrische Sonnenstrahlung; *Qsim* = simulierte Abflusshöhe. Zwei Parameter für das Schneemodell (*Ts* und *Tm*), einer für die Kapazität des Bodenspeichers (*X*1), einer für den Austausch mit benachbarten Einzugsgebieten (*X*5). Die Kapazität des Gebietsspeichers (*X*4) und der Perkolationskoeffizient des Bodenspeichers (*X*2) sind im Standardmodell konstant. In zusätzlichen Modellrechnungen wurden diese teils als freie Parameter verwendet (siehe Tab. 1).

Abbildung 2 zeigt schematisch die verwendete Modellstruktur. Es werden die Prozesse Schneespeicherung und Schneeschmelze, Evapotranspiration, Boden- und Gebietsspeicherung sowie der Wasseraustausch mit benachbarten Einzugsgebieten berücksichtigt. Das Standardmodell (4Pb; Tab. 1) kommt mit nur 4 freien Parametern aus. Die Kapazität des Bodenspeichers (*X*1 [mm]; „production store“) sowie der Austauschkoeffizient (*X*5 [–]), der Ab- (*X*5 < 1) oder Zufluss (*X*5 > 1) aus bzw. von benachbarten Einzugsgebieten erlaubt, sind die zwei freien Parameter des N-A-Modells. Le Moine et al. (2007) konnten zeigen, dass die Verwendung eines Austauschterms in Wasserbilanzmodellen eine wichtige Rolle spielt. Insbesondere in Karstgebieten ist eine hydraulische Wechselwirkung zwischen Einzugsgebieten von großem Interesse. Im Falle des Lurbachsystems ist diese Funktionalität wohl wichtig, da ein Überlauf vom Hammerbach-zum Schmelzbachsystem bekannt ist. Der Perkolationskoeffizient des Bodenspeichers (*X*2 [–]) und die Kapazität des Gebietsspeichers (*X*4 [mm], „routing store“) wurden zunächst wie in Mouelhi et al. (2006) vorgeschlagen konstant gehalten (3 bzw. 60 mm). Durch das Schneemodell kommen als zwei weitere freie

Parameter die Schwellwerttemperaturen für die Trennung von Regen und Schneefall *Ts* [◦C] und der Beginn der Schneeschmelze *Tm* [◦C] hinzu. Um zu untersuchen inwieweit die verschiedenen Parameter bzw. die durch sie repräsentierten Komponenten des Karstsystems einen Einfluss auf die Güte der Modellanpassung und die Prognosefähigkeit des Modells haben, wurden ergänzend zu diesem Standardmodell (4Pb) Varianten mit 2 bis 6 freien Parametern getestet (Tab. 1). Die Niederschlagszeitreihe für die Modellierung wurde durch arithmetische Mittelung aus 6 Stationen in der Umgebung (Semriach und Eichberg (Abb. 1) sowie Frohnleiten, Gratkorn, Schöckl und St. Radegund) erhalten, da einzelne Stationen lückenhafte Datensätze haben und weil lokal ausgeprägte Niederschläge von einzelnen Stationen nicht immer erfasst werden. Temperaturdaten standen nur von der Station Eichberg auf der Murwestseite (Abb. 1; 610 m Seehöhe) für den Zeitraum von 1998–2009 zur Verfügung. Da für diesen Zeitraum auch Abflussdaten des Hammerbachs mit nur kleineren Lücken vorlagen, wurde die N-A-Modellierung für diesen Zeitraum durchgeführt. Die Modellkalibrierung erfolgte mithilfe des Solvers in Excel (Gradientenmethode).

		Modellvarianten							
		2 Parameter „GR2M“	3 Parameter	4 Parameter Variante a	4 Parameter **Standardmodell**	4 Parameter Variante c	5 Parameter	6 Parameter	
	Parameter	2P	3P	4Pa	4Pb	4Pc	5P	6P	**Parameter-beschreibung**
freie (zu kalibrierende) Modellparameter	X_1 [mm]	**Ja**	**Ja**	**Ja**	**Ja**	Nein	**Ja**	**Ja**	Kapazität des Bodenspeichers („production store“)
	X_5 [–]	**Ja**	Nein	Nein	**Ja**	**Ja**	**Ja**	**Ja**	Grundwasser-Austausch-Koeffizient
	T_S [°C]	Nein	**Ja**	**Ja**	**Ja**	**Ja**	**Ja**	**Ja**	Schneefall hört auf, sobald diese Temperatur überschritten wird
	T_M [°C]	Nein	**Ja**	**Ja**	**Ja**	**Ja**	**Ja**	**Ja**	Schneeschmelze setzt ein, sobald diese Temperatur überschritten wird
	X_4 [mm]	Nein	Nein	**Ja**	Nein	**Ja**	**Ja**	**Ja**	Kapazität des Gebietsspeichers („routing store“)
	X_2 [–]	Nein	Nein	Nein	Nein	Nein	Nein	**Ja**	Perkolations-koeffizient des Bodenspeichers

Tab. 1 Übersicht der unterschiedlichen Modellvarianten und der jeweilig verwendeten freien Parameter.

Um die Güte des simulierten Abflusses zu beurteilen, wurde das klassische Nash- Sutcliffe- (Nash & Sutcliffe 1970) sowie das logarithmisch und quadratwurzeltransformierte Nash-Sutcliffe-Effizienzkriterium verwendet. Die Zeitreihen wurden auf alle drei Kriterien gemeinsam optimiert um alle Bereiche des Quellhydrographen (Basisabfluss, Mittelwasser und Spitzenabfluss) gleichermaßen zu berücksichtigen (z. B. Perrin et al. 2001, Krause et al. 2005, Oudin et al. 2006). Der Anschaulichkeit halber wurden die Werte der Effizienzkriterien gemittelt, sodass ein Wertebereich zwischen $-\infty$ und 100 % entsteht. Als Nebenbedingung wurde verlangt, dass jedes einzelne der 3 Kriterien zumindest 60 % erreichen sollte. Zusätzlich wurden die Abweichung zwischen simulierter und beobachteter

Gesamtabflussmenge (Bias) und die Residuen der simulierten und beobachteten Einzelwerte berücksichtigt (hier nicht gezeigt). Die Modellkalibrierung und -validierung wurde nach dem Prinzip des „(differential) split-sample test“ (Klemes 1986) durchgeführt, d. h. es wurden verschiedene Zeitperioden für die Kalibrierung und Validierung definiert. Es wurden drei Zeitabschnitte gewählt, die ein sehr unterschiedliches hydrologisches Verhalten zeigen, einerseits eine gegenüber früheren Aufzeichnungen ungewöhnlich gedämpfte Abflussdynamik nach einem Hochwasserereignis (September 2005 bis Juni 2009) und andererseits einen Zeitraum mit ausgeprägten Niedrigwasserperioden (Juli 2001 bis Juli 2005) sowie einen Zeitbereich, der eher unauffällig („normal“) erscheint (Juli 1998 bis Juli 2001). Zusätzlich wurde der Zeitraum von Juli 2000 bis Juli 2003 gesondert betrachtet, da dieser nur die Niedrigwasserperioden sowie das Trockenjahr 2003 beinhaltet und somit eine weitere Herausforderung im Hinblick auf die Prognosefähigkeit des Modells darstellt. Ergänzend wurde für jede der oben genannten Kalibrierungsperioden auch die Anpassung an die gesamte Datenreihe (Juli 1998 bis Dezember 2009) betrachtet. Um geeignete Anfangsbedingungen zu schaffen, wurden die Wasserstände in den jeweiligen Speichern durch mehrjährige Simulationsperioden (Aufwärmphasen) vor den zu analysierenden Zeiträumen eingestellt. Da Lufttemperaturdaten erst ab 1998 vorliegen, wurden für die Aufwärmphase Monatsmittelwerte der vorhandenen Zeitreihe verwendet.

4. Ergebnisse

Die Kalibrierung und Validierung des Standardmodells (4Pb) an unterschiedlichen Zeitfenstern zeigt generell eine zufriedenstellende Übereinstimmung bis 2005, nicht jedoch für die Zeit danach (Abb. 3 und Tab. 2). Je nach Zeitperiode erreicht das kalibrierte Modell Effizienzkriterien von 55 % bis 79 %, für den Zeitbereich 2005–2009 jedoch nur 28 %. Bei der Validierung ergeben sich in der Regel Effizienzkriterien von wenig unter 50 %, für den Zeitbereich 2005–2009 jedoch stark negative Werte. Entsprechend ergeben sich auch bei Anwendung der kalibrierten Modelle auf die ganze Zeitreihe (1998–2009) etwas geringere Effizienzkriterien (12 % bis 46 %). Für die Periode nach dem Niederschlagsereignis vom August 2005 bis etwa Juni 2009 kann mit den für andere Zeitbereiche kalibrierten Modellen nicht einmal eine minimal zulässige Übereinstimmung (d. h. Werte sind deutlich negativ) gefunden werden (Abb. 3; Tab. 2). Umgekehrt ergibt sich mit dem Parametersatz aus der Kalibrierung für diesen Zeitraum bei Validierung in anderen Zeiträumen keine zufriedenstellende Anpassung. Ebenso werden die geringen Abflüsse der Sommermonate Juli bis September des Trockenjahrs 2003 vom Modell nicht zutreffend simuliert (Abb. 3). Die Niedrigwasserperioden der Jahre 2000 und 2001 werden dagegen recht gut vom Modell nachvollzogen. Betrachtet man die optimalen Parametersätze, die sich für die jeweiligen Zeitbereiche ergeben (Tab. 2), so fällt auf, dass die Kapazität des Bodenspeichers ($X1$) und der Austauschkoeffizient ($X5$) für den Zeitbereich 2005–2009 gegenüber den anderen Perioden deutlich erhöht bzw. erniedrigt sind. Im vorliegenden Fall mit $X5 < 1$ zeigen erniedrigte Werte des Austauschkoeffizienten einen zunehmenden Abfluss in ein anderes Einzugsgebiet an. Effizienzkriterien und Parametersätze von Modellvarianten mit unterschiedlich gewählten freien Parametern sind ebenfalls in Tabelle 2 aufgelistet. Generell ist festzustellen, dass mit keiner Modellvariante eine zufriedenstellende Simulation der

ganzen Zeitreihe möglich ist; die Periode 2005–2009 wird nicht zufriedenstellend simuliert, wenn das Modell auf andere Zeiträume kalibriert wird, und ein auf diese Zeitperiode kalibriertes Modell versagt bei Anwendung auf andere Zeiträume. Beispielhaft sind in Abbildung 4 die simulierten Quellschüttungen der unterschiedlichen Modelle im Vergleich zur Beobachtung durch Kalibrierung auf die Zeitreihe 2001–2005 dargestellt. Wird das Schneemodell weggelassen (Modellvariante „2P“), ergeben sich keine grundlegenden Verschlechterungen bei den Effizienzkriterien. Dies lässt darauf schließen, dass Schneespeicherung und -schmelze zumindest für das Monatsmodell an diesem Standort nicht sehr wichtig sind. Bei Anwendung in stärker alpinen Bereichen (z. B. Wagner et al. 2012) sind diese Prozesse jedoch auch im Monatsmodell von hoher Bedeutung.

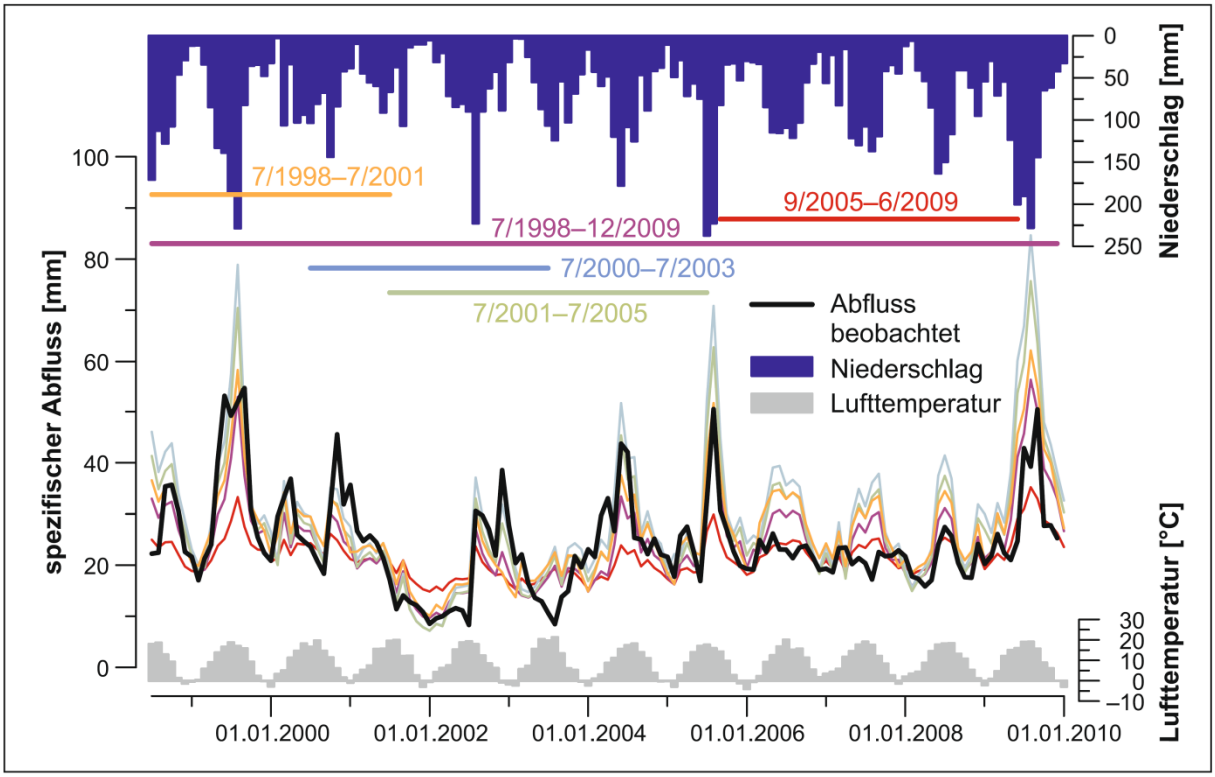

Abb. 3 Beobachtete und simulierte Abflussganglinien der Hammerbachquelle sowie Niederschlagssummen und Temperaturen repräsentativ für das Einzugsgebiet auf Monatsbasis. Die Farbe der Zeitbalken entspricht jener der simulierten Ganglinie, die bei Kalibrierung im entsprechenden Zeitraum erhalten wird (s. Abb. 4).

Eine wesentliche Verschlechterung der Effizienzkriterien ist hingegen sowohl beim 3-Parameter-Modell (3P) als auch beim 4-Parameter-Modell ohne Austauschterm (4Pa) zu beobachten. Lediglich in den Zeiträumen, die durch Niedrigwasserperioden geprägt sind (2001–2005 bzw. 2000– 2003) erreichen diese Modellvarianten Effizienz-Kriterien von über 50 %. Bei der Kalibrierung oder Validierung in anderen Zeiträumen erweisen sich die Varianten ohne Austauschterm dagegen als ungenügend. Im Zeitraum des gedämpften Verhaltens sind selbst beim Kalibrieren stark negative Effizienzkriterien und damit ein Versagen des Modells zu beobachten. Somit scheint in dieser Periode der Austauschterm von großer Bedeutung zu sein. Verwendet man im 4-Parameter-Modell (P4c) statt der Kapazität des Bodenspeichers die des Gebietsspeichers ($X4$ statt $X1$), so ergeben sich vergleichbare Effizienzkriterien (Tab. 2). Auch hier zeigt sich die Notwendigkeit einer starken Erhöhung

des (Gebiets-) Speichers, um das gedämpfte Verhalten in den Jahren 2005 bis 2009 zu reproduzieren. In beiden Modellvarianten (4Pb und 4Pc) gibt es jeweils einen freien Parameter, der die Speicherung beeinflusst, und in beiden ist eine Erhöhung der jeweiligen Speicherkapazität (im Standardmodell *X*1 und in der Modellvariante 4Pc *X*4) notwendig, um das Modell im Zeitbereich 2005–2009 zu kalibrieren. Dies legt den Schluss nahe, dass in dieser Zeit das Speichervermögen im Quelleinzugsgebiet erhöht war, erlaubt jedoch keine eindeutigen Schlüsse in Bezug auf die Art des sich ändernden Speichers. Wird die Kapazität des Gebietsspeichers (*X*4) zusätzlich zu den anderen vier freien Parametern angepasst, so ergibt sich eine geringe Verbesserung der Effizienzkriterien beim Kalibrieren, aber teilweise ein leichter Rückgang beim Validieren. In Übereinstimmung mit den Ergebnissen von Mouelhi et al. (2006) erweist sich ein zusätzlicher (fünfter) freier Parameter hier demnach als kaum gerechtfertigt. Auch mit diesem Modellansatz (5P) ist deutlich zu erkennen, dass der Austausch und die Kapazität des Bodenspeichers in der Periode von 2005 bis 2009 erhöht werden müssen. Die zusätzliche Anpassung des Perkolationskoeffizienten des Bodenspeichers (*X*2) im 6-Parameter-Modell (6P) verbessert die Güte der Kalibrierung weiter. *X*2 schwankt jedoch nur wenig und der Anstieg der Effizienzkriterien bei der Validierung ist nur gering; teilweise sind sogar geringere Effizienzkriterien als bei Modellvarianten mit weniger freien Parametern zu beobachten, was auf eine Überparametrisierung hinweist (Beven 1989, Perrin et al. 2003). Auch hier sind wieder gegenüber den anderen Zeitperioden eine Erhöhung der Kapazität des Bodenspeichers und eine Erniedrigung des Austauschkoeffizienten in der Periode 2005–2009 erforderlich.

N-S-Effizienzkriterien [%]		Kalibrierungszeitraum											
		07/1998–07/2001			07/2001–07/2005			09/2005–06/2009			07/2000–07/2003		
Validierungszeitraum	07/1998–07/2001	52,2	–42,4	15,2	45,3	–42,7	6,8	–15,7	–51,4	8,2	32,8	–42,5	6,1
		54,6	**55,2**	58,9	44,0	**46,4**	43,2	20,1	**–13,6**	–2,9	30,3	**33,6**	41,1
			57,7			41,4			–7,6			29,5	
	07/2001–07/2005	56,4	11,4	32,1	64,6	15,1	52,4	20,4	5,3	26,8	59,8	14,9	51,1
		53,4	**48,6**	54,6	74,4	**65,0**	77,6	43,5	**19,2**	30,6	68,6	**60,1**	73,5
			46,1			73,4			21,5			66,7	
	09/2005–06/2009	–252	–1384,1	–1130,5	–323,4	–1394,5	–964,2	22,7	–1319,6	–860,8	–590,5	–1420,5	–988,3
		–403,3	**–269,6**	–244,2	–314,5	**–328**	–243	–1,8	**27,7**	42,9	–594,3	**–588,4**	–408,1
			–259,1			–352,8			34,3			–625,1	
	07/2000–07/2003	67,9	59,7	66,5	75,7	62,0	80,8	36,5	51,5	46,9	79,0	62,4	82,1
		62,6	**56,8**	63,8	81,4	**75,9**	86,3	39,9	**33,7**	44,6	85,6	**78,9**	89,4
			54,3			81,5			39,0			85,1	
	07/1998–12/2009	49,7	–98,1	–43,3	38,5	–94,6	–26,5	33,4	–104,7	–11,4	12,0	–94,7	–32,1
		26,1	**46,1**	48,4	36,8	**38,4**	45,5	47,9	**33,8**	42,4	9,5	**12,4**	33,2
			46,0			30,6			37,0			7,9	
Modelparameter	X_1 [mm]	4048,09	695,06	326,36	1958,63	788,40	317,98	18361,29	506,23	303,38	1595,59	843,87	307,66
		403,43	**3987,82**	2898,65	403,43	**1964,51**	1052,58	403,43	**17712,04**	9200,38	403,43	**1598,79**	1233,98
			3554,61			415,30			13147,67			823,86	
	X_5 [–]	0,80	1,00	1,00	0,84	1,00	1,00	0,66	1,00	1,00	0,89	1,00	1,00
		0,97	**0,80**	0,81	0,97	**0,84**	0,89	0,96	**0,66**	0,63	0,98	**0,89**	0,88
			0,86			0,97			0,77			0,97	
	T_S [°C]	–	0,37	1,32	–	–0,08	–0,93	–	–0,03	18,45	–	0,29	–1,23
		1,35	**1,58**	0,91	–1,83	**–1,12**	–1,11	–0,294	**0,60**	0,43	–1,99	**–1,04**	–0,62
			0,76			–1,19			0,08			–0,898	
	T_M [°C]	–	–2,19	1,31	–	–3,83	–2,15	–	–5,14	–7,16	–	–3,52	–1,40
		1,32	**–0,83**	0,78	–3,62	**–4,49**	–3,99	–2,47	**–1,42**	–1,21	–6,67	**–5,72**	–5,82
			0,59			–4,38			–1,45			–5,99	
	X_4 [mm]	60,00	60,00	1094,75	60,00	60,00	973,98	60,00	60,00	4978,78	60,00	60,00	805,40
		1440,17	**60,00**	105,86	1129,97	**60,00**	310,53	3090,39	**60,00**	67,65	808,31	**60,00**	204,01
			179,96			812,66			203,44			406,82	
	X_2 [–]	3,00	3,00	3,00	3,00	3,00	3,00	3,00	3,00	3,00	3,00	3,00	3,00
		3,00	**3,00**	2,39	3,00	**3,00**	2,05	3,00	**3,00**	2,16	3,00	**3,00**	1,98
			3,00			3,00			3,00			3,00	

Legende:

Tab. 2 Mittelwert der drei Nash-Sutcliffe-Effizienzkriterien (in %) des N-A-Modells für die jeweiligen Zeitbereiche in denen das Modell kalibriert bzw. validiert wurde (siehe Abb. 3). Die Zahl in der Mitte jeder Box bezieht sich auf das Standardmodell („4Pb“). Die umliegenden kleineren Zahlen beziehen sich auf unterschiedliche Modellvarianten (Tab. 1) entsprechend der Legende. Der untere Teil der Tabelle listet die kalibrierten Modellparameter der einzelnen Perioden bzw. Modellvarianten auf.

5. Diskussion

Der hier verwendete globale Modellansatz liefert selbst mit nur zwei freien Parametern akzeptable Effizienzkriterien bei der Modellkalibrierung. Angesichts der Komplexität des betrachteten binären Karstsystems erweist sich das Modell auch bei der Validierung im Zeitraum bis 2005 als zufrieden stellend und erscheint daher für Prognosezwecke grundsätzlich geeignet. Unabhängig von der Zahl der kalibrierten Modellparameter wird jedoch die Niedrigwasserperiode im Jahr 2003 nicht zutreffend simuliert, selbst wenn sie in den für die Kalibrierung verwendeten Zeitraum (2001–2005) fällt (Abb. 4). Dies legt den Schluss nahe, dass die vereinfachte Abbildung der Abflussbildungsprozesse in der gegebenen Modellstruktur für zuverlässige Prognosen sommerlicher Niedrigwasserperioden nicht ausreicht, sodass hier der Ansatz von instationären Modellparametern, die sich z. B. zwischen trockenen und feuchten Jahren unterscheiden können, notwendig erscheint (Long & Mahler 2013).

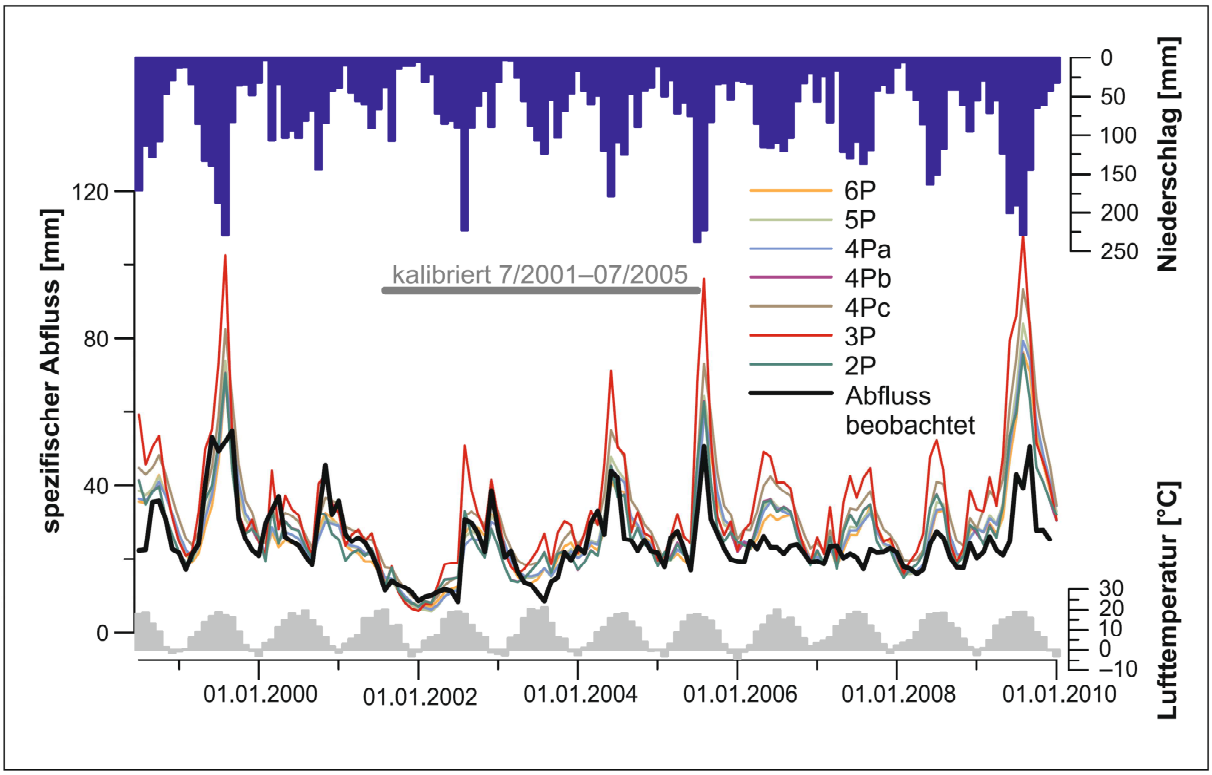

Abb. 4 Beobachtete und simulierte Abflussganglinien der Hammerbachquelle bei Kalibrierung auf den Zeitraum 2001–2005 unter Verwendung der unterschiedlichen Modellvarianten (Tab. 1).

Aus den zuvor erwähnten Markierungsversuchen (Behrens et al. 1992) ist bekannt, dass sich die unterirdischen Abflussverhältnisse in diesem Karstsystem bei Niedrigwassersituationen gegenüber Mittel- oder Hochwassersituationen stark unterscheiden. In Übereinstimmung mit der Beobachtung, dass bei Niedrigwasser keine Verbindung zwischen Hammerbach und Schmelzbach besteht, ergibt sich bei Kalibrierung mit dem durch ausgeprägte Niedrigwassersituationen gekennzeichneten Zeitraum 2000–2003 der höchste Werte für den Austauschkoeffizienten und damit der geringste Wasseraustausch im Modell. Aus demselben Grund ist in diesem (und nur in diesem) Zeitraum auch die Kalibrierung von Modellvarianten ohne Austausch ($X5 = 1$) erfolgreich. Der in anderen Zeiträumen stärkere Abfluss vom Hammerbach ins Schmelzbacheinzugsgebiet kann von diesen Modellen jedoch nicht nachgebildet werden. Umgekehrt gelingt die Simulation der Niedrigwasserperioden mit geringem oder ohne Wasseraustausch nur bedingt, wenn im Kalibrierungszeitraum eher Mittel- oder Hochwassersituationen vorherrschen. Der Einbau eines Schwellwertes, nach dessen Überschreiten der Austausch erst aktiv wird, brachte keine Verbesserung des Modells. Offenbar kann ein Monatsmodell aufgrund der hohen kurzzeitigen Variabilität der Quellschüttung dieses Schwellenwertverhalten nicht zutreffend abbilden. Bei Verwendung einer höheren zeitlichen Auflösung (Tagesmodell) wäre dieser Ansatz aber vermutlich vielversprechend. Im Gegensatz zu den akzeptablen Simulationsergebnissen für den Zeitraum bis 2005, versagt das Modell im Zeitraum 2005–2009. Selbst bei der Kalibrierung liegen die Effizienzkriterien allerModellvarianten deutlich unter 50%und bei der Validierung mit anderen Zeiträumen ergeben sich stark negative Effizienzkriterien. Der Austauschkoeffizient $X5$ ist für diesen Zeitraum kleiner als bei allen anderen Kalibrierungsperioden (Tab. 2). Das

bedeutet, dass in diesem Zeitraum ein größerer Abfluss vom Hammerbach- zum Schmelzbachsystem angenommen werden muss.

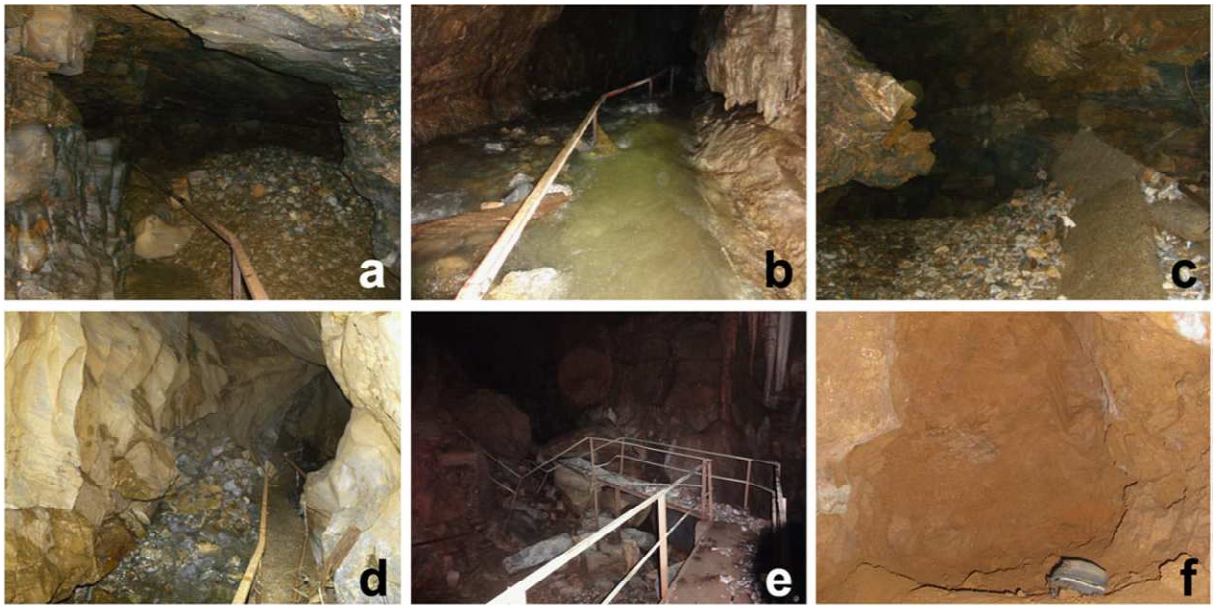

Abb. 5 Feldeindrücke der befahrbaren Teile der Lurgrotte. **(a)** Sedimentumlagerungen im Schauhöhlenbereich der Lurgrotte, Sept. 2008. **(b)** Aktives Gerinne des SB-Höhlenbaches bei erhöhter Wasserführung, Juli 2012. **(c)** Beschädigte Führungssteige in der Lurgrotte 2008. **(d)** Sedimentablagerungen beim Schmelzbachursprung nach einem Hochwasser im Juni 2012. **(e)** Zerstörter Führungssteig im Bereich Blocksberg nach einem Hochwasser im August 2009. **(f)** Mit Sediment verlegte ehemals phreatische Gänge im Tannebenmassiv (Josefinenhöhle; 425 m), vermutlich pleistozänen Alters, November 2008.

Dies ist mit Feldbeobachtungen konsistent. Während eines Markierungsversuchs im Jahre 2008 (Oswald 2009, Wagner et al. 2011) konnte gezeigt werden, dass der Überlauf ins Schmelzbachsystem bereits bei einem gegenüber früheren Untersuchungen geringeren Abfluss des Hammerbachs stattfand (etwa 135 l/s statt 200 l/s) und gleichzeitig der Markierungsstoff verhältnismäßig lange Durchgangszeiten aufwies (> 60 h gegenüber < 40 h bei vergleichbarem Abfluss in früheren Untersuchungen). Gleichzeitig ist in diesem Zeitraum im Modell eine Erhöhung der Speicherung erforderlich, um das gedämpfte Auslaufverhalten der Hammerbachquelle zu ermöglichen. Dies wirft die Frage auf, ob und welche Vorgänge im Hammerbachsystem zu einer Vergrößerung der Speicherkapazität und einem Überlauf ins Schmelzbachsystem bei gegenüber früheren Beobachtungen geringeren Abflüssen geführt haben könnte. In diesem Zusammenhang ist festzuhalten, dass das Abflussverhalten des Hammerbachs ab Ende 2009 anscheinend wieder sprunghafter wird (Abb. 3). Angesichts der in den begehbaren Teilen der Höhle nach größeren Flutereignissen beobachtbaren Sedimentumlagerungen (Abb. 5) liegt es nahe, diese Reversibilität durch ähnliche Vorgänge im Hammerbachsystem zu erklären. Wie von Covington et al. (2009, 2012) gezeigt, sind etwa durch Sedimentablagerungen geschaffene Engstellen plausible geometrische Strukturen, um ein gedämpftes Verhalten einer Quelle zu verursachen. Solche Verengungen würden zudem einen Anstieg des Wasserspiegels oberstromig bewirken und somit einen Überlauf in das benachbarte Schmelzbachsystem bereits bei geringerem Abfluss des Hammerbachs und damit den erhöhten Austauschfluss im Modell im Zeitraum 2005– 2009 erklären. Die Hypothese, dass das gedämpfte Abflussverhalten des Hammerbachs durch Veränderungen im

Karstsystem und nicht durch unterschiedliche Witterungsbedingungen verursacht ist, wird durch die Auswertung von Trockenwetterfalllinien in den unterschiedlichen Zeiträumen gestützt: Vor 2005 zeigt sich generell ein rascheres Auslaufen mit geringeren Basisabflüssen der Hammerbachquelle als im Zeitraum 2005–2009 (Birk &Wagner 2011). Da das Auslaufverhalten von Quellen in Trockenperioden primär durch die hydraulischen Eigenschaften des Grundwasserleiters bestimmt wird, liegt es nahe, dies strukturellen Änderungen im System selbst zuzuschreiben (Kresic & Bonacci 2010, S. 134). Sollte die beobachtete Veränderung des Abflussverhaltens der Hammerbachquelle tatsächlich aufgrund von Sedimentumlagerungen und damit verbundene Änderungen in den hydraulischen Eigenschaften des Karstgrundwasserleiters verursacht sein, so ist es nicht verwunderlich, dass die Kalibrierung in diesem Zeitraum stark veränderte Parameter ergibt. Ein ähnliches Ergebnis wäre dann allerdings auch für physikalisch-basierte Modelle zu erwarten. In Modellszenarien mit MODFLOW kann eine derartige Veränderung des Abflussverhaltens beispielsweise durch Herabsetzung der hydraulischen Leitfähigkeit und Erhöhung des Speicherkoeffizienten von Modellzellen, die den hochdurchlässigen Fließweg von der Lurbachschwinde zum Hammerbach repräsentieren, bewirkt werden (Mayaud et al. 2013). Bis dato werden nach Kenntnis der Autoren allerdings in keinem physikalisch-basierten N-A-Modell durch Sedimenttransport und -ablagerung bedingte Änderungen in Fließquerschnitten (bis hin zu möglichen Verstopfungen von Fließwegen) berücksichtigt (erste Ansätze siehe Covington et al. 2010).

6. Schlussfolgerungen

Zusammenfassend kann festgestellt werden, dass ein parameterarmes N-A-Modell zwar die Quellschüttung des Hammerbaches bis 2005 simulieren kann, nicht aber im Zeit raum 2005 bis 2009. Nur durch Verwendung anderer Parameterwerte kann in diesem Zeitraum eine minimal akzeptable Übereinstimmung gefunden werden. Die erforderlichen Parameteränderungen sind jedoch konzeptionell in Übereinstimmung mit Ergebnissen aus Markierungsversuchen und Auswertungen von Trockenwetterfalllinien, die in diesem Zeitraum auf einen gegenüber früheren Zeiten erhöhten Speicher und einen häufigeren Überlauf zum Schmelzbach hindeuten. Als mögliche Ursache kommen Sedimentumlagerungen während des Hochwasserereignisses im Sommer 2005 in Frage. Durch derartige Prozesse verursachte Parameteränderungen stellen zwangsläufig die Prognosefähigkeit hydrologischer Modelle in Frage. Insofern zeigt sich, dass die hier offenkundige Dynamik von Karstsystemen große Herausforderungen bezüglich hydrologischer Prognosen stellt. Das hier vorgestellte Beispiel zeigt jedoch, dass die Anwendung des konzeptionellen hydrologischen Modells wertvolle Rückschlüsse auf Abflussprozesse und Eigenschaften im Karstsystem erlaubt und damit zur hydrogeologischen Charakterisierung des Quelleinzugsgebietes beiträgt. Die aus der Modellkalibrierung erhaltenen Parameterwerte haben zwar keine unmittelbare physikalische Bedeutung, können jedoch im Sinne konzeptioneller Modellvorstellung interpretiert werden und tragen damit zu einem besseren Prozessverständnis bei. Die untersuchten Modellvarianten zeigen eine in diesem Quelleinzugsgebiet untergeordnete Rolle der Schneespeicherung. Dagegen wird das Abflussverhalten der Quelle bei Mittel- und Hochwasserbedingungen stark vom Überlauf

zum benachbarten Einzugsgebiet beeinflusst. Im vorliegenden Fall können die Modellergebnisse zudem dahingehend bewertet werden, dass die beobachtete Veränderung im Abflussverhalten nicht primär auf Änderungen der meteorologischen Eingangsgrößen, sondern auf Änderungen im Karstsystem (erhöhte Speichereigenschaften, verstärkter Überlauf zum benachbarten Einzugsgebiet) selbst zurückzuführen sind.

Danksagung

Die Daten wurden vom Hydrographischen Dienst Steiermark zur Verfügung gestellt. Dem Team der Lurgrotte Peggau sei für die gute Zusammenarbeit herzlich gedankt. Wir danken dem Land Steiermark (Fachabteilung GIS-Steiermark) für die Bereitstellung der digitalen geologischen Karte sowie des zugrunde liegenden Höhenmodells. Diese Arbeit wurde von der Österreichischen Akademie der Wissenschaften ÖAW (Projekt: Global models of spring catchments) und dem Austrian Science Fund (FWF): L 576-N21 finanziell unterstützt.

Literatur

Abbott, M.B., Bathurst, J.C., Cunge, J.A., O'Connell, P.E., Rasmussen, J.: An introduction to the European hydrological system—systeme hydrologique europeen, "SHE", 1_: history and philosophy of a physically-based, distributed modelling system. J. Hydrol. 87, 45–59 (1986)

Behrens, H., Benischke, R., Bricelj, M., Harum, T., Käss, W., Kosi, G., Leditzky, H.P., Leibundgut, C., Maloszewski, P., Maurin, V., Rajner, V., Rank, D., Reichert, B., Stadler, H., Stichler, W., Trimborn, P., Zojer, H., Zupan, M.: Investigations with natural and artificial tracers in the karst aquifer of the Lurbach system (Peggau-Tanneben-Semriach. Austria Steir. Beitr. Hydrogeol. 43, 9–158 (1992)

Beven, K.: Changing ideas in hydrology—the case of physically based models. J. Hydrol. 105, 157–172 (1989)

Beven, K.: Prophecy, reality and uncertainty in distributed hydrological modelling. Adv. Water Resour. 16, 41–51 (1993)

Birk, S., Wagner, T.: New directions in the application of hydrograph recession models to karst aquifers, IAMG 2011 Publication (2011). In: Proc. IAMG 2011 Conference, Salzburg, September 5–9, 2011. doi:10.5242/iamg.2011.0261

Butscher, C., Huggenberger, P.: Intrinsic vulnerability assessment in karst areas: a numerical modelling approach. Water Resour. Res. 44, W03408 (2008)

Covington, M.D., Wicks, C.M., Saar, M.O.: A dimensionless number describing the effects of recharge and geometry on discharge from simple karstic aquifers. Water Resour. Res. 45, W11410 (2009). doi:10.1029/2009WR008004

Covington, M.D., Luhmann, A.J., Wicks, C., Saar, M.O.: Process length scales: a conceptual tool for karst hydrogeology, geomorphology, and hydroecology. Geol. Soc. Am. Abstracts Programs 42(5), 329 (2010)

Covington, M.D., Banwell, A.F., Gulley, J., Saar, M.O., Willis, I., Wicks, C.M.: Quantifying the effects of glacier conduit geometry and recharge on proglacial hydrograph form. J. Hydrol. 414–415, 59–71 (2012)

Fleury, P., Plagnes, V., Bakalowicz, M.: Modelling of the functioning of karst aquifers with a reservoir model: application to fontaine de vaucluse (South of France). J. Hydrol. 345, 38–49 (2007)

Bundesanstalt, G.: Provisorische Geologische Karte der Republik Österreich, 164–Graz. – Geofast 1:50.000. Wien, Geologische Bundesanstalt (2005)

Geyer, T., Birk, S., Liedl, R., Sauter, M.: Quantification of temporal distribution of recharge in karst systems from spring hydrographs. J. Hydrol. 348, 452–463 (2008)

Gupta, H.V., Beven, K.J., Wagener, T.: Model Calibration and Uncertainty Estimation. Encyclopedia of Hydrological Sciences, Bd. 3, S. 2015–2032. Wiley, Chichester (2005). Part 11, Section 131

Hartmann, A., Lange, J., Weiler, M., Arbel, Y., Greenbaum, N.: A new approach to model the spatial and temporal variability of recharge to karst aquifers. Hydrol. Earth Syst. Sci. 16(7), 2219–2231 (2012)

Jakeman, A.J., Hornberger, G.M.: How much complexity is warranted in a rainfall-runoff model? Water Resour. Bull. 29(8), 2637–2649 (1993)

Jeannin, P.Y., Sauter, M.: Analysis of karst hydrodynamic behaviour using global approaches: a review. Bull. Hydrogéol. (Neuchâtel) 16, 31–48 (1998)

Klemes, V.: Operational testing of hydrological simulation models. Hydrolog. Sci. 31, 13–24 (1986)

Krause, P., Boyle, D.P., Bäse, F.: Comparison of different efficiency criteria for hydrological model assessment. Adv. Geosci. 5, 89– 97 (2005)

Kresic, N., Bonacci, O.: Spring discharge hydrograph. In: Kresic, N., Stevanovic, Z. (Hrsg.) Groundwater Hydrology of Springs: Engineering, Theory, Management, and Sustainability, S. 129–163. Elsevier, Amsterdam (2010). Chapter 4

Kübeck, C., Maloszewski, P.J., Benischke, R.: Determination of the conduit structure in a karst aquifer based on tracer data—Lurbach system. Austria Hydrol. Process. 27, 225–235 (2013)

Le Moine, N., Andréassian, V., Perrin, C., Michel, C.: How can rainfall-runoff models handle intercatchment groundwater flows? Theoretical study based on 1040 French catchments. Water Resour. Res. 43, W06428 (2007). doi:10.1029/2006WR005608

Long, A.J., Mahler, B.J.: Prediction, time variance, and classification of hydraulic responses to recharge in two karst aquifers. Hydrol. Earth Syst. Sci. 17, 281–294 (2013)

Mayaud, C., Wagner, T., Benischke, R., Birk, S.: Understanding changes in the hydrological behaviour within a karst aquifer (Lurbach system, Austria). Carbonate Evaporite (2013). doi:10.1007/s13146-013- 0172-3

Mouelhi, S.,Michel, C., Perrin, C., Andréassian, V.: Stepwise development of a two-parameter monthly water balance model. J. Hydrol. 318, 200–214 (2006)

Nash, J.E., Sutcliffe, J.V.: River flow forecasting through conceptual models. Part I—A discussion of principles. J. Hydrol. 27(3), 282– 290 (1970)

Oswald, S.: Künstliche und natürliche Tracer in einem Karsteinzugsgebiet mit allochthoner Neubildung (Lurbach, Österreich) (2009)

Oudin, L., Hervieu, F., Michel, C., Perrin, C., Andréassian, V., Anctil, F., Loumagne, C.: Which potential evapotranspiration input for a lumped rainfall-runoff model? Part 2—Towards a simple and efficient potential evapotranspiration model for rainfall-runoff modelling. J. Hydrol. 303, 290–306 (2005)

Oudin, L., Andréassian, V., Mathevet, T., Perrin, C., Michel, C.: Dynamic averaging of rainfall-runoff model simulations from complementary model parameterizations. Water Resour. Res. 42, W07410 (2006). doi:10.1029/2005WR004636

Perrin, C., Michel, C., Andréassian, V.: Does a large number of parameters enhance model performance? Comparative assessment of common catchment model structures on 429 catchments. J. Hydrol. 242, 275–301 (2001)

Perrin, C., Michel, C., Andréassian, V.: Improvement of a parsimonious model for streamflow simulation. J. Hydrol. 279, 275–289 (2003)

Rehrl, C., Birk, S.: Hydrogeological characterisation and modelling of spring catchments in a changing environment. Aust. J. Earth Sci. 103(2), 106–117 (2010)

Schubert, G.: Hydrogeological Map of Austria 1:500.000. Geologische Bundesanstalt, Wien (2003)

Wagner, T., Fabel, D., Fiebig, M., Häuselmann, P., Sahy, D., Xu, S., Stüwe, K.: Young uplift in the non-glaciated parts of the Eastern Alps. Earth Planet. Sci. Lett. 295, 159–169 (2010)

Wagner, T., Mayaud, C., Oswald, S., Rinder, T., Leis, A., Stadler, H., Benischke, R., Birk, S.: Understanding intercatchment flow in a karst aquifer—using the Lurbach system example (Eastern Alps– Austria). Geophys. Res. Abstr. 13, (EGU2011) 7962 (2011)

Wagner, T., Themeßl, M., Schüppel, A., Gobiet, A., Stigler, H., Birk, S.: Auswirkungen des Kimawandels auf Abfluss und Wasserkrafterzeugung österreichischer Flüsse, In:

Wasserbau Symposium 2012 Tagungsband, Graz, S. 1–8 (2012). ISBN 978-3-85125-230- 9

Xu, C.-Y., Seibert, J., Halldin, S.: Regional water balance modelling in the NOPEX area: development and application of monthly water balance models. J. Hydrol. 180, 211–236 (1996)

APPENDIX B

CONFERENCE ABSTRACTS RELATED TO THIS THESIS

(PRESENTED AS FIRST AUTHOR)

1. A dual approach to compute groundwater flow in karst aquifers using distributive models: example of the Lurbach system (Austria)
Cyril Mayaud, Kim Maren Lompe, Thomas Reimann, Ralf Benischke and Steffen Birk

2. Changes in the hydrological behaviour of a karst aquifer (Lurbach system, Austria)
Cyril Mayaud, Thomas Wagner, Ralf Benischke and Steffen Birk

3. Recharge time scales and discretization length scales for single-continuum models with turbulent flow in karst catchments
Cyril Mayaud, Thomas Reimann and Steffen Birk

4. New insights into the functioning of the Lurbach system (Central Styrian Karst, Austria)
Cyril Mayaud, Thomas Wagner, Ralf Benischke and Steffen Birk

5. Single event time series analysis in a karst catchment evaluated using a groundwater model
Cyril Mayaud, Thomas Wagner and Steffen Birk

1. A dual approach to compute groundwater flow in karst aquifers using distributive models: example of the Lurbach system (Austria)

Distributive models of different complexity were applied to the binary Lurbach karst system, which is located 20 km north of Graz (Austria). The upper part of the catchment comprises impermeable schists and is drained by a stream, the Lurbach, towards the lower part, the 8.3 km^2 limestone plateau of the Tanneben massif. After it reaches the limestone unit, the Lurbach infiltrates along its course and finally disappears into an inaccessible subterranean sinkhole located in a cave, the Lurgrotte. Then, the water flows through the fissures and conduits of the massif and resurges at two springs, the Hammerbach spring and the Schmelzbach spring, located at the foot of the Peggauer Wand, a 300 m high limestone cliff, at the western border of the catchment. Two different modelling approaches were used to learn more about the behaviour of the karst system:

(A) MODFLOW laminar single-continuum models were implemented using the geological knowledge, tracer results, and spring discharge data. The purpose was to reproduce the response of the two springs under different hydrological conditions.

(B) Idealized catchments served to analyse the transfer of an input signal in a conduit with simple geometrical assumptions (such as varying matrix parameters) to learn more about prevailing effects in the system and to evaluate the significance of pressurized- and open-channel flow.

Three different numerical models were used for the investigation: the hybrid models CFPM1 (USGS), which couples MODFLOW to a discrete pipe network simulating pressurized flow; ModBraC, which couples MODFLOW to a discrete open-channel flow model adapted for karst conduits; and the modified single-continuum model CFPM2, which is a version of MODFLOW that accounts for turbulent flow by appropriately adjusting the hydraulic conductivity of the model cells.

Results lead to the following conclusions:

(A) The MODFLOW simulations in steady and transient state show good agreement with the discharge data. Transient state should be privileged in the future, because karst aquifers are rarely in steady-state conditions. Even though the behaviour of the system is reproduced, the lack of Schmelzbach data was a problem. Further investigations are needed and should use more data.

(B) Studies with synthetic catchments show that the observed damping of the input signal during recharge events at the Hammerbach spring could be a consequence of strong interaction between conduits and the carbonate matrix when pipe flow is pressurized. The model results with the new hybrid model ModBraC show that damping can also be obtained using open-channel flow. As opposed to CFPM1 and CFPM2, ModBraC displays a time lag between the in- and output signal, which is also observed at the field site. First modelling results with a ModBraC regional model, however, show that open-channel flow alone cannot explain the strongly damped discharge curve and the time lag of up to 26 hours between the in- and output signal at the Hammerbach spring. This means that the recharge signal is obviously influenced by a combination of open-channel flow, pressurized flow, and by the

presence of reservoirs along the conduits. However, reasonable results were obtained for the Schmelzbach system using the open-channel flow model.

Finally, results suggest that single-continuum and hybrid models each with turbulent flow representation are adequate to compute spring water discharge in karst aquifers. Nevertheless, information about the conduit geometry and sufficient hydrological data are required.

2. Changes in the hydrological behaviour of a karst aquifer (Lurbach system, Austria)

The purpose of this work is to better understand the processes which influence the global behaviour of a karst aquifer. The area under investigation is the Lurbach system, a binary karst aquifer located 20 km north of Graz (Austria). The upper part of the catchment comprises impermeable schists and is drained by a stream, the Lurbach, towards the lower part, the 8.3 km^2 limestone plateau of the Tanneben massif. After it reaches the limestone unit, the Lurbach infiltrates along its course and finally disappears into an inaccessible subterranean sinkhole located in a cave, the Lurgrotte. Then, the water flows through the fissures and conduits of the massif and resurges at two springs, the Hammerbach spring and the Schmelzbach spring, located at the foot of the Peggauer Wand, a 300 m high limestone cliff, at the western border of the catchment. Climate data, water discharge at the springs and sinkhole as well as chemical data, which are available for different types of hydrological conditions, suggest that the Schmelzbach and Hammerbach springs react very differently during flood, drought or normal water conditions. A number of tracer tests further show that the Hammerbach is the only resurgence of the sinking Lurbach stream at low water conditions, whereas at high water conditions the Lurbach water resurges at both Schmelzbach and Hammerbach.

A thorough analysis using the hydrological data suggests that the behaviour of the Lurbach system has changed due to a large flood in August 2005. Since then, no similar event was recorded and the Hammerbach discharge seems to be strongly damped compared to the Lurbach input data. Recession analysis and cumulative frequency curves support this finding. Analysis of chemical data based on recent tracer experiments are also in good agreement with this hypothesis and further suggest that intercatchment flow now occurs at lower discharge rates than before August 2005. To improve the understanding of the different behaviour of the two springs as well as the changes in their hydrological behaviour, groundwater modelling with process-based distributive models was carried out. Transient MODFLOW models were implemented successfully. Turbulent flow was integrated using a modified version of the free USGS Software Conduit Flow Process Mode 2 for MODFLOW-2005. Considering constricted flow in conduits with reduced hydraulic conductivity, the new behaviour was reproduced by the model. Thus, the change in the system's behaviour might be due to collapse material or sediment aggradation causing a constriction and thus lower hydraulic conductivity of a conduit pathway connecting Lurbach sink and Hammerbach spring.

In summary, this approach was useful to improve the understanding of the Lurbach system and might be easily applied to investigate the hydraulic behaviour of other karst aquifers.

3. Recharge time scales and discretization length scales for single-continuum models with turbulent flow in karst catchments

Karst catchments are known to have dual flow regimes: laminar flow is essentially present in the fissured matrix, whereas turbulent flow occurs through solution conduits. This duality poses great challenges to the application of conventional numerical groundwater models.
For more than 20 years, specific approaches have been developed to reproduce the hydraulic behaviour of karst aquifers (e.g. exhibited by the spring hydrographs) using groundwater models. For instance, Teutsch (1988) introduced the double-continuum approach, where the fissured matrix and the solution conduits are represented by two continuum models that are coupled by a linear exchange term. Later, hybrid models, coupling continuum and discrete approaches, were found to provide adequate representations of the dual flow behaviour of karst aquifers (e.g., Birk et al., 2006). The discrete approaches implemented in hybrid models may also account for turbulent conduit flow. Compared to conventional single-continuum models, these models require higher computational efforts and additional input parameters, which are frequently not available. Earlier research (e.g. Teutsch and Sauter, 1998) suggested that single-continuum models cannot simulate the characteristic hydraulic responses of karst aquifers.
However, Reimann et al. (2011, 2012) recently proposed the concept of conduit type flow in continuum cells (CTFC) and demonstrated that single-continuum models that account for turbulent flow, in principal, have the ability to mimic the realistic behaviour of more complex hybrid models. Yet, in the simple hypothetical catchment considered by Reimann et al. (2011b), the solution conduit was represented by cells with sizes corresponding to the conduit diameter. This is hardly possible in model applications to real karst catchments. Thus, this work examines how far this numerical model concept is capable of reproducing the dualistic behaviour of karst aquifers if the cell sizes are much larger than the conduit size. To this end, the CTFC approach was used for a parameter study in order to identify the influence of the cell discretization on the simulated dynamic response of the karst aquifer. In doing so, the performance of different model set-ups is evaluated for different recharge pulses with varying time duration in order to infer relationships between the recharge time scale and the length scale of the model cells required to provide an adequate representation of the hydraulic aquifer response.

References:

Birk, S., Liedl, R., Sauter M., 2006. Karst spring responses examined by process-based modelling, Groundwater, 44(6), 832-836.

Reimann, T., Birk, S., Rehrl, C., Shoemaker, W.B., 2012. Modifications to the Conduit Flow Process Mode 2 for MODFLOW-2005, Groundwater, 50(1), 144-148. doi 10.1111/Fj.1745-6584.2011.00805.x.

Reimann, T., Rehrl, C., Shoemaker, W.B., Geyer, T., Birk, S., 2011b. The significance of turbulent flow representation in single-continuum models, Water Resour. Res., 47, W09503, doi:10.1029/2010WR010133.

Teutsch, G., 1988. Grundwassermodelle im Karst: Praktische Ansätze am Beispiel zweier Einzugsgebiete im Tiefen und Seichten Malmkarst der Schwäbischen Alb. PhD Thesis, Eberhard-Karls-Universität, Tübingen.

Teutsch, G., Sauter, M., 1998. Distributed parameter modelling approaches in karst-hydrological investigations. Bulletin d'Hydrogéologie, 16: 99-110.

4. New insights into the functioning of the Lurbach system (Central Styrian Karst, Austria)

Keywords: binary Karst, MODFLOW, single-continuum model, groundwater modelling, laminar/turbulent flow, hydrological behaviour

Karst aquifers are widespread (~20% of the ice-free emerged areas are constituted of limestone or similar other karstifiable rocks; Ford and Williams, 2007) and well-known for their large heterogeneities essentially due to a triple porosity, a duality in their storage and a dual flow behaviour. These features need to be addressed in groundwater modelling. Because karstic waters represent an important part of the water supply for the world's population (20-25%; Ford and Williams, 2007) but are highly vulnerable to chemical and bacterial contamination, and under pressure by an intensive agricultural use, it is necessary to improve the global understanding of processes which govern flow through karst aquifers and to assess how changes in these systems might influence the spring behaviour over time.
The here investigated aquifer belongs to the Lurbach system, a 22.3 km^2 binary karst catchment located 15 km north of Graz, in the Central Styrian Karst, Austria. The Lurbach drains the upper low-permeable part of the catchment and disappears into the Lurgrotte cave, some hundred meters after it enters the karstified area. Then, the water flows through the limestone massif and resurges at the Hammerbach spring and the Schmelzbach outlet at the western border of the catchment. Spring hydrograph analyses suggest that a change in behaviour happened in the system between 2005 and 2009. Previous work showed that a redistribution of sediment within the conduits of the Hammerbach network could explain this temporary behaviour (Wagner et al., 2011; Mayaud et al., 2011). The present study uses MODFLOW to investigate whether the behaviour can be reproduced using different hypotheses like a reservoir filling and emptying water over the time. The role of turbulent flow is also investigated using the equivalent porous media approach of the Conduit Flow Process, a MODFLOW-compatible package developed by the USGS (Shoemaker et al., 2008). The study focuses first on the behaviour of the Hammerbach spring where long continuous time series are available; then we investigate the interactions of the Hammerbach/Schmelzbach system where overflow from the Hammerbach system to the Schmelzbach system is known to occur at high water levels.

References:

Ford, D., Williams, P., 2007. Karst Hydrogeology and Geomorphology. John Wiley & Sons, Ltd.

Mayaud, C., Wagner, T., Benischke, R., Birk, S., 2011. Changes in the hydrological behaviour of a karst aquifer (Lurbach system, Austria). Proc. H2Karst, 9th Conference on Limestone Hydrogeology, Besançon (France) 1-4 Sep. 2011, pp. 331-334.

Shoemaker, W.B., Kuniansky, E.L., Birk, S., Bauer, S., Swain, E.D., 2008. Documentation of a Conduit Flow Process (CFP) for MODFLOW-2005. U.S. Geological Survey Techniques and Methods 6-A24.

Wagner, T., Mayaud, C., Oswald, S., Rinder, T., Leis, A., Stadler, H., Benischke, R., Birk, S., 2011. Understanding intercatchment flow in a karst aquifer - using the Lurbach system example (Eastern Alps - Austria). Geophysical Research Abstracts, Vol. 13, EGU2011-7962, EGU General Assembly 2011.

5. Single event time series analysis in a karst catchment evaluated using a groundwater model

The Lurbach-Tanneben karst system (Styria, Austria) is drained by two major springs and replenished by both autogenic recharge from the karst massive itself and a sinking stream that originates in low permeable schists (allogenic recharge). Detailed data from two events recorded during a tracer experiment in 2008 (Oswald et al., EGU2009-9255) demonstrates that an overflow from one of the sub-catchment to the other is activated if the spring discharge exceeds a threshold. Time-series analysis (e.g., auto-correlation, cross-correlation) was applied to examine how far the various available methods support the identification of the transient inter-catchment flow observed in this karst system. As inter-catchment flow is intermittent, the evaluation was focused on single events. In order to support the interpretation of the results from the time-series analysis a simplified groundwater flow model was built using MODFLOW based on the current conceptual understanding of the karst system. The groundwater model represents a synthetic karst aquifer for which the same methods were applied. Using the wetting capability package of MODFLOW, the model simulated an overflow similar to what has been observed during the tracer experiment. Various options of recharge (e.g., allogenic versus autogenic) were used to generate synthetic discharge data for the time-series analysis. In addition, geometric and hydraulic properties of the karst system were varied in several model scenarios. This approach helps to identify effects of recharge and aquifer properties in the results from the time-series analysis. Comparing the results from the time-series analysis of the observed data with those of the synthetic data a good agreement was found. For instance, the cross-correlograms show similar patterns with respect to time lags and maximum cross-correlation coefficients if appropriate hydraulic parameters are assigned to the groundwater model. Thus, the heterogeneity of hydraulic aquifer parameters appears to be a controlling factor. Moreover, the location of the overflow connecting the sub-catchments of the two springs is found to be of primary importance. Thus, time-series analysis of single events can potentially be used to characterize transient inter-catchment flow behaviour of karst systems.

APPENDIX C

CONFERENCES ABSTRACTS TITLES RELATED TO THIS THESIS

(PRESENTED AS CO-AUTHOR)

1. The Lurbach system (Central Styrian Karst - Semriach, Austria) - a complex (but) instructive karst aquifer to evaluate predictive modelling capabilities of rainfall - runoff approaches
Thomas Wagner, Cyril Mayaud, Ralf Benischke and Steffen Birk

2. Changing intercatchment flow in a binary karst system - The Lurbach system, Austria
Thomas Wagner, Cyril Mayaud, Kim Maren Lompe, Thomas Reimann, Ralf Benischke, Stefan Hergarten, Gerfried Winkler and Steffen Birk

3. Understanding intercatchment flow in a karst aquifer - using the Lurbach system example (Eastern Alps - Austria)
Thomas Wagner, Cyril Mayaud, Stefan Oswald, Thomas Rinder, Albrecht Leis, Hermann Stadler, Ralf Benischke and Steffen Birk

4. Evaluating the changing discharge behaviour of a karst spring (Hammerbach, Austria)
Thomas Wagner, Cyril Mayaud, Ralf Benischke and Steffen Birk

5. Thresholds in karst catchments: the example of the Lurbach karst system
Steffen Birk, Thomas Wagner and Cyril Mayaud

REFERENCES

Aguilar, J.P., Michaux, J., Pélissié, T., Sigé, B., 2007. Early late Pliocene paleo karstic fillings predating the major Plio-Pleistocene erosion of the Quercy table, SW-France. Acta Carsologica, 36/3, 469-473.

Amraoui, F., Razack, M., Bouchaou, L., 2003. Turbidity dynamics in karstic systems. Example of Ribaa and Bittit springs in the Middle Atlas (Morocco). - Hydrol. Sci. J., 48, 6, 971-984.

Anderson, M.P., Woessner, W., 1992. Applied Groundwater Modelling. Acad Press, San Diego. ISBN 9780120594856.

Atkinson, T.C., 1977. Diffuse flow and conduit flow in limestone terrain in the Mendip Hills, Sommerset (Great Britain). J. Hydrol., 35, 93-110.

Atkinson, T.C., Smart, P.L., 1981. Artificial tracers in hydrogeology. In: A Survey of British Hydrogeology 1980, 173-190. The Royal Society, London.

Bailly-Comte, V., Jourde, H., Roesch, A., Pistre, S., Batiot-Guilhe, C., 2008. Time series analyses for karst/river interactions assessment: Case of the Coulazou River (southern France), J. Hydrol., 349(1-2), 98-114.

Bailly-Comte, V., Martin, J.B., Screaton, E.J., 2011. Time variant cross correlation to assess residence time of water and implication for hydraulics of a sink-rise karst system, Water Resour. Res., 47, W05547, doi:10.1029/2010WR009613.

Bailly-Comte, V., Borrell-Estupina, V., Jourde, H., Pistre, S., 2012. A conceptual semidistributed model of the Coulazou River as a tool for assessing surface water–karst groundwater interactions during flood in Mediterranean ephemeral rivers, Water Resour. Res., 48, W09534, doi:10.1029/2010WR010072.

Bakalowicz, M., 2005. Karst groundwater: a challenge for new resources. Hydrogeol. J., 13, 148-160 doi: 10.1007/s10040-004-0402-9.

Bastian, F., Alabouvette, C., 2009. Lights and shadows on the conservation of a rock art cave: The case of Lascaux Cave. International Journal of Speleology, 38(1), 55-60. ISSN 0392-6672.

Behrens, H., Benischke, R., Bricelj, M., Harum, T., Käss, W., Kosi, G., Leditzky, H.P., Leibundgut, Ch., Małoszewski, P., Maurin, N., Rajner, V., Rank, D., Reichart, B., Stadler, H., Stichler, W., Trimborn, P., Zojer, H., Zupan, M., 1992. Investigations with Natural and Artificial Tracers in the Karst Aquifer of the Lurbach System (Peggau-Tanneben-Semriach, Austria); Steir. Beitr. z. Hydrogeologie 43, Graz.

Benischke, R., Schaffler, H., Weissensteiner, V., (Eds.) 1994. Festschrift Lurgrotte 1894 - 1994. Eigenverlag Landesverein für Höhlenkunde in der Steiermark, Graz, pp 151-154.

Berkowitz. B., 2002. Characterizing flow and transport in fractured geological media: a review. Adv. Water Resour., 25:861-884.

Bon, C., Berthonaud, V., Fosse, P., Gély, B., Maksud, F., Vitalis, R., Philippe, M., van der Plicht, J., Elalouf, J.M., 2011. Low regional diversity of late cave bears mitochondrial DNA at the time of Chauvet Aurignacian paintings. J. Archaeol. Sci., 38, 1886-1895. doi:10.1016/j.jas.2011.03.033.

Bonacci, O., 1987. Karst Hydrology. Springer Verlag, Heidelberg, Germany.

Bonacci, O., 1995. Ground water behavior in karst – Example of the Ombla Spring (Croatia) J. Hydrol., 165, 113-134.

Bouchaou, L., Mangin, A., Chauve, P., 2002. Turbidity mechanism of water from a karstic spring: example of the Ain-Asserdoune spring (Beni Mellal Atlas, Morocco). J. Hydrol., 265, 34-42.

Budge, T.J., Sharp, J.M., 2009. Modeling the Usefulness of Spatial Correlation Analysis on Karst Systems. Groundwater, 47(3), 427-437.

Chin, D.A., Price, R.M., DiFrenna, V.J., 2009. Nonlinear Flow in Karst Formations, Groundwater, 47(5), 669-674. doi: 10.1111/j.1745-6584.2009.00574.x.

COST Action 65., 1995. Hydrogeological aspects of groundwater protection in karst areas. Final report EUR 16547 EN, Office for Official publications of the European Communities, Luxembourg, 446 pp.

Covington, M.D., Wicks, C.M., Saar, M.O., 2009. A dimensionless number describing the effects of recharge and geometry on discharge from simple karstic aquifers, Water Resour. Res., 45, W11410, doi:10.1029/2009WR008004.

Covington, M.D., Banwell, A.F., Gulley, J., Saar, M.O., Willis, I., Wicks, C.M., 2012. Quantifying the effects of glacier conduit geometry and recharge on proglacial hydrograph form. J. Hydrol., 414-415, 59-71. doi:10.1016/j.jhydrol.2011.10.027.

Cvijić, J., 1893. Das Karstphänomen: Versuch einer morphologischen Monographie, Wien, 113 p. (Geographische Abhandlungen, hrsg. von Prof. Dr Albrecht Penck. V, Heft 3).

Darcy, H., 1856. Les fontaines publiques de la ville de Dijon. Paris, France: Victor Dalmont.

Denmark Hydrology Institute (DHI)., 2007. Mike She User Manual and Reference Guide, December 2007, Denmark (V1 and 2).

DHI-WASY GmbH., 2011. FEFLOW, available at http://www.feflow.info, (last accessed 23th January 2014).

Dörfliger, N., Zwahlen, F., 1998. Practical guide: groundwater vulnerability mapping in karstic regions (EPIK). Environment in practice, Swiss Agency for the Environment, Forests and Landscape (SAEFL), Bern, 56 pp.

Dörfliger, N., Plagnes, V., 2009. Cartographie de la vulnérabilité des aquifères karstiques. Guide méthodologique de la méthode PaPRIKa [Mapping the vulnerability of karst aquifers. Guidelines of the method PAPRIKa]. Rapport BRGM RP-57527-FR, BRGM, Orleans, France, 100 pp.

Eisenlohr, L., Bouzelboudjen, M., Király, L., Rossier, Y., 1997. Numerical versus statistical modelling of natural response of a karst hydrogeological system, J. Hydrol., 202(1-4), 244-262.

Farrant, A.R., Smart, P.L., 2011. Role of sediment in speleogenesis; sedimentation and paragenesis. Geomorphology, 134, 79-93. doi:10.1016/j.geomorph.2011.06.006.

Filipponi, M., 2009. Spatial analysis of karst conduit networks and determination of parameters controlling the speleogenesis along preferential lithostratigraphic horizons, PhD Thesis, Faculté Environnement Naturel, Architectural et Construit, École Polytechnique Fédérale de Lausanne, 303 pp.

Fleury, P., Plagnes, V., Bakalowicz, M., 2007. Modelling of the functioning of karst aquifers with a reservoir model: application to fontaine de vaucluse (South of France). J. Hydrol., 345, 38-49.

Forchheimer, P., 1901.Wasserbewegung durch Boden. Zeitschrift des Vereins deutscher Ingenieure, 45, 1782-1788.

Ford, D., Williams, P., 2007. Karst Hydrogeology and Geomorphology. John Wiley & Sons, Ltd.

Gallegos, J.J., Hu, B.X., Davis, H., 2013. Simulating flow in karst aquifers at laboratory and sub-regional scales using MODFLOW-CFP. Hydrogeol. J., 21, 1749-1760. doi: 10.1007/s10040-013-1046-4.

Geologische Bundesanstalt., 2005. Provisorische Geologische Karte der Republik Österreich, 164-Graz. – Geofast 1:50.000, Geologische Bundesanstalt, Wien.

Genthon, P., Bataille, A., Fromant, A., D'Hulst, D., Bourges, F., 2005. Temperature as a marker for karstic waters hydrodynamics. Inferences from 1 year recording at La Peyrére cave (Ariège, France). J. Hydrol., 311 157-171.

Geyer, T., Birk, S., Reimann, T., Dörfliger, N., Sauter, M., 2013. Differentiated characterization of karst aquifers: some contributions. Carbonate Evaporite, 28 (1-2): 41-46. doi: 10.1007/s13146-013-0150-9.

Ghasemizadeh, R., Hellweger, F., Butscher, C., Padilla, I., Vesper, D., Field, M., Alshawabkeh, A., 2012. Review: Groundwater flow and transport modeling of karst

aquifers, with particular reference to the North Coast Limestone aquifer system of Puerto Rico. Hydrogeol. J., 20, 1441-1461. doi: 10.1007/s10040-012-0897-4.

Gray, D.M., 1970. Handbook on the Principles of Hydrogeology. Secretariat Canadian Nat. Com. For the International Hydrological Decade, Ottawa.

Halford, K.J., 2000. Simulation and interpretation of borehole flowmeter results under laminar and turbulent flow conditions. In Proceedings of the Seventh International Symposium on Logging for Minerals and Geotechnical Applications, Golden, Colorado, October 24-26, 2000, 157-168. Houston, Texas: The Minerals and Geotechnical Logging Society.

Harbaugh, A.W., Banta, E.R., Hill, M.C., McDonald, M.G., 2000. MODFLOW–2000, the U.S. Geological Survey Modular Ground-Water Model - User guide to modularization concepts and the Ground-Water Flow Process: U.S. Geological Survey Open-File Rep 00-92, 121 p.

Harbaugh, A.W., 2005. MODFLOW-2005, The U.S. Geological Survey Modular Ground-Water Model—The Ground-Water Flow Process. U.S. Geological Survey Techniques and Methods Book 6, Chapter A16. Reston, Virginia: USGS.

Harum, T., Stadler, H., 1992. Hydrologic and Climatologic Conditions, in: Behrens, H., Benischke, R., Bricelj, M., Harum, T., Käss, W., Kosi, G., Leditzky, H.P., Leibundgut, Ch., Małoszewski, P., Maurin, N., Rajner, V., Rank, D., Reichart, B., Stadler, H., Stichler, W., Trimborn, P., Zojer, H., Zupan, M., 1992. Investigations with Natural and Artificial Tracers in the Karst Aquifer of the Lurbach System (Peggau-Tanneben-Semriach, Austria); Steir. Beitr. z. Hydrogeologie 43, Graz.

Heinz, B., Birk, S., Liedl, R., Geyer, T., Straub, K.L., Andresen, J., Bester, K., Kappler, A., 2009. Water quality deterioration at a karst spring (Gallusquelle, Germany) due to combined sewer overflow: evidence of bacterial and micro-pollutant contamination. Environ. Geol., 57(4), 797-808. doi: 10.1007/s00254-008-1359-0.

Hill, M.E., Stewart, M.T., Martin, A., 2010. Evaluation of the MODFLOW-2005 Conduit Flow Process, Groundwater, 48 (4), 549-559.

Hubinger, B., Birk, S., 2011. Influence of initial heterogeneities and recharge limitations on the evolution of aperture distributions in carbonate aquifers, Hydrol. Earth Syst. Sci., 15, 3715–15 3729, doi:10.5194/hess-15-3715-2011.

Jeannin, P.Y., Sauter, M., 1998. Analysis of karst hydrodynamic behaviour using global approaches: a review. Bull. Hydrogéol. (Neuchâtel) 16, 31-48.

Jemcov, I., Petrič, M., 2010. Time serie analysis, modeling and assessment of optimal exploitation of the Nemanja spring, Serbia. Acta Carsologica, 39/2, 187-200.

Kavouri, K., Plagnes, V., Tremoulet, J., Dörfliger, N., Rejiba, F., Marchet, P., 2011. PaPRIKa: a method for estimating karst resource and source vulnerability—

application to the Ouysse karst system (southwest France) Hydrogeol. J., 19, 339-353 doi:10.1007/s10040-010-0688-8.

Kiraly, L., 1998. Modelling karst aquifers by the combined discrete channel and continuum approach. Bull. Hydrogéol. (Neuchâtel) 16, 77-98.

Klimchouk, A., 1996. Gypsum karst in the Western Ukraine. International Journal of Speleology, 25: 263-278.

Kong-A-Siou, L., Johannet, A., Borrell Estupina, V., Pistre, S., 2011. Complexity selection of a neural network model for karst flood forecasting: the case of the Lez Basin (southern France). J. Hydrol., 403, 367-380.

Kovačič, G., 2010. Hydrogeological study of the Malenščica karst spring (SW Slovenia) by means of a time series analysis. Acta Carsologica, 39/2, 201-215.

Kralik, M., 2001. Strategie zum Schutz der Karstwassergebiete in Österreich. BE-189 Wien, ISBN 3-85457-585-8 pp 3.

Kresic, N., Stevanovic, Z., 2010. Groundwater Hydrology of Springs: Engineering, Theory, Management, and Sustainability. Elsevier.

Kresic, N., Bonacci, O., 2010. Spring discharge hydrograph, In: Kresic, N., Stevanovic, Z., (Eds.) Groundwater Hydrology of Springs: Engineering, Theory, Management, and Sustainability. Elsevier, Chapter 4, pp 129-163.

Kübeck, C., Małoszewski, P., Benischke, R., 2013. Determination of the conduit structure in a karst aquifer based on tracer data – Lurbach system, Austria. Hydrol. Process., 27, 225-235. doi: 10.1002/hyp.9221.

Kuniansky, E.L., Halford, K.J., Shoemaker, W.B., 2008. Permeameter data verify new turbulence process for MODFLOW, Groundwater, 46(5), 768-771.

Larocque, M., Mangin, A., Razack, M., Banton, O., 1998. Contribution of correlation and spectral analyses to regional study of a large karst aquifer (Charentes, France). J. Hydrol., 205 (3–4), 217-231.

Larocque, M., Banton, O., Razack, M., 2000. Transient-state history matching of a karst aquifer groundwater flow model. Groundwater, 38(6), 939-946.

Le Moine, N., Andréassian, V., Mathevet, T., 2008. Confronting surface- and groundwater balances on the La Rochefoucauld-Touvre karstic system (Charente, France), Water Resour. Res., 44, W03403, doi:10.1029/2007WR005984.

Leroi-Gourhan, A., Michelson, A., 1986. The Religion of the Caves: Magic or Metaphysics? The MIT Press, October, 37, 6-17.

Liedl, R., Sauter, M., Hückinghaus, D., Clemens, T., Teutsch, G., 2003. Simulation of the development of karst aquifers using a coupled continuum pipe flow model. Water Resour. Res., 39, 3, 1057. doi: 10.1029/2001WR001206.

Llasat, M.C., Llasat-Botija, M., Prat, M.A., Porcú, F., Price, C., Mugnai, A., Lagouvardos, K., Kotroni, V., Katsanos, D., Michaelides, S., Yair, Y., Savvidou, K., Nicolaides, K., 2010. High-impact floods and flash floods in Mediterranean countries: The FLASH preliminary database, Adv. Geosci., 23, 47-55, doi:10.5194/adgeo-23-47-2010.

Mangin, A., 1984. Pour une meilleure connaissance des systèmes hydrologiques à partir des analyses corrélatoire et spectrale. J. Hydrol., 67, 25–43.

Marchet, A., 1928. Phosphaterden der Drachenhöhle bei Mixnitz. Mineralogische und petrographische Mitteilungen January 1928, 39(1-2), 28-34. doi: 10.1007/BF03013095.

Maréchal, J.C., Ladouche, B., Dörfliger, N., 2008. Karst flash flooding in a Mediterranean karst, the example of Fontaine de Nîmes. Eng. Geol., 99 138-146.

Marsaud, B., 1996. Structure et fonctionnement de la zone noyée des karsts à partir des résultats expérimentaux, PhD Thesis, Univ. Paris sud, 301 pp.

Martel, E.A., 1894. Les abîmes: les eaux souterraines, les cavernes, les sources, la spéléologie: explorations souterraines effectuées de 1888 à 1893 en France, Belgique, Autriche et Grèce, Paris, Librairie Ch. Delagrave, 578 p.

Massei, N., Dupont, J.P., Mahler, B.J., Laignel, B., Fournier, M., Valdes, D., Ogier, S., 2006. Investigating transport properties and turbidity dynamics of a karst aquifer using correlation, spectral, and wavelet analyses. J. Hydrol., 329, 244-257.

Mayaud, C., 2010. Groundwater modelling in karstic terrains: example of the Lurbach system. Master 2 Sciences de l´Univers, Environnement, Ecologie, Parcours Hydrologie-Hydrogéologie. Université Pierre et Marie Curie, École des Mines de Paris & École Nationale du Génie Rural des Eaux et des Forêts; unpubl master thesis.

Mayaud, C., Wagner, T., Benischke, R., Birk, S., 2013. Understanding changes in the hydrological behaviour within a karst aquifer (Lurbach system, Austria). Carbonate Evaporite. doi: 10.1007/s13146-013-0172-3.

Mayaud, C., Wagner, T., Benischke, R., and Birk, S., (in press) Single event time series analysis in a binary karst catchment evaluated using a groundwater model (Lurbach system, Austria). doi: 10.1016/j.jhydrol.2014.02.024. Accepted for publication by Journal of Hydrology.

Mayaud, C., Walker, P., Hergarten, S., and Birk, S., (under review) Non-Linear Flow Process (NLFP): a new package to compute non-linear flow in MODFLOW. Submitted as Methods Note to Groundwater.

Mithen, S.J., 1996. The prehistory of the mind: a search for the origins of art, religion, and science, London: Thames and Hudson. ISBN 0-500-05081-3.

Moussu. F., Oudin, L., Plagnes, V., Mangin, A., Bendjoudi, H., 2011. A multi-objective calibration framework for rainfall–discharge models applied to karst systems. J. Hydrol., 400, 364–376. doi:10.1016/j.jhydrol.2011.01.047.

Moutsopoulos, K.N, Tsihrintzis, V.A., 2005. Approximate analytical solutions for the Forchheimer equation. J. Hydrol., 309(1–4): 93-103.

Oswald, S., 2009. Künstliche und natürliche Tracer in einem Karsteinzugsgebiet mit allochthoner Neubildung (Lurbach, Österreich). Karl-Franzens-University of Graz; unpubl. bachelor thesis.

Panagopoulos, G., Lambrakis, N., 2006. The contribution of time series analysis to the study of the hydrodynamic characteristics of the karst systems: Application on two typical karst aquifers of Greece (Trifilia, Almyros Crete). J. Hydrol., 329, 368- 376.

Panagopoulos, G., 2012. Application of MODFLOW for simulating groundwater flow in the Trifilia karst aquifer, Greece. Environ Earth Sci 67:1877-1889. doi: 10.1007/s12665-012-1630-2.

Pételet-Giraud, E., Dörfliger, N., Crochet, P., 2000. RISKE: méthode d'évaluation multicritère de la vulnérabilité des aquifères karstiques. Application aux systèmes des Fontanilles et Cent- Fonts (Hérault, Sud de la France) [Risk: methodology for multicriteria evaluation of the vulnerability of karst aquifers. Application to systems Fontanilles and Cent-Fonts Fontanilles (Herault, southern France)]. Hydrogéologie 4, 71-88.

Pezdirc, M., Heath, E., Bizjak-Mali, L., Bulog, B., 2011. PCB accumulation and tissue distribution in cave salamander (Proteus anguinus anguinus, Amphibia, Urodela) in the polluted karstic hinterland of the Krupa River, Slovenia. Chemosphere, 84, 987–993. doi:10.1016/j.chemosphere.2011.05.026.

Pinault, J.L., Plagnes, V., Aquilina, L., Bakalowicz, M., 2001. Inverse modeling of the hydrological and the hydrochemical behavior of hydrosystems: Characterization of karst system functioning, Water Resour. Res., 37, 8, 2191-2204.

Plan, L., Decker, K., 2006. Quantitative karst morphology of the Hochschwab plateau. Eastern Alps, Austria. Z. Geomorph. N.F. 147, 29-54.

Polomčić, D., Dragišić, V., Živanović, V., 2013. Hydrodynamic modeling of a complex karst-alluvial aquifer: case study of Prijedor groundwater Source, Republic of Srpska, Bosnia and Herzegovina. Acta Carsologica, 42/1, 93-107.

Posavec, K., Bačani, A., Nakić, Z., 2006. A Visual Basic Spreadsheet Macro for Recession Curve Analysis. Groundwater, 44(5), 764-767. doi: 10.1111/j.1745-6584.2006.00226.x.

Ravbar, N., Engelhardt, I., Goldscheider, N., 2011. Anomalous behaviour of specific electrical conductivity at a karst spring induced by variable catchment boundaries: the case of the Podstenjšek spring, Slovenia. Hydrol. Process., 25, 2130-2140. doi:10.1002/hyp.7966.

Rehrl, C., Birk, S., 2010. Hydrogeological characterization and modelling of spring catchments in a changing environment. Aust J Earth Sci, 103(2), 106-117.

Reimann, T., Rehrl, C., Shoemaker, W.B., Geyer, T., Birk, S., 2011. The significance of turbulent flow representation 363 in single-continuum models, Water Resour. Res., 47, W09503. doi: 10.1029/2010WR010133.

Reimann, T., Birk, S., Rehrl, C., Shoemaker W.B., 2012. Modifications to the Conduit Flow Process Mode 2 for MODFLOW-2005, Groundwater, 50(1), 144-148. doi :10.1111/Fj.1745-6584.2011.00805.x.

Reimann, T., 2012 Adaptation of numerical modeling approaches for karst aquifer characterization. PhD Thesis. Institute for Groundwater Management, TU Dresden, Dresden, Germany.

Renko, T., Iršič-Žibert, M., 2011. Heavy rain and floods in Croatia and Slovenia. 17-19 September 2010. EUMeTrain document available online at: http://eumetrain.org/data/2/202/navmenu.php (last accessed 2nd February 2014).

Saller, S.P., Ronayne, M.J., Long, A.J., 2013. Comparison of a karst groundwater model with and without discrete conduit flow. Hydrogeol. J., 21, 1555-1566. doi: 10.1007/s10040-013-1036-6.

Salomon, J.N., 2006. Précis de karstologie, Presses Universitaires de Bordeaux, coll.«Scieteren», ISBN 9782867814112.

Sauter, M., 1992. Quantification and forecasting of regional groundwater flow and transport in a karst aquifer (Gallusquelle, Malm, SW. Germany), PhD Thesis, Universität Tübingen, Tübingen (Germany).

Sauter, M., Kovács, A., Geyer, T., Teutsch, G., 2006. Modellierung der Hydraulik von Karstgrundwasserleitern – Eine Übersicht. Grundwasser – Zeitschrift der Fachsektion Hydrogeologie 3/2006. doi: 10.1007/s00767-006-0140-0.

Scanlon, B.R., Mace, R.E., Barrett, M.E., Smith, B., 2003. Can we simulate regional groundwater flow in a karst system using equivalent porous media models? Case study, Barton Springs Edwards aquifer, USA, J. Hydrol., 276(1-4), 137-158.

Schubert, G., 2003. Hydrogeological Map of Austria 1: 500.000. Geologische Bundesanstalt, Wien.

Shen, G., Wu, X., Wang, Q., Tu, H., Feng, X., Zhao, J., 2013. Mass spectrometric U-series dating of Huanglong Cave in Hubei Province, central China: Evidence for early presence of modern humans in eastern Asia. J. Hum. Evol., 65, 162-167.

Shoemaker, W.B., Kuniansky, E.L., Birk, S., Bauer, S., Swain, E.D., 2008. Documentation of a Conduit Flow Process (CFP) for MODFLOW-2005. U.S. Geological Survey Techniques and Methods Book 6, Chapter A24. Reston, Virginia: USGS.

Sidiropoulou, M.G., Moutsopoulos, K.N., Tsihrintzis, V.A. 2007. Determination of Forchheimer equation coefficients a and b. Hydrol. Process., 21, 534-554. doi: 10.1002/hyp.6264.

Teutsch, G., Sauter, M., 1991. Groundwater modelling in karst terranes: scale effects, data acquisition and field validation. Proc. 3rd Conference on Hydrogeology, Ecology, Monitoring and Management of Ground Water in Karst Terranes, Dec. 1991, Nashville.

The Unesco Courier., 1995. Troglodytes: a hidden world. Issue from December 1995. 62 pp.

Thrailkill, J., 1974. Pipe flow models of a Kentucky limestone aquifer. Groundwater, 12(4), 202-205.

Unicef., 2013. Joint Monitoring Programme for Water Supply and Sanitation. 40p. ISBN 978 92 4 150539 0.

Valdes, D., Dupont, J.P., Massei, N., Laignel, B., Rodet, J., 2006. Investigation of karst hydrodynamics and organization using autocorrelation and T-ΔC curves. J. Hydrol., 329, 432-443.

Vesper, D.J., Loop, C.M., White, W.B., 2001. Contaminant transport in karst aquifers. Theor et Appl. Karstol., 13–14 (2001), pp. 101-111.

Wagner, T., Fritz, H., Stüwe, K., Nestroy, O., Rodnight, H., Hellstrom, J., Benischke, R., 2011. Correlations of cave levels, stream terraces and planation surfaces along the River Mur—Timing of landscape evolution along the eastern margin of the Alps. Geomorphology, 134, 62-78. doi: 373 10.1016/j.geomorph.2011.04.024.

Wagner, T., Themessl, M., Schüppel, A., Gobiet, A., Stigler, H., Birk, S., 2012. Auswirkungen des Klimawandels auf Abfluss und Wasserkrafterzeugung österreichischer Flüsse. In: Zenz, G. (ed.), Wasserbau Symposium 2012 Wasser - Energie, Global denken - lokal handeln, Verlag der Technischen Universität Graz: 1-8.

Wagner, T., Mayaud, C., Benischke, R., Birk, S., 2013. Ein besseres Verständnis des Lurbach-Karstsystems durch ein konzeptionelles Niederschlags-Abflussmodell. Grundwasser, 18(4), 225-235. doi: 10.1007/s00767-013-0234-4.

Wen, Z., Huang, G., Zhan, H., 2011. Non-Darcian flow to a well in a leaky aquifer using the Forchheimer equation. Hydrogeol. J., 19, 563-572. doi: 10.1007/s10040-011-0709-2.

Williams, P., Fong, Y., 2011. World map of carbonate rock outcrops v3.0, available at http://www.geog.auckland.ac.nz/research/karst.shtml, (last accessed 14th November 2013).

Worthington, S.R.H., 2007. Ground-water residence times in unconfined carbonate aquifers. Journal of Cave and Karst Studies, v. 69, no. 1, p. 94-102.

Worthington, S.R.H., 2009. Diagnostic hydrogeologic characteristics of a karst aquifer (Kentucky, USA). Hydrogeol. J., 17(7), 1665-1678.

Zheng, Z., Grigg, R., 2006. A Criterious for Non-Darcy Flow in Porous Media. Transport Porous Med., 63, 57-69. doi: 10.1007/s11242-005-2720-3.

THANKS TO…

During this PhD I met many people who helped, guided and advised me. This contributed a lot to improve my vision of sciences, karst, groundwater modelling or just life in general. As the final work wouldn't have been the same without their contribution, I would like to acknowledge all of them in the following section. Of course this is a succinct list and I apologize if I forget someone.

First of all, I want to thank my PhD advisor Steffen Birk, who gave me the opportunity to make a PhD in the field of karst sciences in Graz. Thank you Steffen for being available, for your enthusiasm and all your precious advices and also for giving me so much freedom in my work!

The second person who I'm greatly indebted is my office mate Thomas Wagner. Tom, I have no words to express my profound gratitude for all the interests you continuously showed to my studies. I really enjoyed the many discussions we had about sciences and mountaineering. I think now that I understand better the meaning of the expression "to work in a team".

Because modelling needs to stay close to field observations, I would like to thank warmly Ralf Benischke for sharing me his tremendous knowledge about the Lurbach system and the Central Styrian Karst (and its very rich history). Thank you Ralf, I learned many things from you!

I'm grateful to Stefan Hergarten for his precious help. Thank you for your good mood, for the easy way you found the analytical solution of the Forchheimer equation. I really enjoyed the nice bike tour we shared together (I'm ashamed that we couldn't bike more during the time you were in Graz but I hope we will ride again in the future).

Many good advices were given to me by Gerfried Winkler, my second "unofficial" advisor. Thank you for that and thank you for correcting my mistakes in German!

I shared many funny moments with Abraham and Marcus, the two great guys from the neighboring office: both of you contributed significantly to improve my mood with your smiles and your jokes and I appreciated it a lot! Abraham: አመሰግናለሁ brother!; Marcus: thanks for teaching me this amazing Austrian and Styrian slang! Thanks as well for the kleine Wappler; I will still have my revenge for the keyboard! I hope I will be present at your respective defenses.

Sylvain: thank you for all the discussions we had since three and a half years! I really enjoyed all the lunches we had together speaking about everything and I learned many things from your wisdom.

I would like to thank also all the other members (past and present) of our research group: Michaela, Bernhard, Michi, and Andreas, and from the institute: Claudia, Markus, Patrick, Amon, Yanlong, Tamer, Syed, Mahmoud, Angela, Andreas B, Michi L, Rolland, Felix, Patrica as well as all the PhD students from the UZAG doctoral school. Georg Stegmüller, Franz Tscherne (Hallo servas!), Gertraud Bauer and Erwin Kober are thanked for the administrative and technical support.

During these three and a half years, I took part at many interesting meetings in several different countries. Those meetings contributed a lot to my present work. I would like especially to acknowledge all the participants of the karst modelling workshop from 2011 to 2013 (Rudolf Liedl, Georg Kaufmann, Wolfgang Dreybrodt, Thomas Reimann, Thomas Hiller, Markus Giese, Dushko Romanov, Matija Perne, Matt Covington and Franci Gabrovšek). I thank also Martin, Carole and Manon for the good time we had together during the 20th Karst Summer School in Postojna and all the interesting discussions we had after that. I should also hereby mention my profound gratitude to two teachers I had during my school years: Christophe Huet at high school level and Francois Métivier at university level. Thank you both for transmitting me your passion for geosciences for the first one and your enthusiasm of research for the second one!

Barclay Shoemaker is thanked for his kindness and support with his regular emails coming from the other side of the Atlantic Ocean. A particular thank is addressed to Kim and Christoph for the nice time I had during my stay in Dresden! I enjoyed a lot the hikes and the nice evenings at the Biergarten near the Blaue Wunder with you, and I hope we will see us very soon. Nikos is thanked for his good mood and all the brilliant discussions we had together. Danke mein Kampfgenosse!

The Ginko (Graz), Maharaja and Namasté (Ljubljana) are acknowledged for the nice food they provide. The Triglav National park, the Schöckl and Mixnitz mountains as well as the hills of Novystein, Linecker and Šmarna gora are thanked to exist and to offer so many nice biking and hikking trips. The music of Gojira, Cult of Luna, Explosions in the Sky, Bijelo Dugme, Bajaga i Instruktori and FM4 were really good for my ears and my mind.

I would like to thank all my friends from France and especially those of whom I had a regular contact during the years: Alexandra, Damien, Adrien, Boris le hachoir mon pote de toujours, Pierre, Anne-Lise, Solène, Benji, Camille, Hugo, Lola and Guillaume with a special mention to Séverin who visited me two times.

Nina is thanked a lot for her nice mood as well as her understanding and patience with me during the years ()()*.

Finally my last thought is for my family and especially for my parents Claude and Sylvie: all their love and constant support during the years allowed me to become what I am today.

This work was funded by the Austrian Science Fund (FWF): L 576-N21.

SHORT CV

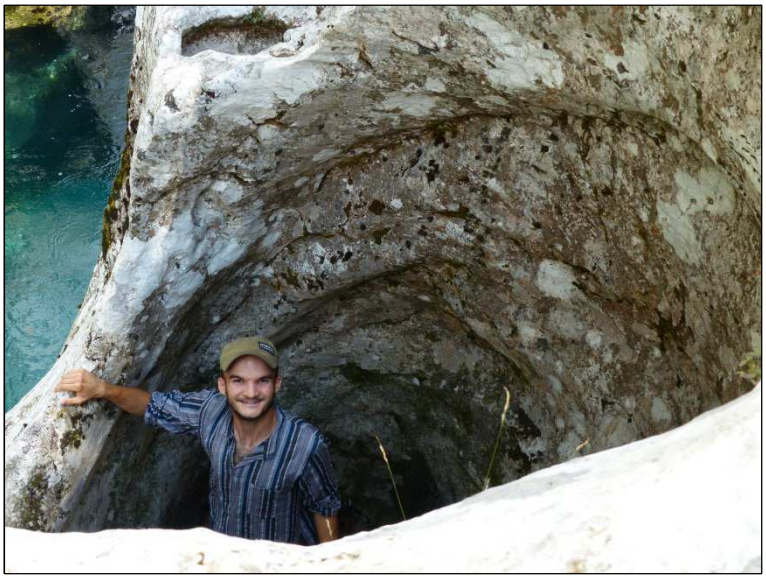

Personal information
Full name: Cyril Mayaud
Date of birth: 01.01.1987
Place of birth: Longjumeau, France
Citizenship: French
Languages: French, German, English

Education

2010-2014:	PhD student, University of Graz, Austria Thesis title: " Groundwater modelling in karst terrains using single-continuum models" Supervisor: Univ. Prof. Dr. Steffen Birk
2009-2010:	MsC studies, Pierre-and-Marie-Curie University, Paris, France Six month exchange at the University of Graz, Austria Thesis title: " Groundwater modelling in karst terrains: example of the Lurbach catchment" Supervisor: Univ. Prof. Dr. Steffen Birk; Dr. Valérie Plagnes
2008-2009:	MsC studies, Paris Diderot University and IPGP, Paris, France Five month at SANTEC-Fuchs compagny, Hürth, Germany Thesis title: "Groundwater and subsoil decontamination with activated carbon"
2006-2008:	BsC studies, Paris Diderot University, Paris, France

Before all things reborn again
You learn the painful breath of time
Cold mourning stretches out your arms
To the mighty warmth of the golden sun
Seem all have gone insane for gold
All was created out of the night
We're all born from the burst of a star
The day you'll come to life you'll realize
Expanding force to life where you belong
And in the winter cold, with opened eyes
You'll find the strength to fight and stand upright
One day you'll walk the world and keep in mind
The heart you've been given in winter time
And through the bitter cold, with opened eyes
You'll find the strength to fight and stand upright
Gojira - Born In Winter